Factors regulating nuclear localization of MIER1 alpha isoforms

by

© Aimee M. Hand, B.Sc.

A thesis submitted to the

School of Graduate Studies

in partial fulfillment of the requirements for the degree of

Masters of Science in Medicine

Faculty of Medicine

Memorial University of Newfoundland

December 2014

St. John's Newfoundland and Labrador

Abstract

Mesoderm induction early response 1 (*MIER1)* gene is located on human chromosome 1p31.2 and encodes a nuclear protein. *MIER1* encodes four distinct proteins with a common internal sequence and variable N- and C-termini. MIER1α, the α C-terminus with 23 amino acids and an LXXLL motif for interaction with nuclear hormone receptors, interacts with the estrogen receptor alpha (ERα) *in vivo* and decreases growth of T47D cells. This study investigated the effect of MIER1α on proliferation and/or survival of human breast adenocarcinoma cells, MCF7, and T47D cells, and the results demonstrated that MIER1α had no effect on cell number.

Previous work has revealed that the subcellular localization of MIER1α changes, and loss of nuclear MIER1α might contribute to the advancement of breast cancer. A third isoform arises at the N-terminus, MIER1-3Aα, and contains a leucine-rich nuclear export signal. Inclusion of this exon in MIER1α, to produce MIER1-3Aα, changes its subcellular localization from nuclear to cytoplasmic. It has been shown that the percentage of cells appearing with nuclear MIER1α is different in MCF7 and T47D cells at 78.9 % and 9.2 %, respectively. These two cell lines are cultured under different serum conditions and therefore, the effect of factors in serum on nuclear localization was investigated. Serum was shown to have an appeared effect on nuclear localization of MIER1 isoforms in MCF7 cells, and MIER1α in T47D cells. To investigate the effect of an extracellular growth factor on localization, insulin was added to the cell culture medium. Insulin was shown to have an appeared effect on localization of MIER1α in MCF7 cells. Our results demonstrate that factors in serum may be important to control the nuclear localization of proteins.

Acknowledgements

"The scientist is motivated primarily by curiosity and a desire for truth."-*Irving Langmuir*

"It helps us being the underdog. We have nothing to lose. Nobody expects us to win except ourselves"- *Daniel Ruffin*

I would first and foremost like to express my utmost appreciation for my supervisor, Dr. Laura Gillespie, for giving me the wonderful opportunity of working in her laboratory. When I initially started my Master's degree, I was insecure and I did not think I deserved my given position within the laboratory however, Dr. Gillespie's continued support and direction gave me the confidence to fully complete my Master's project. Dr. Gillespie is very knowledgeable and I believe I have learned a lot from her supervision. I will always to be truly grateful for this experience. I would like to thank Dr. Gary Paterno for providing additional guidance and support with areas of my project. I would like to thank my supervisory committee members, which include Dr. Gillespie, Dr. Paterno and Dr. Kao, for guiding me in the right direction in order to complete my thesis. I would like to extend a sincere thank you to Corinne Mercer for always being there when I needed your guidance and for your continued encouragements. I would also like to thank the members of the Terry Fox Laboratory, Roya Derwish, Jarratt Rose, Shengnan Li, Leena Derwish, Julia Ferguson, Karley Thorne, Philip Andrews, Tahrim Hasan, Youlian Tzenov and Maryam Vatani. Lastly, I would like to thank my family and my boyfriend, Mark Roebothan, for their continued support, encouragement, and love during the duration of this project.

Table of Contents

List of Figures

List of Tables

List of Abbreviations

+	plus
-	minus
%	percent
α	alpha
β	beta
°C	degrees Celsius
mm	millimeter
ug	microgram
uL	microlitre
Akt	also known as protein kinase B
AR	androgen receptor
β-actin	beta actin
bFGF	basic fibroblast growth factor
Bcl-2	B-cell lymphoma 2
BRCA1	breast susceptibility gene 1
BRCA2	breast susceptibility gene 2
BSA	bovine serum albumin
BrdU	bromodeoxyuridine
CBP	Creb-binding protein
$Cdk4^{WT}$	cyclin-dependent kinase 4 wild type
$Cdk4^{R/R}$	cyclin-dependent kinase 4 mutant
CDKs	cyclin-dependent kinases
CIN	chromosomal instability
CO_2	carbon dioxide
CpGs	CG dinucleotides
CRM1	chromosome region maintenance 1
DAB	3, 3'-diaminobenzidine

DCIS	ductal carcinoma *in situ*
DMEM	Dulbecco's Modified Eagle Medium
DNA	deoxyribonucleic acid
dox	doxycycline
E_2	17β-estradiol
EDTA	ethylenediaminetetraacetic acid
EGFR	epidermal growth factor receptor
EGL27	*Caenorhabditis elegans* protein
E2F	family of transcription factors
ELM2	EGL27 and MTA1 homology
EMP2	epithelial membrane protein-2
EMT	epithelial to mesenchymal transition
ERE	estrogen response elements
ER	estrogen receptor
ERα	estrogen receptor alpha
ERβ	estrogen receptor beta
ERK4	transcription factor
ESR1 & ESR2	estrogen receptors
FBS	fetal bovine serum
FKHR1	member of the forkhead transcription factors
G_0 phase	Gap 0 phase/resting phase
G_1 phase	Gap 1 phase
G418	geneticin
GADPH	glyceraldehyde 3-phosphate dehydrogenase
GAL4	transcriptional activator
GAM-HRP	goat anti-mouse horseradish peroxidase light chain specific
GFP	green fluorescent protein
H_2O	water

HAT	histone acetyltransferase
HDAC1	histone deacetylase 1
HDFs	human diploid fibroblasts
HER2	human epidermal growth factor receptor 2
HIEC	human non immortalized intestinal epithelial crypt cells
hMIER1	human mesoderm induction early response 1 protein
hMIER1	*human mesoderm induction early response 1 gene*
hr	hour
hrs	hours
HR	hormone receptor
ICC	immunocytochemistry
IDC	invasive ductal carcinoma
IGF1R	insulin-like growth factor 1 receptor
IGFBP5	insulin-like growth factor binding protein 5
ILC	invasive lobular carcinoma
IR	insulin receptor
kb	kilobase pair
kDa	kilodalton
KiMSV	Kirsten murine sarcoma virus
KLF6	Kruppel-like zinc finger 6 transcription factor
$KLF6SV_1$	splice variant of KLF6
LPA	lysophosphatidic acid
LXXLL	L=leucine; X=any amino acid
M	molar
MAL	myocardin-related SRF coactivator
MAPK	mitogen-activated protein kinase
MEFs	mouse embryonic fibroblasts
MIER1	*mesoderm induction early response 1 gene*

MIER1	mesoderm induction early response 1 protein
mA	milliamps
mins	minutes
ml	millilitre
mRNA	messenger ribonucleic acid
MSI	microsatellite instability
MTA1	metastasis-associated 1
mTOR	mammalian target of rapamycin
NBCS	newborn calf serum
n.d.	no date
NGB	neuroglobin
NK	natural killer
NLS	nuclear localization signal
nm	nanometer
nM	nanomolar
NOX1	member of the family of NADPH oxidases
p21	cyclin-dependent kinase inhibitor
p27	cyclin-dependent kinase inhibitor
p53	tumour suppressor protein
p85	regulatory subunit of P13K
P1	promoter 1
P2	promoter 2
PBS	phosphate buffered saline
PDGF	platelet derived growth factor
PI3K	phosphatidylinositol 3'-kinase
PIP_3	phosphatidylinositol 3, 4, 5- triphosphate
PKCδ	protein kinase C isoform
PPARγ	peroxisome proliferator-activated receptor

pRb	retinoblastoma protein
PR	progesterone receptor
PTEN	phosphatase and tensin homolog
RB1	*retinoblastoma 1 gene*
RNA	ribonucleic acid
ROS	reactive oxygen species
RTK	receptor tyrosine kinases
S phase	synthesis phase
SAM-HRP	sheep-anti mouse horseradish peroxidase
SANT	homology to the DNA binding domain c-myb
SDS	sodium dodecyl sulfate
SDS-PAGE	sodium dodecyl sulfate polyacrylamide gel electrophoresis
SH3	src homology domain 3
SIRT1	silent information regulator 1
Sp1	specificity protein 1 transcription factor
SRF	serum response factor
SSB	SDS sample buffer
TDc21	control T47D cells
TDα5	MIER1α expressing T47D cells
Tet	tetracycline
TGF-α	transforming growth factor alpha
TGF-β	transforming growth factor beta
TNBC	triple negative breast cancer
TP53	*tumour gene p53*
Tregs	regulatory T cells
UBF1	ribosomal transcription factor
UBF2	ribosomal transcription factor
VEGF	vascular endothelial growth factor

VEGF-2	vascular endothelial growth factor receptor 2
WGA	wheat germ agglutinin
wtKLF6	wild type Kruppel-like zinc finger 6 transcription factor
WRT	Wistar rat thyroid cells
xmier1	*Xenopus mesoderm induction early response 1 gene*
xmier	*Xenopus* mesoderm induction early response 1 protein

Chapter 1- Introduction

1.1 Complexity of Cancer

1.1.1 Cancer Development

Cancer is a complex disease involving dynamic alterations in the genome. It is characterized by abnormal cell growth driven by mutations in hereditary DNA, allowing cancer cells to forgo essential pathways that regulate normal cell growth and homeostasis (Hanahan & Weinberg, 2011). Cancer cells have acquired six capabilities which have given normal cells the ability to transform into malignant phenotypes. These include: self-sustaining proliferative signalling, evading growth suppressors, resisting cell death, enabling replicative immortality, inducing angiogenesis, and activating invasion and metastasis, as shown in Figure 1.1 and discussed below.

Normal cells require the presence of a growth signal in order to proliferate, and the proliferation process is tightly controlled. Cancer cells escape this control and have the ability to proliferate even in the absence of external stimuli (Gutschner & Diederichs, 2012). This leads to unlimited cell growth and is the result of sustained proliferative signalling. Cancer cells have the ability of sustaining proliferative signalling through the production of their own growth factors, which can act in an autocrine or paracrine manner, the altering of growth factor levels and the deregulation of signalling pathways, and also the cancer cells gained independence from exogenous growth factors and the activation of signalling pathways (Gutschner & Diederichs, 2012; Prevarskaya *et al.*,

2010). The production of their own growth factors and the activation of signalling pathways allow cancer cells to grow in the absence of external stimuli.

The cell cycle is a complex process regulated by signalling networks. Cells rely on the action of signalling networks which include the retinoblastoma protein (pRb) and the p53 protein to regulate control of the cell cycle and induce apoptosis in the presence of damaged DNA (Good & Harrington, 2013). Cancer cells have gained the ability to ignore signals that prevent proliferation by inducing cell cycle arrest or apoptosis. This includes signals from transforming growth factor beta (TGF-β), which is involved in limiting proliferation, initiating cell cycle arrest, and initiating DNA damage repair and apoptosis. Cancer cells also have the ability to secrete TGF-β in an autocrine manner, thereby changing the tumour suppressor response to a tumour promoter response (Good & Harrington, 2013; Prevarskaya *et al.*, 2010). Cancer cells have the ability to ignore anti-growth signals and the capability to change the phenotype of a tumour suppressor, TGF-β, and therefore, are capable of evading growth suppressors.

Apoptosis is also one of the challenges cancer cells face and it is detrimental to their survival. Apoptosis can be activated through both extrinsic and intrinsic pathways, and is regulated by pro-apoptotic and anti-apoptotic molecules (Sledge & Miller, 2003). For cancer cells to resist apoptosis, genetic alterations often occur and include mutated *TP53* gene and alterations in pro-apoptotic and anti-apoptotic genes. These mutations allow cancer cells to escape cell death and continue to grow uninhibited.

After each cell division, the telomere length for normal cells is shortened. Cancer cells have the ability to stabilize telomere length, which is important for cancer cells to

maintain the fourth hallmark of cancer, enabling replicative immortality (Kelland, 2007). In normal cells, telomeres are lost during each replication and the telomere length becomes increasingly shorter. The chromosomal DNA becomes unprotected, chromosomal rearrangements occur, and the eventual result is cell death (Prevarskaya *et al.*, 2010). However, in cancer cells, the telomere length is stabilized through the activation of telomerase (Kelland, 2007). The enzyme telomerase is composed of a RNA unit (hTERC) and a catalytic protein (hTERT), and the catalytic protein is common in breast cancers (Kelland, 2007; Sledge & Miller, 2003). The stabilization of telomere length by cancer cells is important for their ability to continuously replicate and escape cell death.

The formation of new blood vessels, angiogenesis, is important for cancer to grow. Angiogenesis is almost always activated, and cancers cells have acquired this ability by an imbalance of pro-angiogenic and anti-angiogenic proteins (Voron *et al.*, 2014). Vascular endothelial growth factor is a pro-angiogenic protein that is up-regulated, and thrombospondin-1 is an anti-angiogenic protein that is down-regulated (Harrington *et al.*, 2007). The up-regulation of pro-angiogenic proteins is important for both the formation of new blood vessels and sustained neoplastic growth.

Invasion and metastasis is the sixth hallmark of cancer required for malignant tumours to invade normal tissues and continue to grow. TGF-β is known to promote invasion into adjacent tissues by inducing epithelial-to-mesenchymal transition (EMT; Haria & Naora, 2013). Several transcription factors induced by TGF-β are involved in EMT and include, Snail, Twist and ZEB families of transcription factors. Another

important factor of the metastatic cascade is E-cadherin, which is involved in the development of epithelial cell layers. Upregulation of E-cadherin expression inhibits metastasis however, E-cadherin expression is lost in human cancers. Invasion of normal tissues by cancer cells is achieved by EMT and the down regulation of E-cadherin expression.

Further research has suggested that two additional hallmarks are involved in the development of cancer: deregulating cellular energetics and avoiding immune destruction. Deregulating cellular energetics is the altering of energy metabolism to stimulate the proliferative process of cancer cells. This hallmark represents the theory that without fuel or energy there would be no proliferation (Sonnenschein & Soto, 2013). In order for cancer cells to proliferate there must be a reprogramming of energy metabolism to aerobic glycolysis. This glycolytic use of energy by the oncogenes, *RAS* and *MYC*, and the mutant tumour suppressor, *TP53*, have proven beneficial in conferring to the hallmark capabilities of cell proliferation and decreased apoptosis (Hanahan & Weinberg, 2011). Without energy there would be no proliferation, and therefore, the reprogramming of energy metabolism is critical for the growth of cancer cells.

The second emerging hallmark, avoiding immune destruction, allows cancer cells to avoid detection by the immune system. The immune system is constantly monitoring cells and tissues and thus, responsible for eliminating cancerous cells (Curigliano, 2011). Cancer cells are capable of avoiding immune destruction by the increased activity of regulatory T cells (Tregs). Tregs suppress T-cell response and natural killer (NK) cells

proliferation, and thereby interfere with the desired immune response. Given the activity of Tregs, cancer cells avoid elimination by the immune response and continue to grow.

Genomic instability is an enabling characteristics of cancer cells, and is responsible for the generation of mutations. There are different forms of genomic instability however, chromosomal instability (CIN) is the most common form (Negrini *et al*., 2010). Chromosomal instability involves a change in the number of chromosomes as well as chromosomal rearrangements in cancer cells compared to normal cells. Microsatellite instability (MSI) is another form of genomic instability and involves the expansion or contraction in the number of repeated DNA nucleotide units in microsatellite sequences (de la Chapelle & Hampel, 2010; Negrini *et al*., 2010). MSI is present in 15 % - 20 % of all colorectal cancers, and CIN contributes to mutations in DNA repair genes leading to the development of certain cancers including breast and ovarian (de la Chapelle & Hampel, 2010; Negrini *et al.*, 2010). Genomic instability is the outcome of mutations in DNA repair genes and the detrimental consequence is cancer development.

The latter enabling characteristic, driven by cells of the immune system, promotes tumour progression through various ways. In the past, tumour-promoting inflammation stimulated tumorigenesis and progression, and thereby allowed neoplasias to attain hallmark capabilities (Hanahan & Weinberg, 2011). Inflammation contributes to tumour progression by providing growth factors, survival factors and inductive signals that aid in proliferation. Inflammatory cells can be present at the beginning stages of neoplastic progression, and can develop neoplasias into advanced cancer. Lastly, inflammatory cells

can release chemicals that are mutagenic and can accelerate cancer cells evolution to malignancy. Tumour-promoting inflammation is a powerful hallmark as it can contribute to tumour progression in a variety of ways. These emerging hallmarks and enabling characteristics are shown in Figure 1.2.

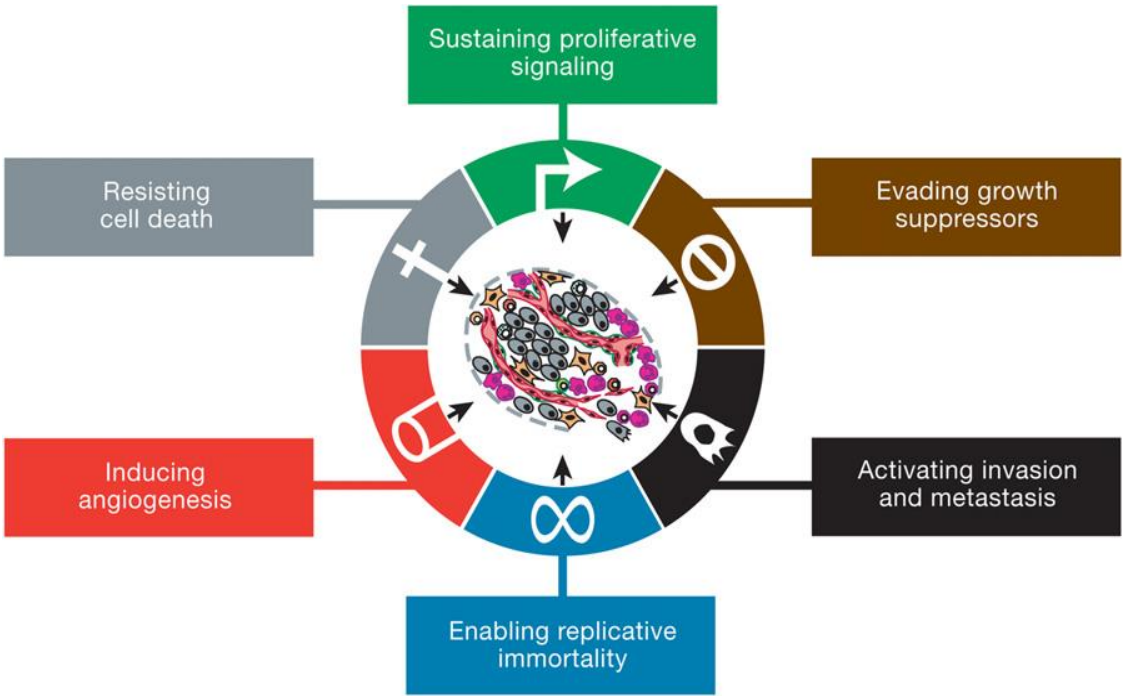

Figure 1.1: Hallmarks of Cancer

This figure, from Hallmarks of Cancer, Hanahan and Weinberg, 2011[1] illustrates the six capabilities of cancer: (1) Sustaining proliferative signaling, (2) Evading growth suppressors, (3) Resisting cell death, (4) Enabling replicative immortality, (5) Inducing angiogenesis and (6) Activating invasion and metastasis.

[1] License agreement between Aimee Hand and Elsevier provided by Copyright Clearance Center. Licence Number: 3499570950357 and Licence Date: October 31st, 2014 (http://www.cell.com/cell/home).

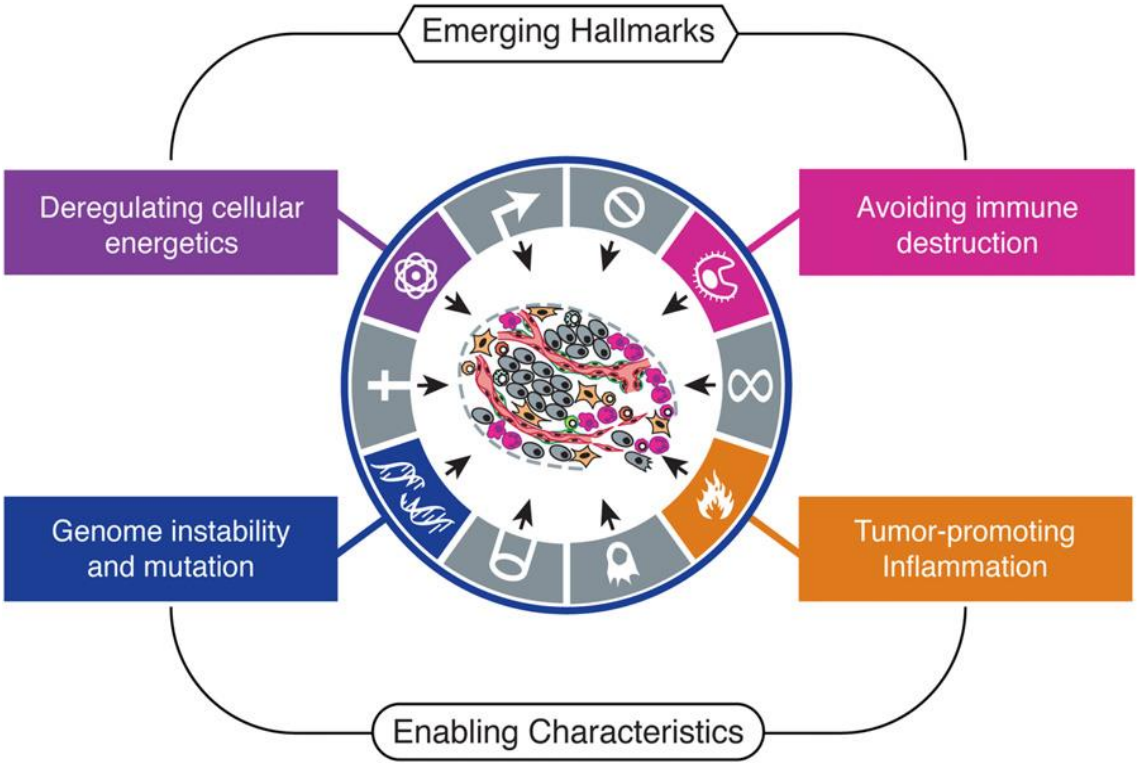

Figure 1.2: Emerging Hallmarks and Enabling Characteristics
This figure, from Hallmarks of Cancer, Hanahan and Weinberg, 2011[2] illustrates the two additional hallmarks involved in the development of cancer and are labelled emerging hallmarks, deregulating cellular energetics and avoiding immune destruction. Cancer cells have acquired these capabilities for tumorigenesis with the help of enabling characteristics, genomic instability and mutation, and tumour-promoting inflammation.

[2] License agreement between Aimee Hand and Elsevier Copyright Clearance Center. License number: 3499570950357 and License Date: October 31st, 2014 (http://www.cell.com/cell/home).

1.1.2 Canadian Cancer Statistics

Cancer is one of the leading causes of death worldwide. It is a devastating disease that is responsible for an estimated 25 % of all deaths in Canada, and approximately 187,600 new cases of cancer to be diagnosed in 2013 (Canadian Cancer Statistics, 2013). Statistical analysis has revealed that the most common types of new cancer cases being diagnosed are lung, breast, colorectal and prostate cancer, with lung cancer being the most devastating. According to these recent statistics, cancer occurs in both males and females, and more frequently in those over the age of 50. The leading cancer for males is prostate cancer and for females is breast cancer at 25 % and 26 % of cases being diagnosed, respectively. However, the incidence rate is higher in males at 45 % (1/2.2) and 42 % (1/2.4) in females. The disease is overwhelming with the five-year relative survival rate at 63 %. Overall, thyroid cancer having the highest five-year relative survival ratio and pancreatic cancer having the lowest five-year relative survival ratio. These staggering statistics emphasize the impact of cancer in Canada.

1.2 Breast Cancer

Breast cancer is an intricate disease and the most frequently diagnosed cancer in women. It is estimated that breast cancer made up 26 % of all cancer cases being diagnosed in Canada in 2013, and an estimated 1.7 million cases will be diagnosed globally by the year 2020 (Canadian Cancer Statistics, 2013; Bhikoo *et al.*, 2011). Breast cancer is the leading cause of cancer-related death among women accounting for 16 % of

cancer deaths and 460,000 deaths worldwide (Engstrøm *et al*., 2013; Florea & Busselberg, 2013).

Breast cancer can be divided into three subtypes based on the presence of receptors on cancer cells. The first, hormone receptor (HR) positive breast cancers, account for 60 % of cases and express estrogen (ER) and/or progesterone (PR) receptors (Tinoco *et al.*, 2013). The other two subtypes are expressed in 20 % of cases and include human epidermal growth factor receptor 2 (HER-2/neu) and triple negative breast cancer (TNBC). Triple negative breast cancer represents those negative for expression of ER, PR and HER-2/neu. There are many risk factors for breast cancer including, but not limited to, age, geographic location, socioeconomic status, familial history of breast cancer, hormones and lifestyle (Florea & Busselberg, 2013). Therefore, women should take all precautionary measures, such as regular breast cancer screening, to avoid diagnosis.

1.2.1 Breast Cancer Tumorigenesis

The progression from normal to malignant breast tissue is a complex process. Breast cancer tumorigenesis occurs when normal breast tissue becomes an invasive cancer via hyperplasia and carcinoma (Kenemans *et al.,* 2004). Once the invasive cancer is established, metastasis can occur through the blood vascular systems. This process is correlated with mutations in regulatory genes involved in cell proliferation, survival and differentiation. These include estrogen receptor genes, cyclin D1 and E genes, tumour suppressor genes *RB1*, *TP53*, and *PTEN*, oncogenes *HER2* and *c-MYC*, and the breast susceptibility genes *BRCA1* and *BRCA2* (Suter & Marcum, 2007). The process of breast

cancer development involves mutations in several genes which will be discussed in more detail in the following sections.

1.2.2 Estrogen and estrogen receptor

Estrogen and estrogen receptor have been implicated in the malignant progression of breast cancer. Estrogen is a mitogenic hormone that is not only important for breast development, but it is expressed at a higher level in breast cancer tissue than normal tissue (Duffy, 2006; Suter & Marcum, 2007). There are two types of estrogen receptors (ERs), ERα and ERβ, with ERα being the most important growth factor receptor in hormone-dependent breast cancer (Kenemans *et al.*, 2004). Once estrogen binds to the ERα, the activated estrogen-ERα shifts to the nucleus, and binds to estrogen response elements (ERE) in the target gene promoter (Saha Roy & Vadlamudi, 2012). When the activated estrogen-ERα binds the ERE, it interacts with coactivator proteins and components of the RNA polymerase II transcription initiation complex, and this stimulates gene transcription (Klinge, 2001). The estrogen and ERα signalling mechanism is responsible for the increased transcription of genes

1.2.3 Cyclins D_1 and E

Cyclins D_1 and E are key regulatory cyclin-dependent kinases involved in the control of transition from G_1 to S phase of the cell cycle. Cyclin D_1 gene, *CCND1*, encodes a 34 kDa protein overexpressed in 30 % - 40 % of breast cancer cases (Suter & Marcum, 2007; Kenemans *et al.*, 2004). When cyclin D_1 is overexpressed, less time is spent in G_1 phase of the cell cycle allowing more cells to enter S phase, leading to an

aggressive form of breast cancer (Suter & Marcum, 2007). Cyclin E gene encodes a 50 kDa protein that is overexpressed 64-fold in some breast cancer cell lines however, never overexpressed at the same time as cyclin D_1. Deregulation of cyclin E in breast cancer leads to phosphorylation of substrates involved in the cell cycle at the inappropriate times and results in increased S phase entry, tumorigenesis and genomic instability (Willmarth *et al.*, 2004). Taken as a whole, cyclin D_1 is upregulated by growth factors, like estrogen, and binds to CDK4/6 (Suter & Marcum, 2007). This leads to phosphorylation of pRb, release of E2F transcription factor, and cyclin E upregulation (Suter & Marcum, 2007). The cyclin E-CDK_2 holoenzyme is then formed and completely phosphorylates pRb, leading to its inactivation. E2F transcription factors are then released, and the cell cycle is initiated. Loss of pRb, the master regulator of the cell cycle, leads to the loss of cell cycle function.

1.2.4 Oncogenes

The *HER2* gene is an oncogene and its receptor is expressed on breast cancer cells, human epidermal growth factor receptor 2. The *HER2* gene, *human epithelial receptor 2*, is a 185 kDa transmembrane tyrosine kinase growth factor receptor which is overexpressed in 25 % - 30 % of breast cancer cases, and linked to poor prognosis (Suter & Marcum, 2007; Tapia *et al.*, 2007). HER2 is known to form heterodimers with HER1 and HER3, other members of the HER family, and aid in tumour formation (Suter & Marcum, 2007). These dimers are known to be involved in signal transduction in a variety of cellular pathways, such as mitogen-activated protein kinase (MAPK) and phosphatidylinositol-3 kinase (P13K) pathways, and influence cell proliferation, survival

and angiogenesis (Chan *et al*., 2006; Suter & Marcum, 2007). Given the role of the *HER2* gene in activation of cellular pathways, the overexpression of the gene in breast cancer cases and the linkage to poor prognosis, the *HER2* gene is a good focus for targeted therapy.

The *c-MYC* gene plays a role in breast cancer progression through deregulation of the cell cycle. *c-MYC* is the cellular homolog to the viral oncogene *v-MYC*, and plays an important role in proliferation and differentiation (Dang, 1999; Suter & Marcum, 2007). The *c-MYC* gene is overexpressed in 25 % - 30 % of breast cancer cases, and required for estrogen-stimulated proliferation of breast cancer cells (Kenemans *et al.*, 2004; Mukherjee & Conrad, 2005). c-MYC (MYC) is involved in cell cycle progression in breast cancer cells by activating cyclin E/Cdk_2 and inhibiting cyclin-dependent kinase inhibitor, $p21^{Cip1}$ (Xu *et al.,* 2010). The p21 family includes wafl (also known as p21, cip1 and pic1) and these proteins are important for G_1 regulation (Schafer, 1998). $p21^{Cip1}$ binds cyclins to prevent cdk from phosphorylating pRb and inducing its release from E2F transcription factors (Schafer, 1998). Inhibition of $p21^{Cip1}$ results in defects in the G_1/S checkpoint activation (Vermeulen *et al*., 2003). c-MYC plays a key role in the progression of breast cancer by inhibition of $p21^{Cip1}$, a key regulator of the cell cycle.

1.2.5 Breast Susceptibility Genes (BRCA1 and BRCA2)

BRCA1 and *BRCA2* are tumour suppressor genes that, if mutated, increase the risk of breast cancer development. The *breast susceptibility gene 1* (*BRCA1*) is located on chromosome 17q12-21 and found in 80 % of familial breast cancer cases and 5 % - 10 % of other cases (Kenemans *et al.,* 2004; Suter & Marcum, 2007). The *BRCA2* gene is

located on chromosome 13q12-13 and is functionally similar to *BRCA1*; however, it is structurally different. *BRCA1* plays an important role in transcription and apoptosis, and *BRCA2* is involved in DNA repair, cell cycle control and transcription (Kenemans *et al.*, 2004). *BRCA1* and *BRCA2* play an important role in double-stranded DNA breaks by homologous recombination, and are responsible for maintaining the integrity of the cell's genome (Narod & Salmena, 2011; Suter & Marcum, 2007). The risk of breast cancer increases with age, and the onset of the disease is much earlier for those who carry mutations in *BRCA1* or *BRCA2* (Suter & Marcum, 2007). Cells with mutations in *BRCA1* and *BRCA2* are unable to repair DNA damage, such as double stand breaks, by homologous recombination. The repair then occurs through error-prone pathways and chromosomal rearrangements result from consecutive cell divisions (Narod & Salmena, 2011). This could result in cell death, but in some cases, mutant daughter cells can produce a cell lineage with metastatic capability. Mutations in the breast susceptibility genes, *BRCA1* and *BRCA2*, result in the inability to repair DNA damage, and consequently, the possible development of a cell lineage with metastatic capability.

1.2.6 Tumour Suppressor Genes

The *retinoblastoma* gene (*RB1*) is a tumour suppressor and the master regulator of the cell cycle. It is located on chromosome 13q14.1 and found to be underexpressed in 20 % of breast cancer cases (Lerebours & Lidereau, 2002). Loss of function of *RB1* is present in one-third of sporadic breast cancer cases and is the result of chromosomal deletion, functional inactivation by cyclin A and E overexpression, transcriptional silencing and intragenic mutation (Suter & Marcum, 2007). The underexpression of *RB1*

in some breast cancer cases and the loss of function of *RB1* in sporadic breast cancer therefore, aids in the progression of breast cancer.

The *TP53* gene encodes a phosphoprotein, p53, another key regulator of the cell cycle. *TP53* is one of the most commonly mutated genes in human breast cancers and is mutated in 20 % - 40 % of breast cancer cases (Fernández-Cuesta *et al.*, 2012; Suter & Marcum, 2007; Walerych *et al.*, 2012). p53 is known as the "guardian of the genome", and its main functions include cell cycle control, DNA damage response and maintaining genomic stability (Suter & Marcum, 2007; Yang *et al.*, 2013). Other functions of p53 include DNA repair and inhibition of angiogenesis (Suter & Marcum, 2007). Mutations in *TP53* gene have been associated with chromosomal abnormalities and resistance to chemotherapeutic drugs (Walerych *et al.*, 2012). Studies have shown that there is a correlation between mutant p53 and Survivin, an anti-apoptotic splice variant. Mutant p53 increases levels of Bcl-2 which is overproduced in triple negative breast cancers (TNBCs; Walerych *et al.*, 2012). Bcl-2 is an anti-apoptotic protein which has shown to lead to the development of cancer through the inhibition of cell death (Gerl & Vaux, 2005). Mutations in the *TP53* gene are one of the most common in breast cancer and mutant p53 increases levels of Bcl-2, an anti-apoptotic protein. Therefore the mutational effects of these factors on breast cancer development are evident.

PTEN, phosphatase and tensin homolog, is a tumour suppressor gene located on chromosome 10q23. *PTEN* plays an important role in cell cycle arrest, programmed cell death, cell adhesion and migration (Suter & Marcum, 2007). PTEN negatively regulates the PI3K/Akt/mTOR signaling pathway by dephosphorylation of phosphatidylinositol 3,

4, 5-triphosphate (PIP_3), and downregulation of Akt. Downregulation of Akt leads to decreased activity of effector mTOR (mammalian target of rapamycin), cell cycle arrest at G_1 and programmed cell death. Germ-line mutations in *PTEN* are responsible for Cowden syndrome, and those female patients with Cowden syndrome are 25 % - 50 % more likely to develop breast cancer (Zhang *et al.*, 2013). Loss of PTEN leads to activation of Akt which then promotes anti-apoptotic and pro-cell cycle entry pathways (Panigrahi *et al.*, 2004). The loss of PTEN results in activation of Akt and unrestricted control of the cell cycle. Therefore, Akt could be an important focus for targeted therapy in the development of breast cancer.

1.3 Nuclear Localization and the Regulation of Tumour Suppressors' Function

The nucleus is an area of the eukaryotic cell, segregated from the cytoplasm, and an area in which proteins play a key role. The nucleus contains genetic material and transcriptional machinery, and is segregated from the cytoplasm by the double membrane of the nuclear envelope (Hoelz *et al.*, 2011). The two membranes which form the nuclear envelope are composed of a lipid bilayer, a structure formed from three classes of lipids including glycerolipids, sterols and sphingolipids (Pomorski *et al.*, 2001). Proteins play important roles in the nucleus. They are responsible for DNA repair, replication, transcription, and RNA processing and therefore, must be localized in the nucleus in order to complete their function (Marfori *et al.*, 2011; Turpin *et al.*, 1999). Translation occurs in the cytoplasm and therefore, RNA must leave the nucleus and enter the cytoplasm to be translated into protein (Hoelz *et al.,* 2011*)*. In recent years, the nuclear transport of proteins has become increasingly important in the regulation of protein

function (Thompson, 2010). The function of tumour suppressors have been altered by the change in nuclear and cytoplasmic distributions, and include the retinoblastoma tumour suppressor protein (pRb) and the Kruppel-like zinc finger 6 transcription factor (KLF6; Clements *et al.,* 2012). This altering of tumour suppressors' function by the change in nuclear and cytoplasmic distributions was shown in a study that examined the effect of cyclin-dependent kinase (Cdk) phosphorylation on nuclear localization of retinoblastoma tumour suppressor protein (pRb) in mouse embryonic fibroblasts (MEFs; Jiao *et al.*, 2006). The pRb protein is a nuclear protein that is a negative regulator of cell proliferation and is inactivated in a variety of human tumours. The pRb protein was found to be localized in the nucleus of cyclin-dependent kinase 4 wild-type ($Cdk4^{WT}$) MEFs, and localized in both the nucleus and cytoplasm of cyclin-dependent kinase 4 R24C mutant ($Cdk4^{R/R}$) MEFs. The change in subcellular localization of the pRb protein is due to the $Cdk4^{R/R}$ mutation. This mutation was generated by site-directed mutagenesis to convert arginine at position 24 to cysteine. The results revealed increased phosphorylation of pRb protein in $Cdk4^{R/R}$ cells and dispersion throughout the nucleus and cytoplasm. The cells that exhibited distributed pRb had increased growth rate and tumorigenesis. This was shown in another study which investigated the localization of KLF6 tumour suppressor. KLF6 is present in both the nucleus and cytoplasm, and is inactivated in prostate cancer (Rodríguez *et al.*, 2010; Narla *et al.*, 2005). Wild-type Kruppel-like zinc finger 6 transcription factor KLF6 (wtKLF6) decreases cell growth through p53-independent transactivation of $p21^{Cip1}$ (Narla *et al.*, 2005). However, the splice variant of KLF6, KLF6-SV_1, is predominantly localized in the cytoplasm, and promotes tumour growth, metastasis and development in prostate cancer and other human cancers

(Rodríguez *et al.*, 2010). In the cytoplasm, KLF6-SV_1 antagonizes wild-type KLF6 (wtKLF6), leading to decreased $p21^{Cip1}$ expression and increased cell growth (Narla *et al.*, 2005). These studies emphasize the importance of studying subcellular localization of tumour suppressors.

1.4 Effect of Serum on Nuclear Localization

Serum contains a high amount of growth factors, hormones, vitamins, spreading factors, transport proteins and other components. Spreading factors are attachment promoting molecules and include serum spreading factor as shown in Appendix 1 (Reilly & Nash, 1988; Brunner *et al.*, 2010). Transport proteins are responsible for transport, such as transferrin and the transport of iron to cells and tissues (Zhang *et al.*, 2007). The other components of serum are shown in Appendix 1, and include epidermal growth factor, fibroblast growth factor and insulin, to name a few. The presence of these factors have been shown to have an effect on subcellular localization of proteins. This was shown when the effect of calf serum on p27 localization was investigated (Lewis *et al.*, 2004). p27 belongs to a family of KIP cyclin dependent kinase inhibitors, $p27^{Kip1}$ that inhibit cyclin D and cyclin E activated kinases (Ellis *et al.,* 1999). In quiescent rat thyroid cells, $p27^{Kip1}$ is located in the nucleus, however, treatment with 5 % calf serum decreased nuclear localization of $p27^{Kip1}$ in quiescent Wistar rat thyroid cells (WRT). To confirm calf serum was responsible for nuclear export of $p27^{Kip1}$, quiescent WRT cells were treated for 60 minutes with leptomycin B, an inhibitor of nuclear export. The cells were then treated with calf serum for 24 hours and subjected to immunostaining. The results showed that the percentage of cells showing nuclear staining of $p27^{Kip1}$ in the presence of

leptomycin was 61 %, compared to only 18 % in the absence of leptomycin B (Lewis *et al.*, 2004). Another example of the effect of serum on localization is a study that investigated the localization of myocardin related serum response factor (SRF) coactivator MAL (Miralles *et al.*, 2003). In serum starved NIH3T3 cells, MAL exhibits diffuse cytoplasmic staining however, after just 10 minutes treatment with serum, MAL becomes predominantly nuclear. Growth factors in serum were also shown to have an effect on nuclear localization of proteins, and this was shown in a study that investigated the effect of growth factors on nuclear translocation of MAP kinase, ERK ($p44^{MAPK}$), in CCL39 fibroblasts (Lenormand *et al.*, 1993). In G_0 arrested CCL39 cells, ERK ($p44^{MAPK}$) is localized in the cytoplasmic region however, treatment for 180 minutes with 10 U/mL α thrombin induced G_0/G_1 nuclear translocation of ERK ($p44^{MAPK}$). Serum contains several components that could be responsible for the change in subcellular localization of the proteins discussed above.

1.4.1 Insulin and Insulin-like growth factor 1

Insulin and insulin-like growth factor are both components of serum as shown in Appendix 1. Insulin and insulin-like growth factors (IGF-1 and IGF-2) belong to a family of receptor tyrosine kinases (RTKs), and IGF-1 plays important roles in cell processes including cell proliferation, differentiation and inhibition of apoptosis (Kaplan *et al.*, 2005; Lamothe *et al.*, 1998). Insulin-like growth factor 1 (IGF-I) is a 70 amino acid peptide, and a member of the family of insulin related peptides (Laron, 2001). Insulin is an exogenous growth factor that promotes cell growth of many cell types *in vitro*, with

only a few nanograms/mL needed to be effective (Hunt *et al.*, 1997). It has been shown that insulin receptor content is six times higher in human breast cancer specimens than normal breast tissue (Milazzo *et al.*, 1992). MCF7 cells express insulin receptors significantly higher than non-malignant transformed breast cells, and exhibit increased insulin binding capacity. In MCF7 cells, insulin stimulates insulin receptor tyrosine kinase activity, and initiates a mitogenic effect via the insulin receptors and IGF-1 receptors (IGF-1R; Milazzo *et al.*, 1992). Studies have shown that both insulin and IGF-1 have an effect on nuclear localization of proteins. This was shown in a study which investigated the localization of cyclin D_1 in MCF-7S cells after IGF-1 stimulation (Hamelers *et al.*, 2002). Cyclin D_1 is perinuclear in serum-starved cells however, after treatment with 20 ng/mL IGF-1 for 16 hours, cyclin D_1 localization is 94 % nuclear. In another study, the localization of protein kinase C isoform, PKCδ protein, in L_6 sketal muscle cells was investigated (Horovitz-Fried *et al.,* 2008). The results showed that stimulation with 10^{-7} M insulin for 5 minutes increased nuclear and cytoplasmic localizations of PKCδ. To further confirm the observed role of insulin on nuclear localization, cells were treated with an inhibitor of nuclear import, wheat germ agglutinin (WGA), before insulin stimulation. The results showed that blockage of nuclear import had no effect on insulin-induced nuclear localization of PKCδ. These studies suggest a potential role of insulin on subcellular localization of proteins.

1.5 Mesoderm Induction Early Response 1 (MIER1)

Mesoderm induction early response 1 (*MIER1)* gene is located on human chromosome 1p31.2 and encodes a nuclear protein that functions as a transcriptional regulator. *MIER1* was first discovered as a fibroblast growth factor early response gene from *Xenopus* embryonic cells (Paterno, 1997). A human orthologue of *xmier1*, human *MIER1* (*hMIER1*), was cloned using a testes cDNA library and is highly conserved in evolutionarily with 95 % identity between human and mouse sequences (Clements *et al.,* 2012). Research revealed the structure and protein isoforms of human *MIER1* gene through its role as a transcriptional regulator and its involvement in embryonic development (Paterno *et al*., 2002). The structure of the human *MIER1* gene and its protein isoforms will be discussed in the following sections.

1.5.1 *MIER1* Gene and Protein Isoforms

Mesoderm induction early response 1 (*MIER1*) gene is 63 kb, contains 17 exons and encodes four functionally distinct proteins. The four distinct proteins arise through exon skipping, facultative intron usage, alternative polyadenylation sites and the use of two alternate promoters, P1 and P2 (Paterno *et al.*, 2002). The encoded proteins contain a common internal sequence with variable amino (N-) and carboxy (C-) termini. The two C-termini are the α C-terminus and the β C-terminus.

Two C-termini result from alternate use of a facultative intron, intron 15. The α C-terminus has 23 amino acids, arises from removal of facultative intron 15 and contains a LXXLL motif for interaction with nuclear hormone receptors (Clements *et al.,* 2012). The β C-terminus has 102 amino acids, arises from inclusion of intron 15 and includes a

nuclear localization signal (NLS; Paterno *et al*., 2002; Post *et al.*, 2001). The two C-termini differ in size and sequence and, the β C-terminus possesses a NLS.

Two functionally distinct N-termini are generated by alternate promoter usage and splicing. N-termini, named N2 and N3, result from transcriptional start at P1 and P2 promoters respectively (Clements *et al*., 2012). They are identical except for the first two amino acids after the start methionine and have no detectable difference in function or activity. A second functionally distinct N-terminal isoform results from transcriptional start at the P1 promoter and includes sequence from exon 3A. This results in N1, a variant with additional sequence at its N-terminus that includes a nuclear export sequence (Clements *et al*., 2012). The alternate use of two promoters and the inclusion of sequence from exon 3A produces two functional different N-termini.

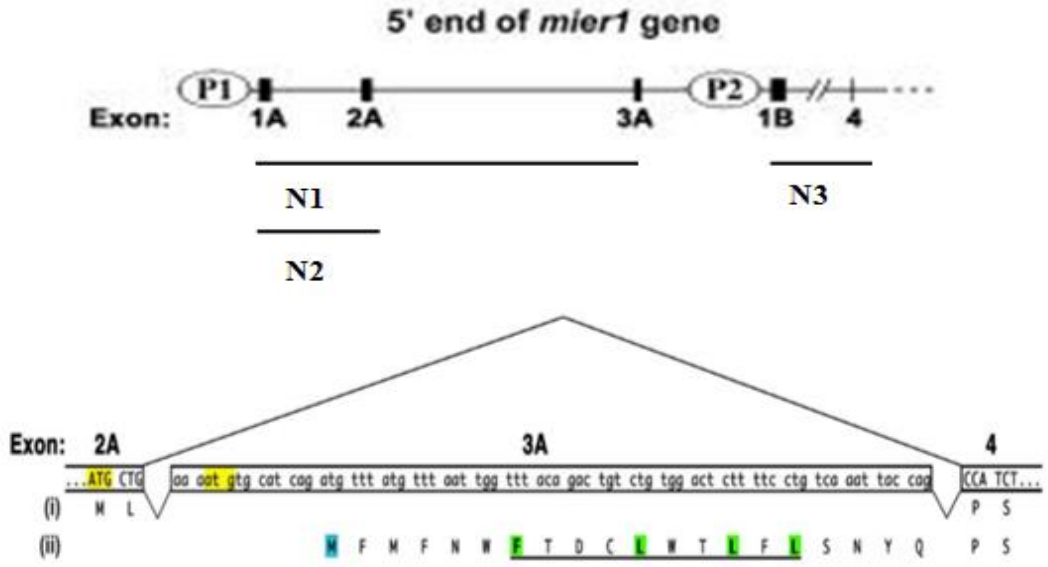

Figure 1.3: 5' end of the *MIER1* gene and the amino acid sequence encoded by exon 3A

The top image of this figure illustrates the two alternate transcriptional start sites for both *MIER1* promoters, P1 and P2. Transcriptional start at P1 and P2 result in N2 and N3, which are identical except for the first two amino acids after the start methionine. N1 also results from transcriptional start at P1 but includes the amino acid sequence from exon 3A, MFMFNWFTDCLWTLFLSNYQ, which is shown in the bottom image (adapted from Clements *et al.,* 2012).

1.5.2 MIER1 Domains

Close examination of the human MIER1 (hMIER1) protein structure led to the identification of several conserved domains. These domains are found in the common internal region and are important for regulating transcription (Paterno *et al.*, 2002). These include the acidic activation domain, the ELM2 domain, of EGL-27 and MTA1 homology, the SANT domain, with homology to the DNA binding domain c-myb, and the proline-rich domain.

1.5.2.1 Acidic Activation Domain

Located in the N-terminus of MIER1 is the acidic activation domain. When fused to GAL4 DNA binding domain, the acidic activation domain was shown to activate transcription and first led to the belief that MIER1 was a transcriptional activator (Paterno, 1997). However, further studies have revealed that MIER1 also acts as a transcriptional repressor through the SANT and ELM2 domains, as described below.

1.5.2.2 ELM2 Domain

The ELM2 domain is located downstream from the acidic activation domain, and plays an important role in transcriptional regulation. The ELM2 domain is of EGL-27, *Caenorhabditis elegans* protein, and MTA1, a metastasis-associated protein 1, homology (Ding *et al.,* 2003; Millard *et al.,* 2013). Most ELM2 containing proteins have a SANT domain, such as MIER1 and MTA1, with the latter having a functional relationship between the two (Millard *et al.*, 2013). In the first study to determine a functional role of

the ELM2 domain, it was determined that through this domain both hMIER1α and hMIER1β recruit HDAC1 and repress transcription (Ding *et al*., 2003). Class 1 histone deacetylases (HDAC1) are a class of enzymes that remove acetyl groups from lysine residues in histone tails, and these HDAC1s are recruited to transcriptional repression complexes resulting in a more condensed chromatin structure and repression of gene transcription (Millard *et al*., 2013). The results showed that both hMIER1α and β repress transcription in a dose-dependent manner (Ding *et al.*, 2003). Further analysis illustrated that both hMIER1α and hMIER1β physically associate with HDAC1 *in vivo* and repress transcription. Another study investigated the ability of MIER1 to interact with Creb-binding protein (CBP) and regulate its histone acetyltransferase activity (HAT; Blackmore *et al., 2008*). It was determined that the N-terminal half, consisting of the acidic activation and ELM2 domains of MIER1, was able to bind to CBP (Blackmore *et al.*, 2008). The functional significance of the MIER1-CBP binding concluded that cells transfected with CBP alone produced high levels of HAT activity however, those transfected with MIER1β produced no measurable levels of HAT activity (Blackmore *et al*., 2008). This study illustrated a method by which MIER1 can repress transcription.

1.5.2.3 SANT Domain

Located downstream from the ELM2 domain is the SANT domain. The SANT domain has been identified in histone-modifying enzymatic complexes and based on its homology to the DNA binding domain c-myb (Badri *et al*., 2008; Boyer *et al*., 2002). This domain is the most conserved and a hallmark of chromatin remodelling complexes,

protein-protein interactions and DNA binding, and is found in Swi3, Ada2, the co-repressor NCoR, TFIIIB, and ISWI (Sterner *et al.*, 2002). The SANT domain was found to repress transcription by interfering with the binding of transcription factor (Sp1) to its respective binding site on *hMIER1* promoter (Ding *et al.*, 2004). This domain, as well as the ELM2 domain, highlights the role of MIER1 as a transcriptional repressor.

1.5.2.4 LXXLL Motif

The C-terminus of MIER1α contains a LXXLL motif, not found in MIER1β. This motif can interact with nuclear hormone receptors (Paterno *et al.*, 2002). The ability of MIER1α to interact with estrogen receptor-α (ERα) was investigated and the results revealed that MIER1α interacted with ERα both in the presence and absence of E2 ligand (McCarthy *et al.*, 2008). MIER1α interacts with the ERα *in vivo* and decreases growth of T47D breast carcinoma cells in the presence of oestrogen. The LXXLL motif allowed MIER1α to interact with ERα and decrease growth of T47D cells.

1.5.2.5 Proline-rich Region

Located in the C-terminus of MIER1 is the proline-rich region. This region confirms to the consensus SH3 binding domains, Src homology 3 domains, which are protein modules often found in intracellular signalling proteins (Teplitsky *et al.*, 2003; Yu *et al.*, 1994). One study focused on the effects of *xmier1,* a gene from *Xenopus laevis,* on *Xenopus* embryonic development and the importance of functional domains in the protein sequence (Teplitsky *et al.*, 2003). The effects of xmier1 overexpression on *Xenopus* embryonic development was examined, and the results revealed deficiencies in both anterior and

posterior structures. Furthermore, the effects of xmier1 overexpression on mesoderm induction were investigated, and the results revealed xmier1 inhibited mesoderm induction when compared to the control. The region of xmier1 responsible for the effects on *Xenopus* development was determined. Embryos were injected with control, wild-type xmier1, or mutant constructs, and mutation of the proline-rich region resulted in a percentage of abnormal embryos similar to that of the control. To determine if the proline or serine was the critical residue, the mutated residues were injected into embryos. The results revealed that mutated ^{365}P eliminated the effects of xmier1 on development and mutated ^{366}S had no effect on xmier1. Therefore, it was determined that ^{365}P is the critical residue responsible for the developmental effects of xmier1 (Teplitsky *et al.*, 2003). Lastly, the effect of ^{365}P mutant on mesoderm induction was investigated and the results showed that ^{365}P mutant had no effect on mesoderm induction when compared to the H_2O-injected controls, and confirmed that ^{365}P is the critical residue for embryonic development and mesoderm induction (Teplitsky *et al.*, 2003). The proline-rich region is the domain responsible for embryonic development and mesoderm induction.

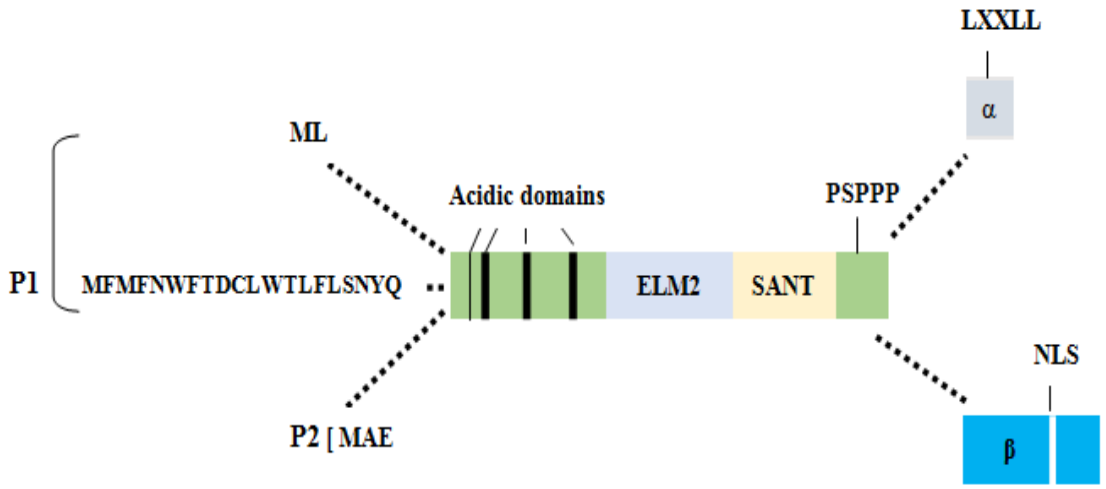

Figure 1.4: The Functional Domains of the MIER1 Protein

This figure, from Gillespie and Paterno, 2012 shows the functional domains of MIER1, described above, and their location. The two C-terminal domains, α and β, and the two alternate promoters, P1 and P2 are indicated. Reprinted and adapted from MIER1 (mesoderm induction early response 1 homolog (Xenopus laevis)). Gillespie LL, Paterno GD. Atlas Genet Cytogenet Oncol Haematol. 2012; 16(2):127-130. (http://atlasgeneticsoncology.org//Genes/MIER1ID50389ch1p31.html) by permission of the Atlas.

1.5.3 Subcellular Localization of MIER1

In a previous study by McCarthy *et al.* (2008), the subcellular localization of MIER1α in normal tissue samples and tumour samples was examined. Normal tissue and hyperplasia showed 74.7 % and 76.5 % nuclear MIER1α staining respectively, compared to 50.7 % in ductal carcinoma *in situ* (DCIS), 25.3 % in invasive lobular carcinoma (ILC) and only 4.4 % in invasive ductal carcinoma (McCarthy *et al*., 2008). The change in subcellular localization of MIER1α from normal breast tissue to invasive breast carcinoma, indicates a potential role of MIER1α in breast cancer progression.

A more recent study by Clements *et al*. (2012), examined whether differential splicing in MIER1α to produce MIER1-3Aα altered subcellular localization. MIER1-3Aα is the third N-terminal isoform and arises from inclusion of cassette exon, exon 3A, which contains a leucine rich nuclear export signal. The results showed 81 % of cells exhibited nuclear staining of MIER1α, and the remainder showed whole cell staining (Clements *et al.,* 2012). MIER1-3Aα expressing cells showed staining was 66 % cytoplasmic and 32 % whole cell. In comparison to MIER1α cells, MIER1-3Aα cells showed no staining that was nuclear. MIER1β contains a NLS and is predominantly nuclear in most cells. Therefore, this study examined whether the inclusion of exon 3A would change the nuclear localization of MIER1β. Inclusion of exon 3A to produce MIER1-3Aβ did not alter subcellular localization, 80% of the cells showed nuclear staining and none were exclusively cytoplasmic. This study revealed that inclusion of exon 3A affects nuclear localization of MIER1α.

1.6 The objectives of this study

The breast cancer cells lines, MCF7 and T47D, were used because they are both estrogen receptor (ER) positive cell lines, and MCF7 cells are useful for breast cancer studies because the cell line has retained many characteristics of differentiated mammary epithelium. In MCF7 cells, MIER1α is transiently expressed and therefore, only some of the cells will express the gene. The T47D cell line is stably transfected with MIER1α therefore, all cells should express the gene because it becomes integrated into the cell genome and can be replicated (Smith, 2013). The T47D cell line was used because theoretically all cells would be expressing MIER1α rather than a proportion of cells, and no stable Tet-ON MCF7 cell line was available. Therefore, the stably transfected T47D cell was used.

MIER1α interacts with ERα *in vivo* and decreases anchorage-independent growth of T47D breast carcinoma cells (McCarthy *et al.,* 2008). Colony formation in soft agar is a hallmark of transformation and the measurement of anchorage-independent growth (Fukazawa *et al.*, 2002). Anchorage-independent growth is the ability of cells to survive and proliferate without attachment to substratum (Fukazawa *et al.*, 1995). Therefore, it was suggested that MIER1α may play a role in breast carcinoma proliferation. Cell proliferation is a different type of measurement and measures the increase in cell number when cells are attached to the tissue culture dish. It was also determined that the subcellular localization of MIER1α changes with breast cancer progression from predominantly nuclear in normal breast tissue, to predominantly cytoplasmic in invasive breast carcinoma. This suggested that loss of nuclear MIER1α might contribute to breast

cancer progression. This change in MIER1α nuclear localization to cytoplasmic localization in invasive breast carcinoma could affect the ability of MIER1α to apply its gene/chromatin repressor functions (McCarthy *et al.*, 2008). Therefore, it was hypothesized that MIER1α might affect cell proliferation and/or survival of breast cancer cell lines, MCF7 and T47D.

The localization of MIER1α in MCF7 cells is predominantly nuclear as determined by confocal microscopy and shown in studies by Li *et al.* (2013) and Clements *et al.* (2012). Inclusion of exon 3A in MIER1α, to produce MIER1-3Aα, changes its subcellular localization from nuclear to cytoplasmic (Clements *et al.*, 2012). Previous work has revealed that the percentage of cells with nuclear MIER1α is different in MCF7 cells and T47D cells at 78.9 % and 9.2 %, respectively. MCF7 cells are cultured in DMEM medium supplemented with newborn calf serum (NBCS) and fetal bovine serum (FBS), and T47D cells are cultured in RPMI medium supplemented with Tet-approved fetal bovine serum. Tet-FBS is used in Tet-on/Tet-off systems and this FBS is charcoal-stripped and therefore, contains lower levels of steroid, thyroid and peptide hormones, in particular estradiol and insulin (Cao *et al.,* 2009). Thus, it was hypothesized that factors in serum may have an effect on MIER1α localization in MCF7 and T47D cells. For this study, confocal microscopy was not used to determine localization of MIER1 isoforms in MCF7 and T47D cells, immunocytochemistry (ICC) was used. Therefore, for the purposes of this study, the words "appear" or "appeared" will be used when referring to the localization of MIER1 isoforms. To successfully complete this study, the following objectives were explored.

Objective 1: Determine if MIER1α has an effect on proliferation of breast carcinoma cell lines.

Objective 2: To determine if factors in serum effect localization of MIER1 isoforms, MIER1α and MIER1-3Aα, in MCF7 cells, and MIER1α in T47D cells.

Objective 3: Determine if MIER1 isoforms, MIER1α and MIER1-3Aα, localization changes in MCF7 cells in different types of serum.

Objective 4: Determine the effect of insulin on MIER1α localization in MCF7 cells.

Chapter 2- Materials and Methods

2.1 Cell culture

2.1.1 Cell Lines

Human breast adenocarcinoma cells (MCF7) were cultured in Dulbecco's Modified Eagle Medium (DMEM) (Life Technologies, Grand Island, NY, 11965092) supplemented with 10 % serum [2.5 % fetal bovine serum (FBS) (Life Technologies, Grand Island, NY, 12483020) and 7.5 % newborn calf serum (NBCS) (Life Technologies, Grand Island, NY, 16010142)], 1 % sodium pyruvate (Life Technologies, Grand Island, NY, 11360070) and 0.5 % penicillin/streptomycin (Life Technologies, Carlsbad, CA, 15140122). The T47D Tet-On cell line was cultured in RPMI-1640 medium (Life Technologies, Grand Island, NY, 11875093) supplemented with 10 % serum [10 % Tet-approved FBS (Life Technologies, Grand Island, NY, 26140079)], 1 M HEPES (Life Technologies, Grand Island, NY, 15630080), 0.8 % hygromycin B (Life Technologies, Carlsbad, CA, 10687010) and 0.16 % geneticin (G418) (Life Technologies, Carlsbad, CA, 11811031).

For experiments in which I varied serum concentration, MCF7 cells were cultured in DMEM + 10 % serum, as described above and in DMEM supplemented with 0.2 % serum (0.05 % FBS and 0.15 % NBCS), 1 % sodium pyruvate and 0.5 % penicillin/streptomycin at 37 ˚C in 5 % CO_2. For experimental procedures, T47D cells were cultured in RPMI + 10 % serum, as described above and also in RPMI-1640

medium supplemented with 0.2 % serum (0.2 % Tet-approved FBS), 1 M HEPES, 0.8 % hygromycin B and 0.16 % G418.

To determine if Tet-approved FBS had an effect on localization of MIER1 isoforms in MCF7 cells, cells were cultured in DMEM supplemented with 10 % serum (10 % Tet- approved FBS), 1 % sodium pyruvate and 0.5 % penicillin/streptomycin at 37 ˚C in 5 % CO_2. To determine if insulin has an effect on nuclear localization of MIER1α in MCF7 cells, cells were cultured in DMEM supplemented with 10 % serum (2.5 % FBS and 7.5 % NBCS), 1 % sodium pyruvate, 0.5 % penicillin/streptomycin and 4 ug/mL of insulin (Life Technologies, Carlsbad, CA, 12585014). A description of the Media used are shown in Table 2.1

Cells were cultured in 100 mm plates (Corning, Corning, NY, 0877222) containing 10 mL of respective medium and incubated at 37 °C containing 5 % CO_2. The cells were sub-cultured when they reached approximately 80 % confluence by aspirating the media from the 100 mm cell culture plate. Next, the cells were washed with 10 mL 1 x PBS (Sigma Aldrich, St. Louis, MO, P3813), aspirated and replaced with 1.5 mL of 0.025 % trypsin (Life Technologies, Carlsbad, CA, 15090046) containing [ethylenediaminetetraacetic acid (EDTA); pH 8.0 (Thermo Fisher Scientific BP120-500)] in 1 x PBS to promote detachment of the cells. Once the cells were detached from the plate, 1.5 mL of media was added and the cells were pipetted multiple times up and down to resuspend the cells. From this plate, 1 mL of cell suspension was added to three 100 mm cell culture plates already containing 10 mL of media for a 1:3 cultivation ratio.

Table 2.1: The Cell Culture Media used for these Experiments

Media	Description	Collection	Components
Fetal Bovine Serum (FBS)	Shows strong activity and therefore, most frequently used serum in cell culture (Ferruzza *et al.*, 2013)	Harvested from bovine fetuses by means of cardiac puncture (Brunner *et al.,* 2010)	Transport proteins, hormones, and growth factors such as, insulin-like growth factor, fibroblast growth factor and epidermal like growth factor, to name a few (Brunner *et al.*, 2010)
Newborn Calf Serum (NBCS)	-Another animal sera commonly used in cell culture media -NBCS is often used as an alternative to FBS (Sera for Cell Culture, n.d.)	Harvested from 3 to 10 day old calves (Sera for Cell Culture, n.d.)	Contains a higher number of proteins and immunoglobins than FBS but a lower number of growth factors (Sera for Cell Culture, n.d.)
Tet-FBS	Another type of FBS used in Tet-on/Tet-off systems and this FBS is charcoal-stripped (Cao *et al.,* 2009)	N/A	Contains lower levels of steroid, thyroid and peptide hormones, in particular estradiol and insulin (Cao *et al.,* 2009)

2.2 Plasmids

2.2.1 Plasmid Constructs

pCS3+MT, pCS3+MT*MIER1*α, pCS3+*MTMIER1-3Aα*

pCS3+MT is a myc-tagged control plasmid and was a kind gift from Dr. David Turner. Human *MIER1α* and *MIER1-3Aα* were cloned into the pCS3+MT vector by Corinne Mercer. The plasmids pCS3+MT and pCS+MT*MIER1*α were used for the studies on cell proliferation in MCF7 cells. Secondly, the plasmids, pCS3+MT, pCS3+MT*MIER1*α, pCS3+MT*MIER1-3Aα*, were used to determine the effect of factors of serum on localization of MIER1 isoforms in MCF7 cells. Lastly, pCS3+MT and pCS3+MT*MIER1*α plasmids were used to determine the effect of insulin on nuclear localization of MIER1α in MCF7 cells.

2.3 Electroporation

To determine the effect of MIER1α on cell proliferation, the effect of factors of serum on localization of MIER1 isoforms, and the effect of insulin on nuclear localization of MIER1α in the MCF7 human breast adenocarcinoma cell line, pCS3+MT-tagged control, pCS3+MT*MIER1*α (MIER1α) and pCS3+MT*MIER1-3Aα* (MIER1-3Aα) plasmids were transfected into MCF7 cells. MCF7 cells were detached from the plate using trypsin, resuspended in media, counted, and centrifuged for 4 minutes. Following centrifugation, the media was aspirated from the cellular pellet and the cells were resuspended in an equal volume of 1 x PBS. The cells were then centrifuged for an additional 4 mins and resuspended in Resuspension Buffer R (Life Technologies,

Carlsbad, CA, MPK1096) for $3x10^5$cells/10 uL. The electroporation tube was filled with 3 mL of Electrolytic Buffer (Life Technologies, Carlsbad, CA, MPK1096) and the tube was placed into the station to get the system ready for use.

In three 1.7 mL microcentrifuge tubes (Thermo Fisher Scientific, Fair Lawn, NJ, 07200535), the correct volume of each plasmid (pCS3+MT-tagged control, pCS3+MT*MIER1*α and pCS3+MT*MIER1-3A*α) was added (0.5 ug of plasmid DNA per well of a 12-well plate). The appropriate volume of cell suspension ($3x10^5$cells/10 uL for each 0.5 ug of plasmid) was added to each tube and mixed gently with the pipette tip. The electroporation pipette tip was then inserted onto the pipette by pressing down on the pipette button until the clamp picked up the mount of the pipette tip. Then, pushed down on the pipette button and immersed the tip in the cell-DNA mixture, slowing releasing the push button to prevent bubbles which can lead to incorrect transfection. The pipette was then inserted in the electroporation device and the start button pressed to begin the electroporation protocol. The optimal electroporation conditions used for the plasmid constructs in MCF7 cells are shown in Table 2.2. Following the electric pulse, the pipette was slowly removed from the tube and the cell suspension transferred to the appropriate well in the 12-well plate. Following electroporation, cells were cultured in a 12-well plate containing DMEM supplemented with 10 % serum (2.5 % FBS and 7.5 % NBCS) and 1 % sodium pyruvate. The 12-well plate was then gently rocked to evenly distribute the cells and the plate placed at 37 °C in a 5 % CO_2 incubator for 24 hours.

Table 2.2: Electroporation Conditions for the Plasmid Constructs in MCF7 Cells

Plasmids	Pulse Voltage	Pulse Width	Number of Pulses
pCS3+MT	1000	30	2
pCS3+MT*MIER1α*	1000	30	2
pCS3+MT*MIER1-3Aα*	950	40	2

2.4 Stably Transfected T47D Cell Clones and Doxycycline Induction

The human ductal mammary carcinoma T47D Tet-On cell line was purchased from Clontech (Palo Alto, CA, 630923). Establishment of MIER1α stably transfected Tet-On T47D cell line which expresses MIER1α, was achieved as described by Ding *et al.* (2004). Control cell lines (TDc21) were transfected with the pTRE2 empty vector and stable clones (TDα5) were generated using the *hMIER1*α coding region inserted into the pTRE2 vector (Ding *et al.*, 2004).

2.5 CellTiter 96® Aqueous One Cell Proliferation Assay

To investigate the effect of MIER1α on MCF7 cells, non-transfected cells, cells transfected with pCS3+MT tagged control (denoted pCS3+MT), and pCS3+MT*MIER1*α (denoted MIER1α) or mock transfected cells, were incubated for 24 hrs in DMEM medium without antibiotics. Following 24 hrs, transfected cells were resuspended and seeded as triplicates at a density of 6500 cells/100 uL per well in two 96-well plates (Corning, Corning NY, 3599) in DMEM medium. Immediately after one plate was seeded, 20 uL of CellTiter 96® Aqueous One Solution (Promega, Madison, WI, PRG3580) was added to each well containing 100 uL of medium, incubated for 3 hrs at

37 °C, and read at 492 nm to obtain baseline values. Ninety-six hours after transfection, the second 96-well plate was removed from the incubator and 20 uL of CellTiter 96® Aqueous One Solution was added to each well containing 100 uL of medium, incubated for 3 hrs at 37 °C, and read at 492 nm. A separate 96-well plate was seeded into triplicate wells, with cell dilutions ranging from 0 to 20,000 cells/100 uL of MCF7 cells in order to create a standard curve. This plate was incubated for 3 hrs at 37 °C in order to generate a standard curve between cell number and absorbance at 492 nm. Following incubation, the plates were read on a microplate reader (POLARstar OPTIMA; BMG Labtechnologies Inc., Durham, NC) at 492 nm. To determine transfection efficiency, an 8-well chamber slide (BD Biosciences, Bedford, MA, 354118) was seeded with 50,000 cells/200 uL per well of non-transfected cells, cells transfected with pCS3+MT tagged control, and pCS3+MT*MIER1*α or mock transfected cells. Ninety-six hours following transfection, cells were fixed using 4 % paraformaldehyde (pH 7.2; Thermo Fisher Scientific, Fair Lawn, NJ, T353500) and analyzed using immunocytochemistry (ICC) with an anti-myc tag antibody (as described later in section 2.6). The anti-myc tag antibody was prepared from supernatant from 9E10 cells supplemented with 1 % Opti-Mab monoclonal antibody production enhancer (Blackmore *et al.*, 2008). To confirm protein expression of MIER1α, a twenty-four well plate (Corning, Corning, NY, 3526) was also seeded with 40,000 cells/500 uL per well of non-transfected cells, cells transfected with pCS3+MT tagged control, and pCS3+MT*MIER1*α or mock transfected cells, and incubated for 96 hrs after transfection. Protein extraction was performed by adding 40 uL of sodium dodecyl sulfate (SDS) sample buffer (1 x SSB: 2.5 mL stacking gel buffer of pH 6.8, 2.5 mL 20 % SDS, 1.25 mL β-mercaptoethanol (β-ME), 2.5 mL glycerol, 3.75 mL H_2O, and crystals of

bromophenol blue) to each well and expression of myc-tagged MIER1α was confirmed by Western blot (procedure described in section 2.8), of whole cell lysates using an anti-myc tag antibody.

To investigate the effect of MIER1α on T47D cells, TDα5 and TDc21 were induced or not induced with 1 ug/mL doxycycline (Clontech, Mountain View, CA, 631311) for 48 hrs, then cells were resuspended and seeded in triplicate wells at a density of 10,000 cells/100 uL per well in two 96-well plates in RPMI media + and - dox 1 ug/mL dox. Immediately after one plate was seeded, 20 uL of CellTiter 96® Aqueous One Solution was added to each well containing 100 uL of medium, incubated for 3 hrs at 37 °C, and read at 492 nm to obtain baseline values. Five days after the start of dox induction, the second 96-well plate was removed from the incubator and 20 uL of CellTiter 96® Aqueous One Solution was added to each well containing 100 uL of medium, incubated for 3 hrs at 37 °C, and read at 492 nm. Separate 96-well plates were seeded into triplicate wells, with cell dilutions ranging from 0 to 80,000 cells/100 uL per well of T47D cells in order to create standard curves. The 96-well plates were incubated for 3 hrs at 37 °C in order to generate a standard curve between cell number and absorbance at 492 nm. Following incubation, the plates were read on the POLARstar OPTIMA microplate reader at 492 nm. The absorbance value generated for each well was directly proportional to the number of live cells. To determine the percentage of cells expressing, an 8-well chamber slide was seeded with 20,000 cells/200 uL per well of TDα5 cells (+ and - dox) and TDc21 cells (+ and - dox). Five days after the start of dox induction, cells were fixed using 4 % paraformaldehyde (pH 7.2) and analyzed using ICC

(as described later in section 2.6) with an anti-myc tag antibody. To confirm protein expression of MIER1α a 24-well plate was also seeded with 40,000 cells/500 uL per well of MIER1α expressing cells (+ and - dox) and control T47D cells (+ and - dox) for 5 days after the start of dox induction. Protein extraction was performed by adding 40 uL of 1 x SSB to each well and expression of myc-tagged MIER1α was confirmed by Western blot (procedure described in section 2.8), of whole cell lysates using an anti-myc tag antibody.

2.6 Immunocytochemistry

In order to determine the transfection efficiency of MIER1α in MCF7 cells, and the percentage of cells expressing MIER1α in T47D cells, cells were seeded in 8-well chamber slides at a density of $5x10^4$ cells/200 uL per well and $2x10^4$cells/200 uL per well, respectively. These chamber slides were incubated for 96 hrs after transfection in MCF7 cells and for 5 days after the start of doxycycline induction in T47D cells. To determine if factors of serum have an effect on localization of MIER1 isoforms in MCF7, and MIER1α in T47D cells, these cells were seeded in 8-well chamber slides at a density of $5x10^4$ cells/200 uL per well and incubated for 72 and 96 hrs after transfection and 3, 4 and 5 days after the start of doxycycline induction, respectively. To determine if insulin has an effect on nuclear localization of MIER1α in MCF7 cells, cells were seeded in 8-well chamber slides at a density of $2x10^4$cells/200 uL per well and incubated for 28 hrs after transfection. After the required incubation periods, the slides were removed from the incubator and washed in 250 mL of 1 x PBS. This was aspirated, and the slides were fixed by adding 200 uL of 4 % parafomaldehyde (pH 7.2) to each well for 10 mins in a humidified container to prevent the slides from drying out. Following fixation, the slides

were washed in 1 x PBS, then permeabilized with 0.1 % Triton (Sigma Aldrich, St. Louis, MO, T8787) in 1 x PBS for 5 mins. After incubation, the 0.1 % Triton in 1 x PBS was aspirated and 200 uL of 5 % sheep serum (Sigma Aldrich, St. Louis, MO, S3772) in 1 x PBS blocking buffer was added to each well for 1 hr incubation. After incubation, the cells were washed in 1 x PBS and 200 uL of 0.6 % hydrogen peroxide in 1 x PBS added to each well for 30 mins. Following incubation, the cells were washed again in 1 x PBS and primary antibody was added to each well. The primary antibody used was monoclonal anti-myc tag antibody at 1:200 dilution in 3 % BSA/1 x PBS (Bovine Serum Albumin, RIA grade powder #A-7888-10g; Sigma Aldrich, St. Louis, MO) at a final volume of 200 uL. The primary antibody was incubated overnight on the slides at 4 ˚C. The following day, the primary antibody was aspirated, the slide was washed in 0.1 % Triton in 1 x PBS, and incubated in 250 mL beaker of 1 x PBS for 5 mins. Then, 200 uL of sheep-anti-mouse horseradish-peroxidase (SAM-HRP; GE Healthcare, Little Chalfont, Buckinghamshire, UK, NA931V) antibody in 3 % BSA/1 x PBS was added to each well for 1 hr. After incubation, the cells were washed in 0.1 % Triton in 1 x PBS then incubated in 1 x PBS for 5 minutes. The 1 x PBS was aspirated, 200 uL of 3,3-diaminobenzidine (DAB; Sigma Aldrich, St. Louis, MO, D4168-50) diluted in de-ionized water (1 silver and 1 gold tablet per 1 mL of water) was added to each well and incubated for 30 mins. This reaction results in a brownish product which can be visualized under the microscope. After the 30 mins, the DAB was aspirated, the cells washed in 1 x PBS for 5 mins and the gasket removed very carefully. Once the gasket was removed, any remaining PBS was aspirated from the slide and 50 uL of 10 % glycerol in 1 x PBS was added to each well. A cover slide was then placed on the slide, and the slide tilted to

remove any excess glycerol remaining. The slide was sealed with clear nail polish and left to dry. Once dried, the staining was viewed using Olympus BH-2 microscope (Carsen) and photo micrographs were obtained in both phase-contrast and bright field using CoolSnap camera software. Slides were kept in a dark box at 4 °C to prevent degradation of staining.

2.7 Cell Lysis & Protein Extraction

For the studies investigating the effect of MIER1α on MCF7 and T47D cells, 96 hrs after transfection and 5 days after the start of dox induction respectively, the 24-well plates were removed from the incubator, placed on ice, and the cell culture media aspirated from each well. The cells were washed with 1 mL of 1 x PBS and following aspiration of the 1 x PBS, protein extraction was performed by adding 40 uL of 1 x SSB to each well. The cells were then scraped from each well using a yellow pipette tip, the lysate pipetted up and down to break up the cell pellet, and collected in 1.7 mL microcentrifuge tubes to be analyzed. Each sample was stored at -20 °C. The cell extracts were collected as described previously for Western blot analysis, and used to confirm protein expression of MIER1α and MIER1-3Aα in MCF7 cells, and MIER1α in T47D cells respectively.

For the effect of factors in serum on localization of MIER1 isoforms, MIER1α and MIER1-3Aα, in MCF7 cells, and MIER1α in T47D cells, 72 and 96 hrs after transfection and 3, 4 and 5 days after the start of doxycycline induction respectively, the 24-well plates containing cells were removed from the incubator, placed on ice, and the

cell culture media aspirated from each well. The cells were washed with 1 mL of 1 x PBS and following aspiration of the 1 x PBS, protein extraction was performed by adding 40 uL of 1 x SSB to each well. The cells were then scraped from each well using a yellow pipette tip, the lysate pipetted up and down to break up the protein and collected in 1.7 mL microcentrifuge tubes to be analyzed. Each sample was stored at -20 °C.

2.8 Western Blot to Confirm Protein Expression

When determining the effect of MIER1α on MCF7 and T47D cells, cells were seeded at a density of $4x10^4$cells/500 uL in a 24-well plate for 96 hrs after transfection and 5 days after the start of doxycycline induction, respectively. Cell extracts were collected (as stated in section 2.7) to confirm protein expression.

Cell extract samples were boiled for 4 minutes and placed back on ice. The samples were loaded on a 7 % SDS-PAGE gel and run for approximately 1.5 hours at 15 mA in order to separate the protein by molecular weight. Once the gels were run, the proteins were transferred onto a membrane using the Trans-Blot® Turbo™ mini transfer packs (Bio-Rad, Hercules, CA, 170-4156) at 25 volts, 2.5 amps and 10 mins in the Trans-Blot® Turbo™ Transfer System (Bio-Rad, Hercules, CA, 170-4155).The membrane was then blocked for 1 hour in 5 % skim milk powder/1 x TBST at room temperature. Specific protein detection was performed using mouse monoclonal anti-myc tag antibody (day 10 and 14) at 1:1000 dilution for day 10 and 1:2000 dilution for day 14 in 5 % skim milk powder/1 x TBST shaking overnight at 4 ˚C. The following day, the membrane was washed for 1 hour with approximately 1 litre of 1 x TBST. The membrane was then

probed with sheep anti-mouse horseradish peroxidase (SAM-HRP) antibody at 1:3000 dilution for 1 hour. Finally, the membrane was washed for an additional 1 hour with 1 litre of 1 x TBST, then analyzed with ECL Western Blotting System (GE Healthcare, Little Chalfont, Buckinghamshire, UK, RPN2109) and visualized on Amersham Hyperfilm ECL, high performance chemiluminescence film (GE Healthcare, Little Chalfont, Buckinghamshire, UK, 28-9068-39).

To demonstrate equivalent protein loading of the different samples, β-Actin was used. The membranes for Figures 3.1 C and 3.2 C were washed for 1 hr with 1 litre of 1 x TBST, then probed with anti β-actin antibody (Sigma Aldrich, St. Louis, MO, A5441) at 1:5000 dilution in 5 % skim milk powder/1 x TBST for 1 hr. The membrane was washed for 1 hr with approximately 1 litre of 1 x TBST, then probed with goat anti-mouse horseradish peroxidase light chain specific (GAM-HRP; Cedarlane Jackson, Burlington, ON, 115035174) at 1:10,000 dilution in 5 % skim milk powder/1 x TBST for 1 hr. The membrane was washed for an additional 1 hr with 1 litre of 1 x TBST, then analyzed with Clarity Western ECL Substrate (Bio-Rad, Hercules, CA, 170-5061) and visualized on Amersham Hyperfilm ECL, high performance chemiluminescence film.

To confirm protein expression of MIER1α and MIER1-3Aα in MCF7 cells, and MIER1α expression in T47D cells, incubated in different serum concentrations, cells were seeded at a density of $4x10^4$ cells/500 uL per well in a 24-well plate for 72 and 96 hrs after transfection and 3, 4 and 5 days after the start of doxycycline induction. After the indicated incubation periods, cell extracts were collected (as described in section 2.7) to confirm protein expression.

Cell extract samples were boiled for 4 mins and placed back on ice. The samples were loaded on a 7 % SDS-PAGE gels and run for approximately 1.5 hrs at 30 mA in order to separate the protein by molecular weight. Once the gels were run, the Trans-Blot® Turbo™ midi-size PVDF membrane (Bio-Rad, Hercules, CA, 10025917) was soaked in methanol (Thermo Fisher Scientific, Montreal, Quebec, 67-56-1). The Trans-Blot® Turbo™ midi-size PVDF membrane and the two Trans-Blot® Turbo™ midi-size transfer stacks (Bio-Rad, Hercules, CA, 170-4272) were washed in 60 mL water, 20 mL ethanol (Thermo Fisher Scientific, Brampton, ON, 64-17-5) and Trans-Blot® Turbo™ 5 X Transfer Buffer (Bio-Rad, Hercules, CA, 170-4272). The proteins were then transferred on the membrane at 25 volts, 2.5 amps and 10 mins in the Trans-Blot® Turbo™ Transfer System. The membrane was then blocked for 1 hr in 5 % skim milk powder/1 x TBST at room temperature. Western blot detection was performed using mouse monoclonal anti-myc tag antibody (day 14) at 1:2000 dilution for day 14 in 5 % skim milk powder/1 x TBST shaking overnight at 4 ˚C. The following day, the membrane was washed for 1 hr with approximately 1 litre of 1 x TBST, then probed with β-actin antibody at 1:5000 dilution in 5 % skim milk powder/1 x TBST for 1 hr. The membrane was washed for an additional 1 hr with 1 litre of 1 x TBST, then probed with sheep anti-mouse horseradish peroxidase (SAM-HRP) antibody at 1:3000 dilution in 5 % skim milk powder/1 x TBST for 1 hr. Finally, the membrane was washed for an additional 1 hour with 1 litre of 1 x TBST, then analyzed with Clarity Western ECL Substrate and visualized on Amersham Hyperfilm ECL, high performance chemiluminescence film.

2.9 Mirus™ *Trans*IT-LT1 Transfection (Lipofection)

To determine the effect of insulin on nuclear localization of MIER1α in MCF7 cells, MCF7 cells were seeded at a density of 20,000 cells/200 uL in two 8-well chamber slides and incubated in DMEM medium supplemented with 10 % serum (2.5 % FBS and 7.5 % NBCS), 1 % sodium pyruvate and 0.5 % penicillin/streptomycin overnight. Twenty-four hours later, the media in each well of the 8-well chamber slides was replaced with 150 uL of fresh DMEM medium (described previously) and placed back in the incubator. The *Trans*IT-LT1 transfection reagent (MJS Biolynx, Brockville, ON, MIR2300) was warmed to room temperature and vortexed before use. In two 1.7 mL microcentrifuge tubes, added the appropriate volume (for 1 well, added 50 uL Opti-MEM) of Opti-MEM Reduced-Serum Medium (Life Technologies, Grand Island, NY, 51985034) and *Trans*IT-LT1 (0.5 ug of DNA per well, 3 uL of *Trans*IT-LT1 to 1 ug of plasmid DNA = 3 uL of *Trans*IT-LT1 for 2 wells). Added plasmid DNA, pCS3+MT tagged control or pCS3+MT*MIER1*α (0.5 ug per well), to the Opti-MEMI and *Trans*IT-LT1 mixture and pipette gently to mix. These 1.7 mL microcentrifuge tubes were then incubated for 15 mins at room temperature. Following the 15 mins incubation, the *Trans*IT-LT1 and DNA mixture were added to wells in a drop-wise manner and gently rocked the slides to evenly distribute the mixture. The chamber slides were then incubated overnight. Following 24 hrs incubation, the chamber slides were removed from the incubator and the media aspirated from each well. In one slide, added 200 uL of DMEM medium (as described previously) and in the other slide, added DMEM medium (as described previously) with 4 ug/mL insulin. The slides were incubated for 28 hrs after

transfection, then removed from the incubator to be fixed for ICC (as described in section 2.8).

2.10 Statistical Analysis

To perform statistical analysis, Microsoft Office Excel 2007 software was used. For the effect of MIER1α on MCF7 and T47D cell proliferation, the two-tailed unpaired t-tests were performed. For the decrease in expression of MIER1α in T47D cells over a 9 day incubation period, the two-tailed unpaired t-tests were performed. For the localization studies, the two-tailed z-tests for two proportions were performed. The significance level for these tests was set at $p < 0.05$. For the studies on the effect of MIER1α on cell number, the null hypothesis states that there is no difference between the two samples being compared and therefore, MIER1α has no effect on cell number. The alternative hypothesis states that there is a difference between the two samples being compared and therefore, MIER1α has an effect on cell number. For the studies on the expression of MIER1α in T47D cells over a 9 day incubation period, the null hypothesis states that there is no difference between the two incubation periods being compared. The alternative hypothesis states that there is a difference between the two incubation periods being compared. For the localization studies, the null hypothesis states that there is no difference between the relative distribution of proteins in the total cell versus nuclear versus cytoplasmic compartments, and the alternative hypothesis states there is a difference between the relative distributions of proteins in the total cell versus nuclear versus cytoplasmic compartments being compared.

Chapter 3- Results

3.1 The Effect of MIER1α on MCF7 Cell Proliferation

Previously, MIER1α has been shown to interact with ERα *in vivo* and reduce oestrogen-stimulated anchorage-independent growth of T47D cells (McCarthy *et al*., 2008). Colony formation in soft agar is the measurement of anchorage-independent growth, and the ability of cells to survive and proliferate without attachment to substratum (Fukazawa *et al*., 1995). Therefore, it was suggested that MIER1α may play a role in breast carcinoma proliferation. Cell proliferation is a different type of measurement and measures the increase in cell number when cells are attached to a substratum. The study by McCarthy *et al*. (2008) also determined that the subcellular localization of MIER1α changes with breast cancer progression from predominantly nuclear in normal breast tissue, to predominantly cytoplasmic in invasive breast carcinoma. This revealed that loss of nuclear MIER1α might contribute to breast cancer progression. This change in MIER1α nuclear localization to cytoplasmic localization in invasive breast carcinoma could affect the ability of MIER1α to apply its gene/chromatin repressor functions (McCarthy *et al*., 2008). Therefore, this present study investigates the effect of MIER1α on proliferation of MCF7 cells.

To investigate the effect of MIER1α on MCF7 proliferation, the CellTiter 96® Aqueous One Solution Proliferation Assay was performed on non-transfected cells, cells transfected with pCS3+MT tagged control, and pCS3+MT*MIER1*α or mock transfected cells 96 hrs after transfection. Figure 3.1 A shows the fold increase in cell number of non-transfected cells, in cells transfected with pCS3+MT tagged control, and in

pCS3+MT*MIER1*α as well as mock transfected cells after 96 hrs of incubation. Fold increase in cell number was calculated by dividing the mean final cell number by the mean initial cell number from each experiment, and averaging those values. As shown in Figure 3.1 A, the fold increase in the cell number of MIER1α (indicated with yellow bar) is 3.0 fold compared to the non-transfected (red bar), to the pCS3+MT tagged control (green bar) and to the mock transfected (blue bar) cells at 3.4 fold, 3.8 fold and 3.0 fold, respectively.

Immunocytochemistry (ICC) was performed to determine the transfection efficiencies of pCS3+MT tagged control and MIER1α, and was determined by dividing the number of stained cells by the total number of cells and multiplying by 100. Figure 3.1 B are representative ICC images of transfected MCF7 cells, non-transfected MCF7 cells, and the MIER1α control. The MIER1α control represents MCF7 cells transfected with pCS3+MT*MIER1*α but not stained with the primary antibody, anti-myc tag antibody, when ICC was performed. Therefore, the secondary antibody has no primary antibody to bind and as a result no staining was observed. The pCS3+MT tagged control shows staining because it expresses an N-terminus MYC-tag consisting of 6 myc epitopes which produce a short protein recognized by the 9E10 antibody. The transfection efficiencies of pCS3+MT and pCS3+MT*MIER1α* were 35 % and 56 %, respectively.

Western blot analysis was performed to confirm protein expression of MIER1α in MCF7 cells. Figure 3.1 C represents the Western blot indicating the molecular weight of the MIER1α protein.

MIER1α is transiently expressed in MCF7 cells and therefore, only some of the cells originally expressed the gene. After 96 hours incubation, fewer cells expressed the gene because in transient transfection, the gene is not integrated into the cell's genome and therefore, expression is lost over time through successive cell division (Smith, 2013). It therefore became of interest to determine whether MIER1α would have a similar effect in a stable cell line, in which expression of the gene is under the control of doxycycline. A stable cell line was used because theoretically all the cells express MIER1α. All cells should express the gene because, unlike transient transfection, stably transfected cells express the gene and integrate the gene into their genome. Therefore, the stably transfected gene can be replicated. A stable cell line was used because the gene becomes integrated into the cell's genome and can be replicated.

Figure 3.1: The Effect of MIER1α on MCF7 Cell Proliferation

MCF7 transfected cells, non-transfected cells and mock transfected cells, were incubated for 24 hrs in DMEM medium without antibiotics. The cells were then seeded at a density of 6500 cells/100 uL per well of a 96-well plate. Ninety-six hours after transfection, the cell number was determined by adding 20 uL of CellTiter 96® Aqueous One Solution to each well containing 100 uL of cell suspension, incubating the plate at 37 °C for 3 hrs, then reading the plate at 492 nm. Figure 3.1 A represents the effect of MIER1α on MCF7 cell number ± S.D. /√n (n=3). The y-axis represents the fold increase in cell number and the x-axis represents the MIER1 constructs. MIER1α has no effect on MCF7 cell number when compared to the non-transfected (p=0.78), to the pCS3+MT tagged control (p=0.46) and to the mock transfected (p=1) fold increase in cell number. Figure 3.1 B represents the ICC images at 200x magnification of non-transfected MCF7 cells (i); cells transfected with pCS3+MT tagged control (ii); pCS3+MT*MIER1*α (denoted MIER1α) (iii); or mock transfected cells (iv); and the control pCS3+MT*MIER1*α (denoted MIER1α) (v) 96 hrs after transfection. The latter images, vi, vii, viii, ix, and x were taken in bright field. Figure 3.1 C represents the Western blot indicating the molecular weight of MIER1α protein in the first lane, the pCS3+MT tagged control cell extracts loaded in lane 2, mock transfected cell extracts loaded in lane 3 and non-transfected cell extracts loaded in lane 4. β-actin was used as a loading control.

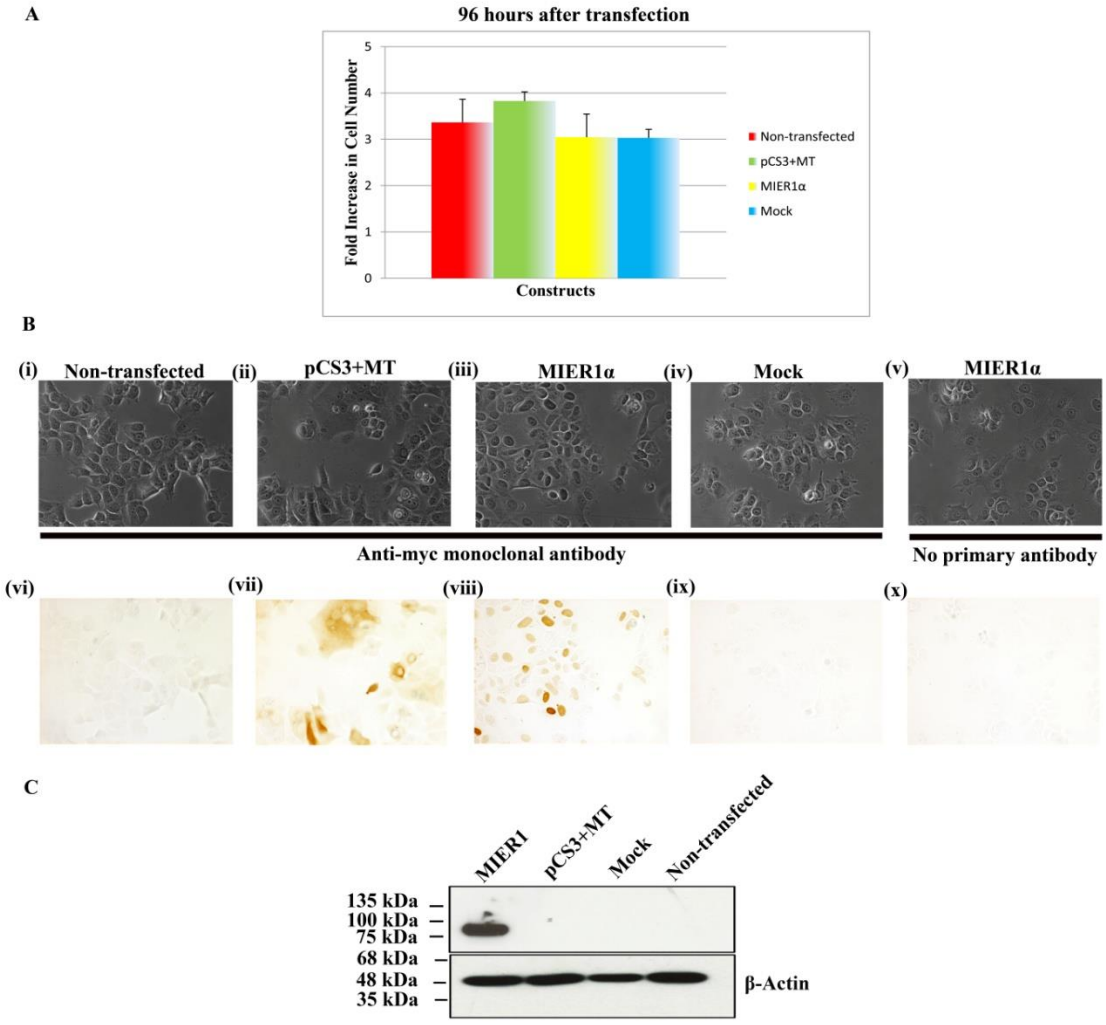
A
96 hours after transfection
Fold Increase in Cell Number
0
1
2
3
4
5
Constructs
Non-transfected
pCS3+MT
MIER1α
Mock
B
(i) Non-transfected
(ii) pCS3+MT
(iii) MIER1α
(iv) Mock
(v) MIER1α
Anti-myc monoclonal antibody
No primary antibody
(vi)
(vii)
(viii)
(ix)
(x)
C
MIER1
pCS3+MT
Mock
Non-transfected
135 kDa
100 kDa
75 kDa
68 kDa
48 kDa
35 kDa
β-Actin

3.2 The Effect of MIER1α on Proliferation of the Stably Transfected T47D Cell Line

The stably transfected T47D cell line was used because a system was needed in which all cells express MIER1α. This system was used to determine if the reason no effect on proliferation was observed with MCF7 cells was not due to the low transfection rate. MIER1α expressing T47D cells (TDα5) are stably transfected cell clones that are induced to express MIER1α with doxycycline (dox).

To investigate the effect of MIER1α on T47D cell number, the CellTiter 96® Aqueous One Solution Proliferation Assay was used on TDα5 and TDc21 cells 5 days after the start of dox induction. Figure 3.2 A shows the fold increase in cell number of TDα5 and TDc21 cells 5 days after the start of dox induction. The fold increase of TDα5 cells was 5.9 fold (+ dox) and 5.7 fold (- dox), and the fold increase in cell number of TDc21 cells was 3.0 fold (+ dox) and 2.9 fold (- dox).

Immunocytochemistry (ICC) was performed to determine the percentage of cells expressing for TDα5 cells (+ dox), and was determined by dividing the number of stained cells by the total number of cells and multiplying by 100. Figure 3.2 B are representative ICC images for control T47D cells, MIER1α expressing T47D cells and MIER1α expressing T47D control cells. The MIER1α expressing T47D control cells are MIER1α expressing T47D cells (TDα5) induced to express MIER1α with dox but, not stained with primary antibody, anti-myc tag antibody, when ICC was performed 5 days after the start of dox induction. Therefore, the secondary antibody has no primary antibody to bind and as a result no staining was observed. Figure 3.2 B (ix) represents the percentage of cells expressing for MIER1α expressing T47D cells (+ dox) 5 days after the start of dox induction. The percentage of cells expressing for MIER1α expressing T47D cells (+ dox)

was 33 %. Western blot analysis was performed to confirm protein expression of MIER1α in MCF7 cells. Figure 3.1 C represents the Western blot indicating the molecular weight of the MIER1α protein.

These experiments show that the percentage of cells expressing MIER1α five days after the start of dox induction is unexpectedly low, as shown in Figure 3.2 B (ix). Therefore, it is difficult to determine the real effect of MIER1α on T47D cell number. These experiments also revealed a decrease in MIER1α expression over time, which was further investigated.

3.3 Decrease in Expression of MIER1α in the Stably Transfected T47D Cell Line over a 9 Day Period

To determine if there is a decrease in the expression of MIER1α over time, TDα5 cells were induced with 1 ug/mL doxycycline to express MIER1α, and grown in a medium supplemented with geneticin (G418) for 48 hrs. The cells were then seeded in 8-well chamber slides and incubated for 5, 7 and 9 days after the start of dox induction. The selection pressure was maintained on these cells by seeding the cells in RPMI medium supplemented with G418.

Figure 3.2: The Effect of MIER1α on Proliferation of the Stably Transfected T47D Cell Line

TDα5 and TDc21 cells were induced with 1 ug/mL doxycycline or not induced (+ and - dox) for 48 hrs, then seeded at a density of 10,000 cells/100 uL per well of a 96-well plate. Five days after the start of dox induction, cell number was determined by adding 20 uL of CellTiter 96® Aqueous One Solution to each well containing 100 uL of cell suspension, incubating the plate at 37 °C for 3 hrs, then reading the plate at 492 nm. Figure 3.2 A represents the effect of MIER1α on T47D cell number ± S.D. /√n (n=3). The y-axis represents the fold increase in cell number and the x-axis represents the constructs. There is no effect of MIER1α on TDα5 cells (+ dox) when compared to TDα5 cells (- dox) (p=0.90). There was no difference between the TDc21 cells (+ and - dox) (p=0.87). Figure 3.2 B are representative ICC images at 100x magnification for TDc21 cells (- dox) (i); TDc21 cells (+ dox) (ii); TDα5 cells (- dox) (v); TDα5 cells (+ dox) (vi); and the MIER1α control cells (+ dox) (vii) 5 days after the start of dox induction. The latter pictures, iii, iv, viii, ix, and x were taken in bright field. The arrows in Figure 3.2 B (ix) show nuclear staining of MIER1α in TDα5 cells (+ dox). Figure 3.2 C represents the Western blot with the TDc21 cell extracts (+ dox) loaded in lane 3, TDc21 cell extracts (- dox) loaded in lane 5, TDα5 cell extracts (+ dox) loaded in lane 7 and TDα5 cell extracts (- dox) loaded in lane 9. β-actin was used as a loading control.

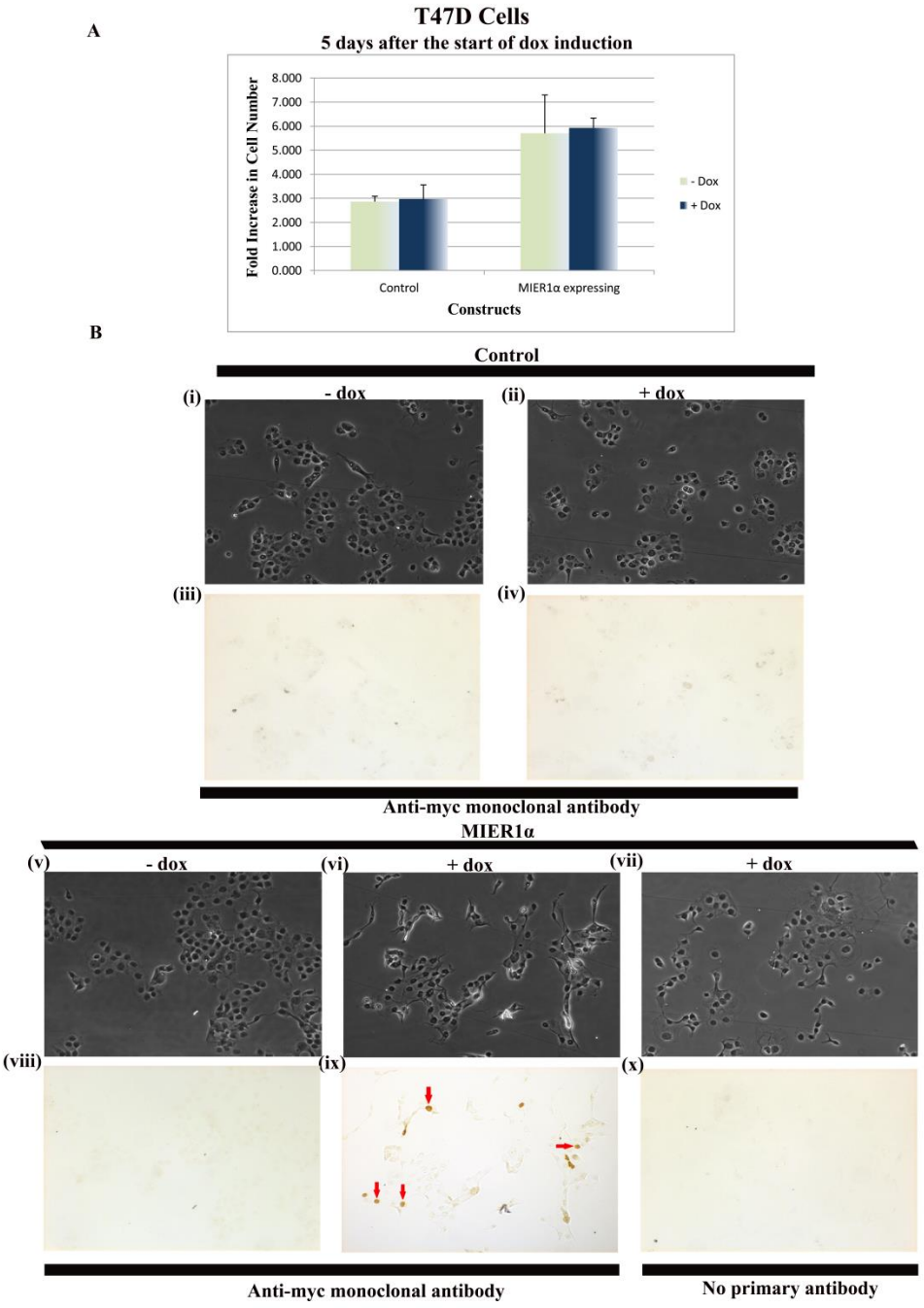
A
T47D Cells
5 days after the start of dox induction
Fold Increase in Cell Number
8.000
7.000
6.000
5.000
4.000
3.000
2.000
1.000
0.000
Control
MIER1α expressing
Constructs
- Dox
+ Dox
B
Control
(i)
- dox
(ii)
+ dox
(iii)
(iv)
Anti-myc monoclonal antibody
MIER1α
(v)
- dox
(vi)
+ dox
(vii)
+ dox
(viii)
(ix)
(x)
Anti-myc monoclonal antibody
No primary antibody
C
Control (+ dox)
Control (- dox)
MIER1α expressing (+ dox)
MIER1α expressing (- dox)
135 kDa
100 kDa
75 kDa
63 kDa
48 kDa
β-Actin

The percentage of cells expressing MIER1α for each time period was determined by dividing the number of stained cells by the total number of cells and multiplying by 100. Figure 3.3 represents the steady decrease in MIER1α expression over the 9 day period. As shown in this figure, percentage of TDα5 cells expressing MIER1α 5 days after the start of dox induction was 32.8 %, 7 days after the start of dox induction was 12.7 % and 9 days after the start of dox induction was decreased to only 1 %.

3.4 Expression of MIER1α in the Stably Transfected T47D Cell Line over a 9 Day Period when Dox and Media were Replaced every 48 hours

In the Tet-On system, gene expression is controlled by the adding of doxycycline to cell culture medium (Zhou *et al.*, 2006). Doxycycline has a half-life of 24 hrs in cell culture and therefore, to maintain stable expression, dox should be replaced in medium every 48 hrs (Tet-Off and Tet-On Gene Expression Systems User Manuel, 2012). To determine if the decrease in the expression of MIER1α over the 9 day period was the result of not replacing the dox and the media every 48 hours, TDα5 cells were induced with 1 ug/mL doxycycline to express MIER1α and grown in a medium supplemented with geneticin (G418) for 48 hrs. The cells were then seeded in 8-well chamber slides and incubated for 5, 7 and 9 days after the start of dox induction. The selection pressure was maintained on these cells by seeding the cells in RPMI medium supplemented with G418. Every 48 hours the media was aspirated from the culture slides and fresh media with 1 ug/mL dox was added.

Figure 3.3: Decrease in Expression of MIER1α in the Stably Transfected T47D Cell Line over a 9 Day Period

TDα5 cells were induced with 1 ug/mL doxycycline to express MIER1α, and seeded at a density of 20,000 cells/well of 8-well chamber slides. The chamber slides were incubated for 5 (n=3), 7 (n=2) and 9 (n=2) day periods after the start of dox induction. Following the indicated incubation periods, the slides were fixed using 4 % paraformaldehyde and ICC performed using an anti-myc tag antibody. Figure 3.3 represents the steady decrease in MIER1α expression over the 9 day period ± S.D.. The asterisk represents a significant difference between incubation periods. The decrease in expression of MIER1α from 5 days to 7 days incubation, and 7 days to 9 days incubation were significant ($p=0.029$ and $p=0.00014$).

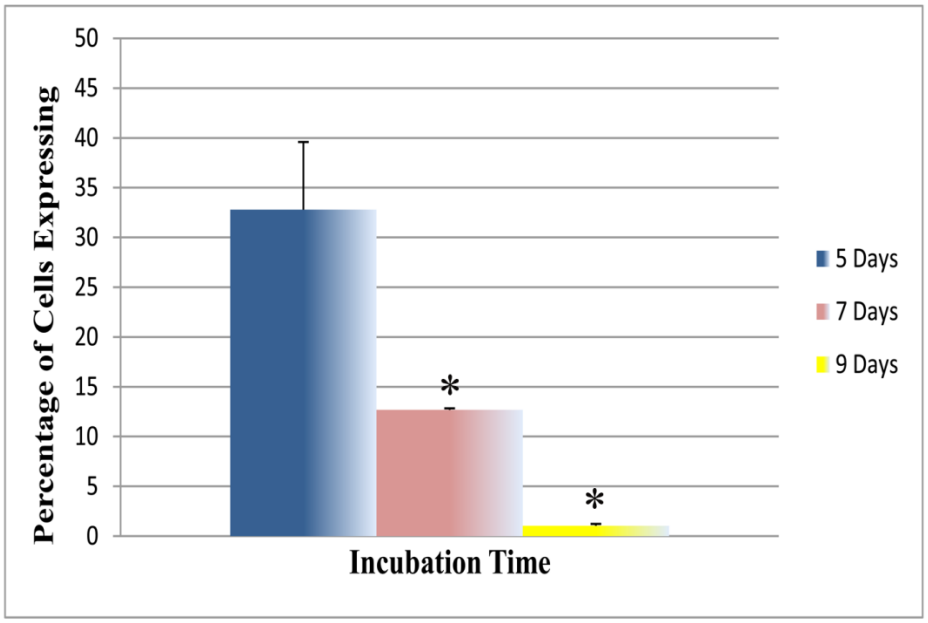
50
45
40
35
30
25
20
15
10
5
0
Percentage of Cells Expressing
*
*
Incubation Time
5 Days
7 Days
9 Days

The percentage of cells expressing MIER1α for each time period was determined by dividing the number of stained cells by the total number of cells and multiplying by 100. Figure 3.4 represents the steady decrease in MIER1α expression over the 9 day period. As shown in this figure, percentage of TDα5 cells expressing MIER1α 5 days after the start of dox induction was 7.2 %, 7 days after the start of dox induction was 3.4 % and 9 days after the start of dox induction was 1.7 %. These experiments revealed that replacing the dox and media every 48 hours does not increase the expression of MIER1α as expected. A small increase in expression of MIER1α was observed after 9 days incubation at 1.7 % compared to 1 % when dox and media were not replaced every 48 hours (Figure 3.3).

3.5 Change in the Localization of MIER1α in the Stably Transfected T47D Cell Line over a 9 Day Period

When investigating the decrease in MIER1α expression over time (Figure 3.3), a change in the localization of MIER1α in T47D cells was observed. I decided to further investigate this change in localization. TDα5 were induced with 1 ug/mL doxycycline to express MIER1α, and grown in a medium supplemented with geneticin (G418) for 48 hrs. The selection pressure was maintained on these cells by seeding the cells in RPMI medium supplemented with G418. The cells were then seeded in 8-well chamber slides and incubated for 5, 7 and 9 days after the start of dox induction.

Figure 3.5 A represents the different localization categories. The arrow in Figure 3.5 A (i) indicates nuclear, the arrows in (ii) indicate whole cell and the arrows in (iii) indicate cytoplasmic staining of MIER1α. Figure 3.5 B are the ICC images representing

the change in localization of MIER1α 5, 7 and 9 days after the start of dox induction. Figure 3.5 C represents the localization of MIER1α in TDα5 cells 5, 7 and 9 days after the start of dox induction. Five days after the start of dox induction, 24.8 % of the cells appear to show nuclear staining, 55.6 % of the cells appear to show whole cell staining, and 19.5 % of the cell appear to show cytoplasmic staining of MIER1α. Seven days after the start of dox induction, 7.7 % of the cells appear to show nuclear staining, 68.6 % of the cells appear to show whole cell staining, and 23.7 % of the cells appear to show cytoplasmic staining of MIER1α. Nine days after the start of dox induction, 0 % of the cells appear to show nuclear staining, 26.8 % of the cells appear to show whole cell staining, and 73.2 % of the cells appear to show cytoplasmic staining of MIER1α.

This change in localization of MIER1α over the 9 day period was an unexpected result and something to be further investigated. The media on the cells was not changed during the incubation period, and therefore this could be causing the change in MIER1α localization. This could be the result of growth factor production by autocrine signalling. Autocrine production of growth factors in low serum has been investigated, and has been shown to allow the continued growth of cells in the absence of growth factors (van Zoelen *et al.*, 1984). Therefore, TDα5 cells could be producing growth factors to promote growth, and these growth factors could be acting on MIER1α and transporting it out of the nucleus. To investigate this change in localization, incubation in different serum concentrations were explored.

Figure 3.4: Expression of MIER1α in the Stably Transfected T47D Cell Line over a 9 Day Period when Dox and Media were Replaced every 48 hours

TDα5 were induced with 1 ug/mL doxycycline to express MIER1α, and seeded at a density of 20,000 cells/well of 8-well chamber slides. The chamber slides were incubated for 5 (n=6), 7 (n=2) and 9 (n=2) day periods after the start of dox induction. Every 48 hours, the dox and media were changed on the cells. Following the indicated incubation periods, the slides were fixed using 4 % paraformaldehyde and ICC performed using an anti-myc tag antibody. Figure 3.4 represents the expression of MIER1α over the 9 day period when dox and media were replaced every 48 hours ± S.D.. The asterisk represents a significant difference between incubation periods. The decrease in expression of MIER1α from 7 days to 9 days incubation was significant ($p=0.0061$).

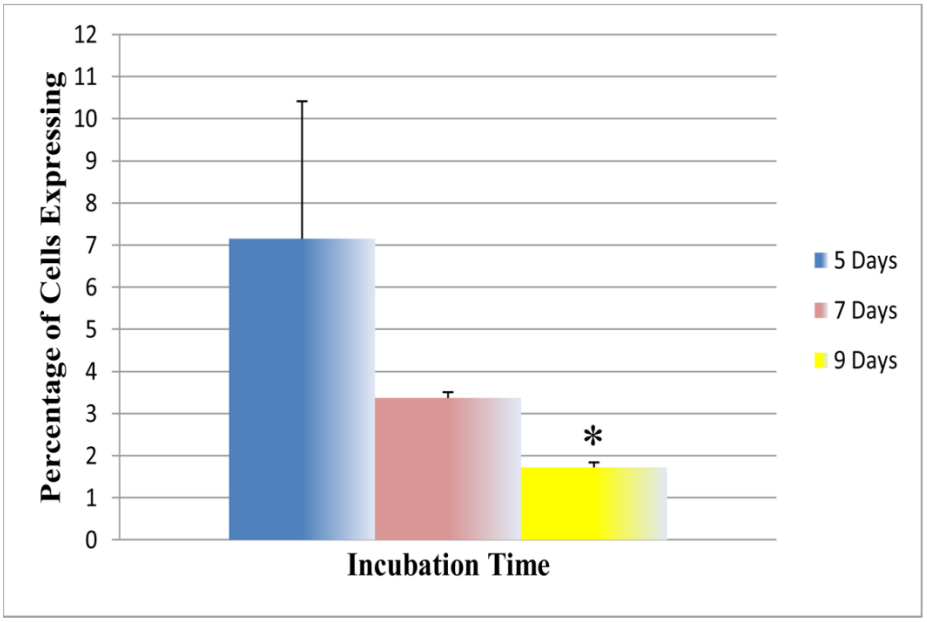
Percentage of Cells Expressing
12
11
10
9
8
7
6
5
4
3
2
1
0
*
Incubation Time
5 Days
7 Days
9 Days

Figure 3.5: Change in Localization of MIER1α in the Stably Transfected T47D Cell Line over a 9 Day Period

TDα5 were induced with 1 ug/mL doxycycline to express MIER1α, and seeded at a density of 20,000 cells/well of 8-well chamber slides. The chamber slides were incubated for 5, 7 and 9 day periods after the start of dox induction. Following the indicated incubation periods, ICC was performed using an anti-myc tag antibody. Figure 3.5 A are representative ICC images at 200x magnification of the different localization categories. The arrow in Figure 3.5 (i) indicates nuclear, the arrows in (ii) indicate whole cell and the arrows in (iii) indicate cytoplasmic staining of MIER1α. Figure 3.5 B represents ICC images at 200x magnification of the change in localization of MIER1α after 5, 7 and 9 days incubation. Figure 3.5 C represents the localization of MIER1α in TDα5 cells 5 (n=4), 7 (n=5) and 9 days (n=4) after the start of dox induction ± S.D. /√n. The appeared percentage of TDα5 cells showing nuclear localization of MIER1α 5 days after dox induction compared to the percentage of TDα5 cells showing nuclear localization of MIER1α 7 and 9 days after dox induction were significant (p=0.0000064 and p=0.000000000011, respectively). The appeared percentage of TDα5 cells showing whole cell localization of MIER1α 7 days after dox induction compared to the percentage of TDα5 cells showing whole cell localization of MIER1α 5 and 9 days after dox induction were significant (p=0.0068 and p=0.000000000000040, respectively). The appeared percentage of TDα5 cells showing cytoplasmic localization of MIER1α 9 days after dox induction compared to the percentage of TDα5 cells showing cytoplasmic localization of MIER1α 5 and 7 days after dox induction were significant (p=0.00 and p=0.00, respectively).

A

(i) Nuclear (ii) Whole cell (iii) Cytoplasmic

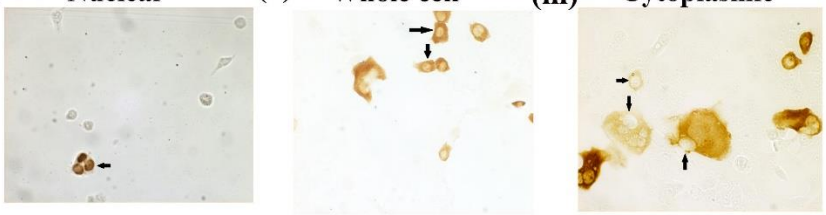

B

(i) 5 days (ii) 7 days (iii) 9 days

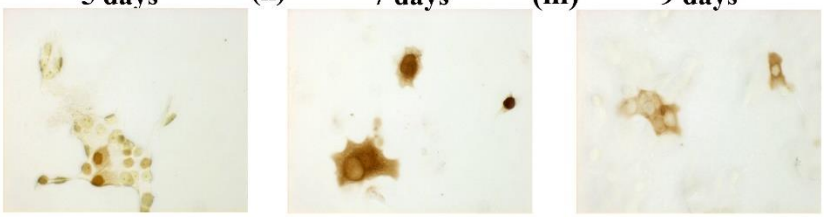

C

	Days						
Localization	5	± S.D./√n	7	± S.D./√n	9	± S.D./√n	p-value
Nuclear	24.8 %	± 4.5	7.7 %	± 1.7	0 %	± 0	p=0.0000064 & p=0.000000000011
Whole cell	55.6 %	± 7.6	68.6 %	± 16.1	26.8 %	± 2.3	p=0.0068 & p=0.000000000000040
Cytoplasmic	19.5 %	± 7.9	23.7 %	± 2.8	73.2 %	± 8.9	p=0.00 & p=0.00

3.6 Effect of Serum Concentration on Nuclear Localization of MIER1α in T47D Cells

TDα5 were induced with 1 ug/mL doxycycline or not induced (+ and - dox) for 48 hrs, then seeded in 8-well chamber slides in 0.2 % and 10 % Tet-approved FBS for 3, 4 and 5 day incubation periods after the start of dox induction. The selection pressure was maintained on these cells by seeding the cells in RPMI medium supplemented with G418. Following the indicated incubation periods, ICC was performed using an anti-myc tag antibody to analyze localization. The stained cells were categorized as having nuclear, cytoplasmic or whole cell staining.

The 10 % Tet-approved FBS was used because this serum is charcoal stripped, and therefore contains a lower level of steroid, thyroid and peptide hormones, and in particular estradiol (Cao *et al.,* 2009). The 0.2 % Tet-approved FBS was used because this serum is also charcoal stripped, and contains an even lower level of hormones than 10 % Tet-approved FBS. These two serums were used to determine if a serum containing a lower level of hormones has a different effect on localization of MIER1α in stably transfected T47D cells when compared to a serum containing a higher level of hormones.

Figures 3.6.1 A, 3.6.2 A and 3.6.3 A represent the localization of MIER1α in TDα5 cells incubated in 0.2 % Tet-approved FBS compared to those incubated in 10 % Tet-approved FBS for 3, 4 and 5 days after the start of dox induction, respectively. As shown in Figure 3.6.1 A, 3 days after the start of dox induction, incubation in 0.2 % Tet-approved FBS appeared to increase the percentage of TDα5 cells showing nuclear localization of MIER1α to 53.3 % compared to incubation in 10 % Tet-approved FBS which appeared to decrease the percentage of TDα5 cells showing nuclear localization of

MIER1α to 4.3 %. Three days after the start of dox induction, incubation in 10 % Tet-approved FBS appeared to increase the percentage of TDα5 cells showing cytoplasmic localization of MIER1α to 38.4 % compared to incubation in 0.2 % Tet-approved FBS with 0 % of TDα5 cells showing cytoplasmic localization of MIER1α. Five days after the start of dox induction, the percentage of TDα5 cells showing nuclear localization of MIER1α appeared to decrease, and the percentage of TDα5 cells showing whole cell and cytoplasmic localizations of MIER1α appeared to increase in 0.2 % Tet-approved FBS at 1.7 %, and 65.9 % and 32.4 %, respectively compared to incubation in 10 % Tet-approved FBS (Figure 3.6.3 A). Five days after the start of dox induction, the percentage of TDα5 cells showing nuclear localization of MIER1α appeared to increase, and the percentage of cells showing whole cell and cytoplasmic localizations of MIER1α appeared to decrease in 10 % Tet-approved FBS at 17.6 %, and 49.2 % and 33.2 % respectively compared to incubation in 0.2 % Tet-approved FBS (Figure 3.6.3 A).

As shown in Figure 3.6.1 A, the percentage of TDα5 cells with nuclear localization of MIER1α in 0.2 % Tet-approved FBS appeared to start high and decrease over time. In comparison, the percentage of TDα5 cells with nuclear localization of MIER1α in 10 % Tet-approved FBS appeared to start off low and increase over time. Therefore, it was hypothesized that factors in serum are responsible for the nuclear localization of MIER1α. The appeared increase in the percentage of TDα5 cells showing nuclear localization of MIER1α in 0.2 % Tet-approved FBS 3 days after the start of dox induction, could be due to the fact that this FBS is charcoal stripped and therefore, contains lower levels of peptide, steroid and thyroid hormones than untreated FBS.

Therefore, less components are present in 0.2 % Tet-approved FBS that could be acting on MIER1α and exporting it out of the nucleus. The appeared decrease in the percentage of TDα5 cells showing nuclear localization of MIER1α in 0.2 % Tet-approved FBS 5 days after the start of dox induction, could be the result of autocrine production of growth factors to allow continued growth. These growth factors could then be acting on MIER1α and transporting it out of the nucleus. The appeared decrease in the percentage of TDα5 cells showing nuclear localization and the appeared increase in cytoplasmic localization of MIER1α in 10 % Tet-approved FBS three days after the start of dox induction, could be due to the higher levels of hormones present in 10 % Tet-approved FBS than 0.2 % Tet-approved FBS that could be acting on MIER1α and transporting it out of the nucleus. The appeared increase in the percentage of TDα5 cells showing nuclear localization of MIER1α in 10 % Tet-approved FBS five days after dox induction, could be due to the depletion of components from the medium.

Figures 3.6.1 B, 3.6.2 B and 3.6.3 B are representative ICC images of MIER1α expressing T47D cells induced or not induced (+ and - dox) and MIER1α expressing T47D control cells, incubated in 0.2 % and 10 % Tet-approved FBS for 3, 4 and 5 days after the start of dox induction. The MIER1α expressing T47D control cells are TDα5 cells induced to express MIER1α with dox but, not stained with primary antibody, anti-myc tag antibody, when ICC was performed 5 days after the start of dox induction. Therefore, the secondary antibody has no primary antibody to bind and as a result no staining was observed. These ICC images represent the localization of MIER1α in TDα5 cells (+ dox) at the indicated times.

From these results it was determined that there is an appeared effect of serum concentration on the nuclear localization of MIER1α in T47D cells. Therefore, I decided to investigate if different types of serum also have an effect on nuclear localization of MIER1 isoforms, MIER1α and MIER1-3Aα, in MCF7 cells.

Figure 3.6.1: Effect of Serum Concentration on Nuclear Localization of MIER1α in the Stably Transfected T47D Cell Line 3 Days after the start of dox induction

TDα5 were induced with 1 ug/mL doxycycline or not induced (+ and - dox) for 48 hrs, then seeded at a density of 50,000 cells/well of 8-well chamber slides. The chamber slides were incubated for 3 days after the start of dox induction and ICC performed using an anti-myc tag antibody. Figure 3.6.1 A represents the localization of MIER1α in TDα5 T47D cells incubated in 0.2 % Tet-approved FBS compared to those incubated in 10 % Tet-approved FBS for 3 days after the start of dox induction ± S.D. (n=6). The asterisk represents a significant difference between two categories. The y-axis represents the percentage of cells expressing and the x-axis represents the different localization categories. The appeared increase in nuclear localization of MIER1α in 0.2 % Tet-approved FBS compared to incubation in 10 % Tet-approved FBS after 3 days of incubation was significant ($p=0.00000000000000000000000000000000000000000019$). The appeared decrease in cytoplasmic localization of MIER1α in 0.2 % Tet-approved FBS compared to incubation in 10 % Tet-approved FBS after 3 days of incubation was significant ($p=0.0000000000000084$). Figure 3.6.1 B represents ICC images at 200x magnification of TDα5 cells - dox (v and vi), TDα5 cells + dox (vii and viii), and TDα5 control cells (i and ii) incubated in 0.2 % and 10 % Tet-approved FBS 3 days after the start of dox induction. The latter images, iii, iv, ix, x, xi and xii of Figure 3.6.1 B were taken in bright field.

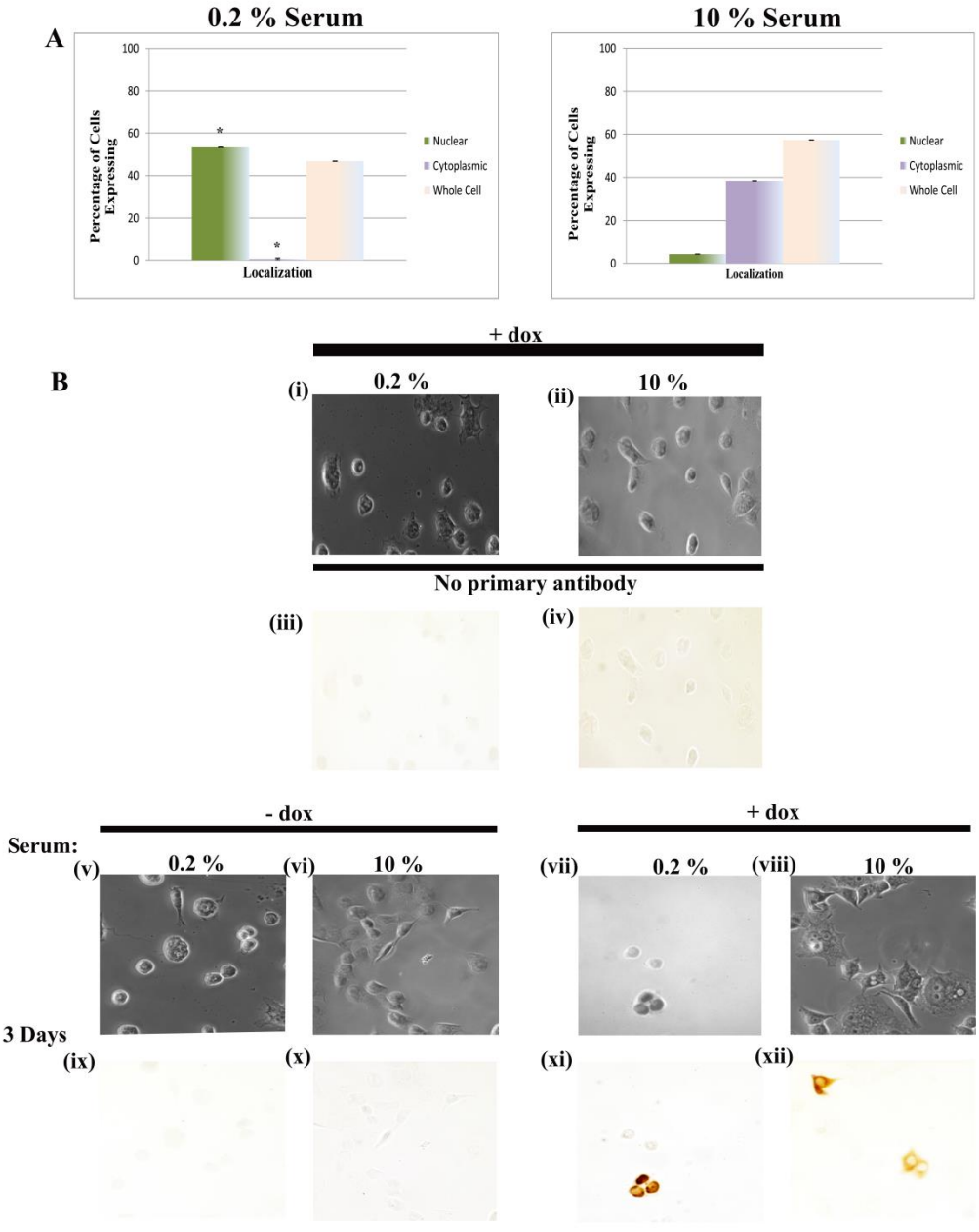
A
0.2 % Serum
10 % Serum
Percentage of Cells Expressing
Localization
Nuclear
Cytoplasmic
Whole Cell
B
+ dox
(i) 0.2 %
(ii) 10 %
No primary antibody
(iii)
(iv)
- dox
+ dox
Serum:
(v) 0.2 %
(vi) 10 %
(vii) 0.2 %
(viii) 10 %
3 Days
(ix)
(x)
(xi)
(xii)

Figure 3.6.2: Effect of Serum Concentration on Nuclear Localization of MIER1α in the Stably Transfected T47D Cell Line 4 Days after the start of dox induction

TDα5 were induced with 1 ug/mL doxycycline or not induced (+ and - dox) for 48 hrs, then seeded at a density of 50,000 cells/well of 8-well chamber slides. The chamber slides were incubated for 4 days after the start of dox induction and ICC performed using an anti-myc tag antibody. Figure 3.6.2 A represents the localization of MIER1α in TDα5 T47D cells incubated in 0.2 % Tet-approved FBS compared to those incubated in 10 % Tet-approved FBS for 4 days after the start of dox induction ± S.D. (n=5). The y-axis represents the percentage of cells expressing and the x-axis represents the different localization categories. The appeared nuclear localization of MIER1α after 4 days of incubation in 0.2 % Tet-approved FBS compared to incubation in 10 % Tet-approved FBS was significant (p=0.000000085). The appeared increase in MIER1α whole cell localization after 4 days of incubation in 0.2 % Tet-approved FBS compared to incubation in 10 % Tet-approved FBS was also significant (p=0.0016). The appeared decrease in cytoplasmic localization of MIER1α after 4 days of incubation in 0.2 % Tet-approved FBS compared to incubation in 10 % Tet-approved FBS was significant (p=0.0000000018). The asterisks represent significant differences between two categories. Figure 3.6.2 B represents ICC images at 200x magnification of TDα5 cells - dox (v and vi), TDα5 + dox (vii and viii), and TDα5 control cells (i and ii) incubated in 0.2 % and 10 % Tet-approved FBS 4 days after the start of dox induction. The latter images, iii, iv, ix, x, xi and xii of Figure 3.6.2 B were taken in bright field.

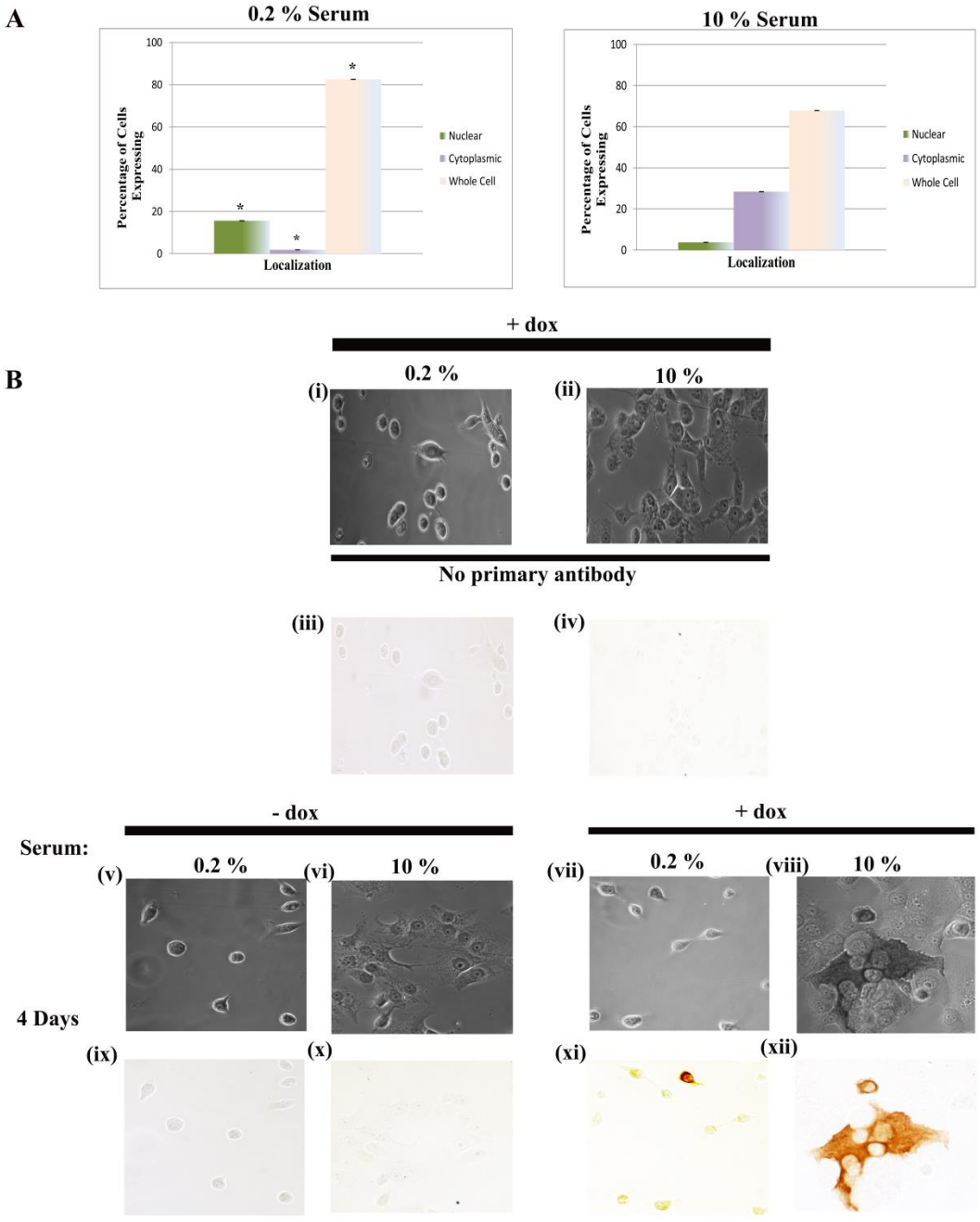
A
0.2 % Serum
10 % Serum
Percentage of Cells Expressing
Localization
Nuclear
Cytoplasmic
Whole Cell
B
+ dox
0.2 %
10 %
(i)
(ii)
No primary antibody
(iii)
(iv)
- dox
+ dox
Serum:
(v)
(vi)
(vii)
(viii)
4 Days
(ix)
(x)
(xi)
(xii)

Figure 3.6.3: Effect of Serum Concentration on Nuclear Localization of MIER1α in the Stably Transfected T47D Cell Line 5 Days after the start of dox induction

TDα5 were induced with 1 ug/mL doxycycline or not induced (+ and - dox) for 48 hrs, then seeded at a density of 50,000 cells/well of 8-well chamber slides. The chamber slides were incubated for 5 days after the start of dox induction and ICC performed using an anti-myc tag antibody. Figure 3.6.3 A represents the localization of MIER1α in TDα5 T47D cells incubated in 0.2 % Tet-approved FBS compared to those incubated in 10 % Tet-approved FBS for 5 days after the start of dox induction ± S.D. (n=6). The y-axis represents the percentage of cells expressing and the x-axis represents the different localization categories. The appeared decrease in MIER1α nuclear localization and the appeared increase in MIER1α whole cell localization after 5 days of incubation in 0.2 % Tet-approved FBS compared to incubation in 10 % Tet-approved FBS were significant ($p=0.000000067$ and $p=0.000051$, respectively). The asterisks represent significant differences between two categories. Figure 3.6.3 B represents ICC images at 200x magnification of TDα5 cells - dox (v and vi), TDα5 cells + dox (vii and viii), and TDα5 control cells (i and ii) incubated in 0.2 % and 10 % Tet-approved FBS 5 days after the start of dox induction. The latter images, iii, iv, ix, x, xi and xii of Figure 3.6.3 B were taken in bright field.

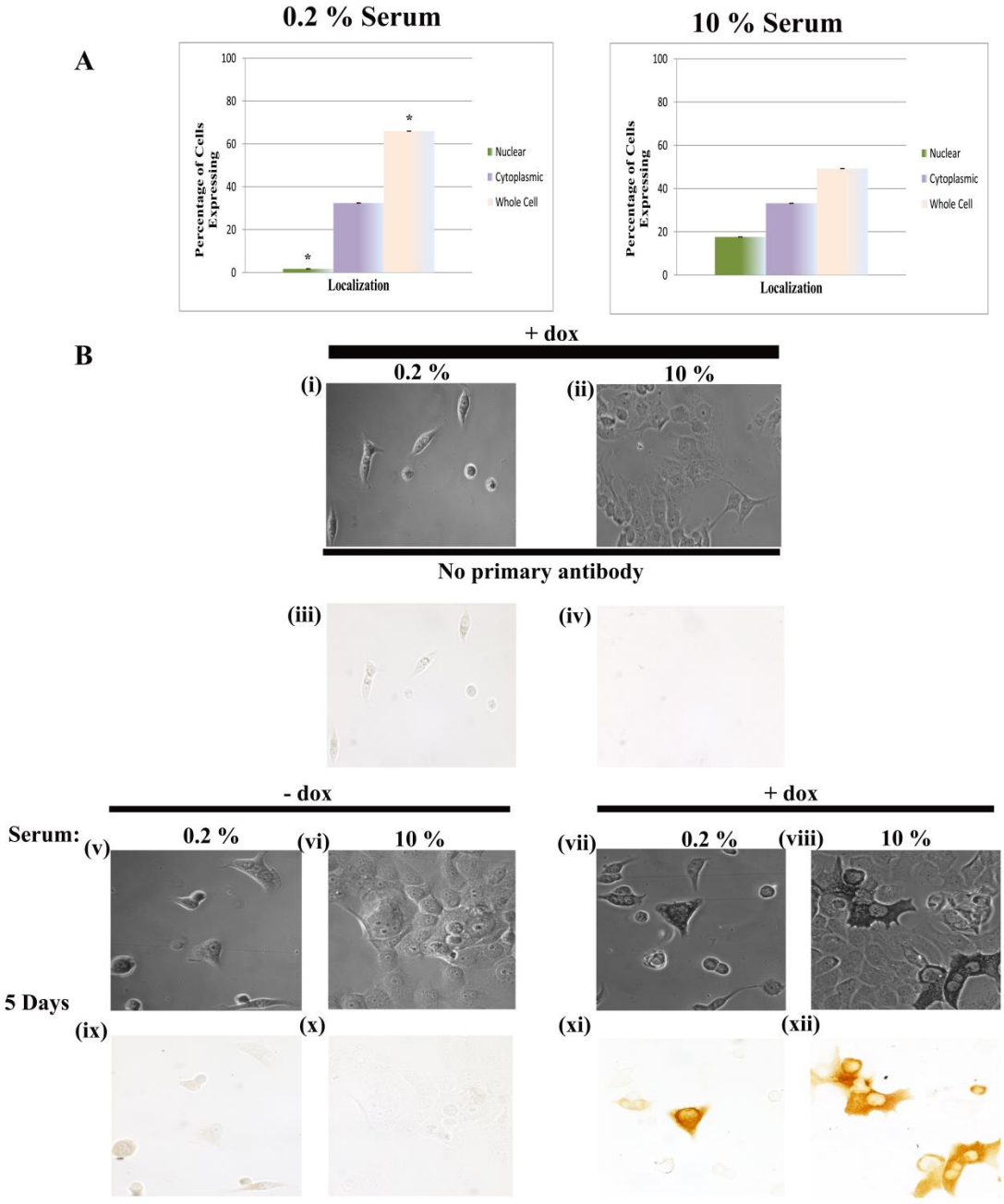
A
0.2 % Serum
10 % Serum
Percentage of Cells Expressing
Localization
Nuclear
Cytoplasmic
Whole Cell
B
+ dox
0.2 %
10 %
(i)
(ii)
No primary antibody
(iii)
(iv)
- dox
+ dox
Serum:
(v)
(vi)
(vii)
(viii)
5 Days
(ix)
(x)
(xi)
(xii)

3.7 MIER1α Protein Expression in the Stably Transfected T47D Cell Line Incubated in 0.2 % Tet-approved FBS and 10 % Tet-approved FBS for 3 days, 4 days and 5 days after the start of Doxycycline Induction

To confirm the protein expression of MIER1α in T47D cells, TDα5 cells induced with 1 ug/mL doxycycline or not induced (+ and - dox) were seeded at a density of 40,000 cells/well of a 24-well plate. The cells were grown in RPMI medium supplemented with 0.2 % and 10 % Tet-approved FBS for 3, 4 and 5 day incubation periods after the start of dox induction. The selection pressure was maintained on these cells by seeding the cells in RPMI medium supplemented with G418. Following the indicated incubation periods, cell lysates were prepared by adding 40 uL of 1 x SSB to each well. Expression of MYC-tag MIER1α was confirmed by Western blot of whole cell lysates using an anti-myc tag antibody.

3.8 The Effect of Different Types of Serum on the Localization of MIER1 Isoforms in MCF7 Cells

To investigate the effect of different types of serum on the localization of MIER1 isoforms, MIER1α and MIER1-3Aα, in MCF7 cells, cells transfected with pCS3+MT tagged control, pCS3+MT*MIER1*α and pCS3+MT*MIER1-3A*α, were seeded in two 8-well chamber slides and incubated in MCF7 DMEM media supplemented with 10 % NBCS and FBS and 10 % Tet-approved FBS for 72 and 96 hrs after transfection.

The 10 % NBCS and FBS was used because this serum is untreated and therefore, contains levels of growth factors, hormones and other components as shown in Appendix 1. The 10 % Tet-approved FBS was used because, unlike untreated serum, this serum is

Figure 3.7: MIER1α Protein Expression in the Stably Transfected T47D Cell Line Incubated in 0.2 % Tet-approved FBS and 10 % Tet-approved FBS for 3 days, 4 days and 5 days after the start of Doxycycline Induction

TDα5 were induced with 1 ug/mL doxycycline or not induced (+ and - dox) for 48 hours, then seeded at a density of 40,000 cells/well of a 24-well plate and grown in RPMI medium supplemented with 0.2 % and 10 % Tet-approved FBS for 3, 4 and 5 day incubation periods after the start of dox induction. Following the indicated incubation periods, cell lysates were prepared as described in the Materials and Methods section and loaded onto the gel for Western blot. The molecular weight of the proteins is indicated on the right. Figure 3.7 A represents the protein expression of MIER1α 3 days after the start of dox induction. In lanes 6 and 8, TDα5 cells induced with dox and incubated in 10 % and 0.2 % Tet-approved FBS, respectively. In lanes 7 and 9, TDα5 cells not induced with dox and incubated in 10 % and 0.2 % Tet-approved FBS. Figure 3.7 B represents the protein expression of MIER1α 4 days after the start of dox induction. In lanes 6 and 8, TDα5 cells induced with dox and incubated in 10 % and 0.2 % Tet-approved FBS, respectively. In lanes 7 and 9, TDα5 cells not induced with dox and incubated in 10 % and 0.2 % Tet-approved FBS. Figure 3.7 C represents the protein expression of MIER1α 5 days after the start of dox induction. In lanes 6 and 4, TDα5 cells induced with dox and incubated in 10 % and 0.2 % Tet-approved FBS, respectively. In lanes 5 and 3, TDα5 cells not induced with dox and incubated in 10 % and 0.2 % Tet-approved FBS. β-actin was used as a loading control.

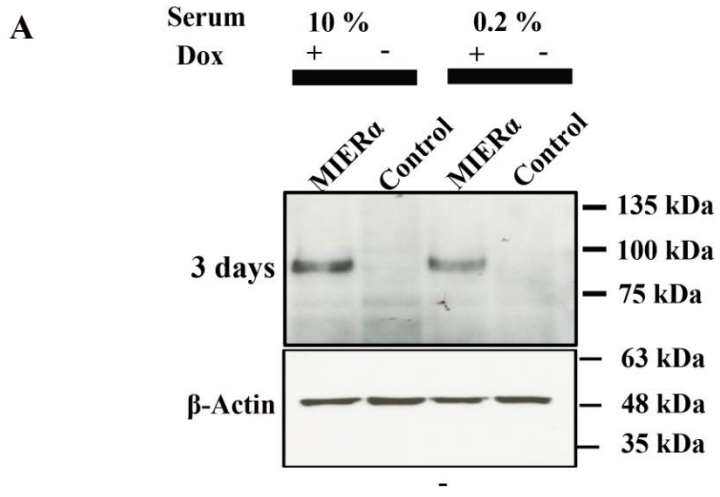
A
Serum
Dox
10 %
0.2 %
+ - + -
MIERα
Control
MIERα
Control
3 days
β-Actin
135 kDa
100 kDa
75 kDa
63 kDa
48 kDa
35 kDa

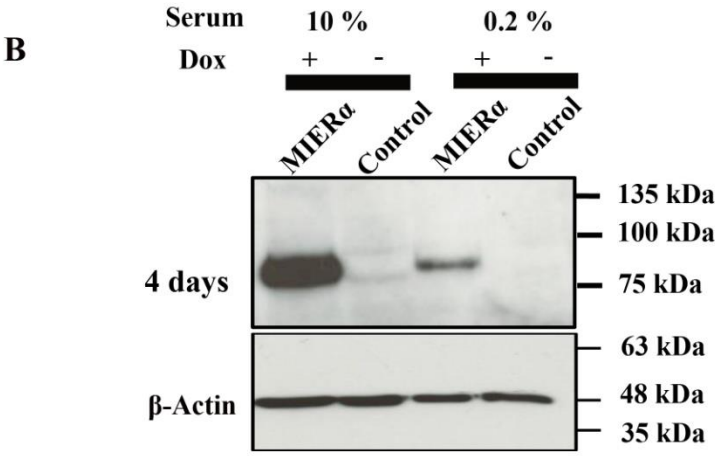
B
Serum
Dox
10 %
0.2 %
+ - + -
MIERα
Control
MIERα
Control
4 days
β-Actin
135 kDa
100 kDa
75 kDa
63 kDa
48 kDa
35 kDa

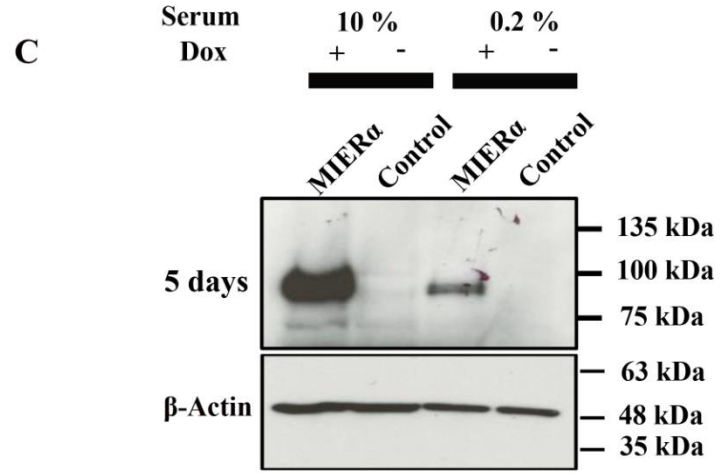
C
Serum
Dox
10 %
0.2 %
+ - + -
MIERα
Control
MIERα
Control
5 days
β-Actin
135 kDa
100 kDa
75 kDa
63 kDa
48 kDa
35 kDa

charcoal stripped. Therefore, this serum contains lower levels of steroid, thyroid and peptide hormones, and in particular estradiol (Cao *et al.*, 2009). These two serums were used to determine if factors present in NBCS and FBS have a different effect on localization of MIER1 isoforms when compared to Tet-approved FBS.

Figures 3.8.1 A and 3.8.2 A represent the proportion of cells in each localization category for the different MIER1 isoforms 72 and 96 hrs after transfection in 10 % NBCS and FBS. Figures 3.8.3 A and 3.8.4 A represent the proportion of cells in each localization category for the different MIER1 isoforms 72 and 96 hrs after transfection in 10 % Tet-approved FBS. After 72 hrs of incubation in 10 % Tet-approved FBS (Figure 3.8.3 A), MIER1α localization appeared nuclear in 96.4 % of cells compared to 90.8 % of cells in 10 % NBCS and FBS (Figure 3.8.1 A). After 72 and 96 hrs of incubation in 10 % Tet-approved FBS (Figure 3.8.3 A and 3.8.4 A), MIER1-3Aα localization appeared nuclear in 8.5 % and 16.1 % of cells respectively, compared to 1.8 % and 1.6 % of cells in 10 % NBCS and FBS (Figure 3.8.1 A and 3.8.2 A). As shown in Figures 3.8.3 A and 3.8.4 A, MIER1α localization appeared whole cell in 3.6 % and 14.4 % of cells after 72 hrs and 96 hrs of incubation in 10 % Tet-approved FBS compared to 7.7 % and 7.1 % in 10 % NBCS and FBS (Figure 3.8.1 A and 3.8.2 A). After 72 hrs of incubation in 10 % Tet-approved FBS (Figure 3.8.3 A), MIER1-3Aα localization appeared whole cell in 77.5 % of cells compared to 63.6 % of cells in 10 % NBCS and FBS (Figure 3.8.1 A). After 72 and 96 hrs of incubation in 10 % Tet-approved FBS (Figure 3.8.3 A and 3.8.4 A), MIER1α and MIER1-3Aα appeared cytoplasmic in 0 % and 0 % of cells respectively, and

14.1% and 6.9 % compared to 1.5 % and 1.3 % of cells respectively, and 34.5 % and 31.1 % of cells in 10 % NBCS and FBS (Figure 3.8.1 A and 3.8.2 A).

Figure 3.8.1 B and 3.8.2 B are representative ICC images of transfected MCF7cells and the MIER1α control 72 and 96 hrs after transfection in 10 % NBCS and FBS. The MIER1α control represents MCF7 cells transfected with pCS3+MT*MIER1*α but, not stained with primary antibody, anti-myc tag antibody, 72 and 96 hrs after transfection. Therefore, the secondary antibody has no primary antibody to bind and as a result no staining was observed.

Figure 3.8.3 B and 3.8.4 B are representative ICC images of transfected MCF7cells, and the MIER1α control 72 and 96 hrs after transfection in 10 % Tet-approved FBS. The MIER1α control represents MCF7 cells transfected with pCS3+MT*MIER1*α but, not stained with primary antibody, anti-myc tag antibody, 72 and 96 hrs after transfection. Therefore, the secondary antibody has no primary antibody to bind and as a result no staining was observed.

These results showed that Tet-approved FBS and untreated NBCS and FBS have different effects on the localization of MIER1 isoforms in MCF7 cells. The percentage of cells with nuclear localization of MIER1α and MIER1-3Aα appeared to increase after incubation in 10 % Tet-approved FBS compared to incubation in 10 % NBCS and FBS for 72 hrs, and 72 and 96 hrs respectively. Tet-approved FBS slightly appeared to decrease the percentage of cells with whole cell staining of MIER1α after 72 hours incubation compared to incubation in 10 % NBCS and FBS. The percentage of cells with whole cell staining of MIER1-3Aα and MIER1α appeared to increase after 72 and 96 hrs

incubation in 10 % Tet-approved FBS respectively, compared to incubation in 10 % NBCS and FBS. Tet-approved FBS also decreased cytoplasmic localization of MIER1α and MIER1-3Aα after 72 and 96 hrs of incubation compared to incubation in 10 % NBCS and FBS. From these results, it became of interest to determine if low serum concentrations also have an effect on MIER1α and MIER1-3Aα localization in MCF7 cells.

3.9 Protein Expression of MIER1 Isoforms, MIER1α and MIER1-3Aα, Incubated in Different Types of Serum for 72 and 96 hours after Transfection

To confirm the protein expression of MIER1α and MIER1-3Aα in MCF7 cells, MCF7 transfected cells were seeded at a density of 40,000 cells/well of 24-well plates and grown in MCF7 DMEM media supplemented with 10 % NBCS and FBS and 10 % Tet-approved FBS for 72 and 96 hrs after transfection. Following the indicated incubation periods, cell lysates were prepared by adding 40 uL of 1 x SSB to each well. Expression of MYC-tagged MIER1α and MIER1-3Aα were verified by Western blot of whole cell lysates using an anti-myc tag antibody.

Figure 3.8.1: The Effect of 10 % NBCS and FBS on the Localization of MIER1 Isoforms in MCF7 Cells 72 hours after Transfection

MCF7 cells were transfected with pCS3+MT tagged control (denoted pCS3+MT), pCS3+MT*MIER1*α (denoted MIER1α) and pCS3+MT*MIER1-3A*α (denoted MIER1-3Aα), and incubated for 24 hrs in DMEM without antibiotics. Following the 24 hrs, MCF7 transfected cells were seeded at a density of 50,000 cells/well of 8-well chamber slides and grown in MCF7 DMEM media supplemented with 10 % NBCS and FBS. The chamber slides were incubated for 72 hrs after transfection and ICC performed using an anti-myc tag antibody to analyze localization. Figure 3.8.1 A represents the localization of pCS3+MT tagged control (denoted pCS3+MT) (n=6) pCS3+MT*MIER1*α (denoted MIER1α) (n=6) and pCS3+MT*MIER1-3A*α (denoted MIER1-3Aα) (n=6) in MCF7 cells incubated in 10 % NBCS and FBS for 72 hrs after transfection ± S.D.. The y-axis represents the percentage of cells in each category and the x-axis represents the MIER1 constructs. The appeared increase in MIER1α and MIER1-3Aα nuclear localizations in 10 % Tet-approved FBS (Figure 3.8.3) compared to incubation in 10 % NBCS and FBS after 72 hrs of incubation were significant ($p=0.000031$ and $p=0.023$, respectively). The appeared increase in whole cell localization of MIER1-3Aα in 10 % Tet-approved FBS (Figure 3.8.3) compared to incubation in 10 % NBCS and FBS after 72 hrs of incubation was significant ($p=0.016$). The appeared decrease in MIER1α whole cell localization in 10 % Tet-approved FBS (Figure 3.8.3) compared to incubation in 10 % NBCS and FBS after 72 hrs of incubation was significant ($p=0.0012$). The appeared decrease in MIER1α and MIER-3Aα cytoplasmic localizations in 10 % Tet-approved FBS (Figure 3.8.3) compared to incubation in 10 % NBCS and FBS after 72 hrs of incubation were significant ($p=0.0010$ and $p=0.00013$, respectively). Figure 3.8.1 B are representative ICC images at 200x magnification of MCF7 cells transfected with pCS3+MT tagged control (denoted pCS3+MT) (i); pCS3+MT*MIER1*α (denoted MIER1α) (ii); pCS3+MT*MIER1-3A*α (denoted MIER1-3Aα) (iii); and MIER1α control (iv) and incubated in the DMEM media supplemented with 10 % NBCS and FBS for 72 after transfection. The latter images, v, vi, vii and viii, of Figure 3.8.1 B were taken in bright field.

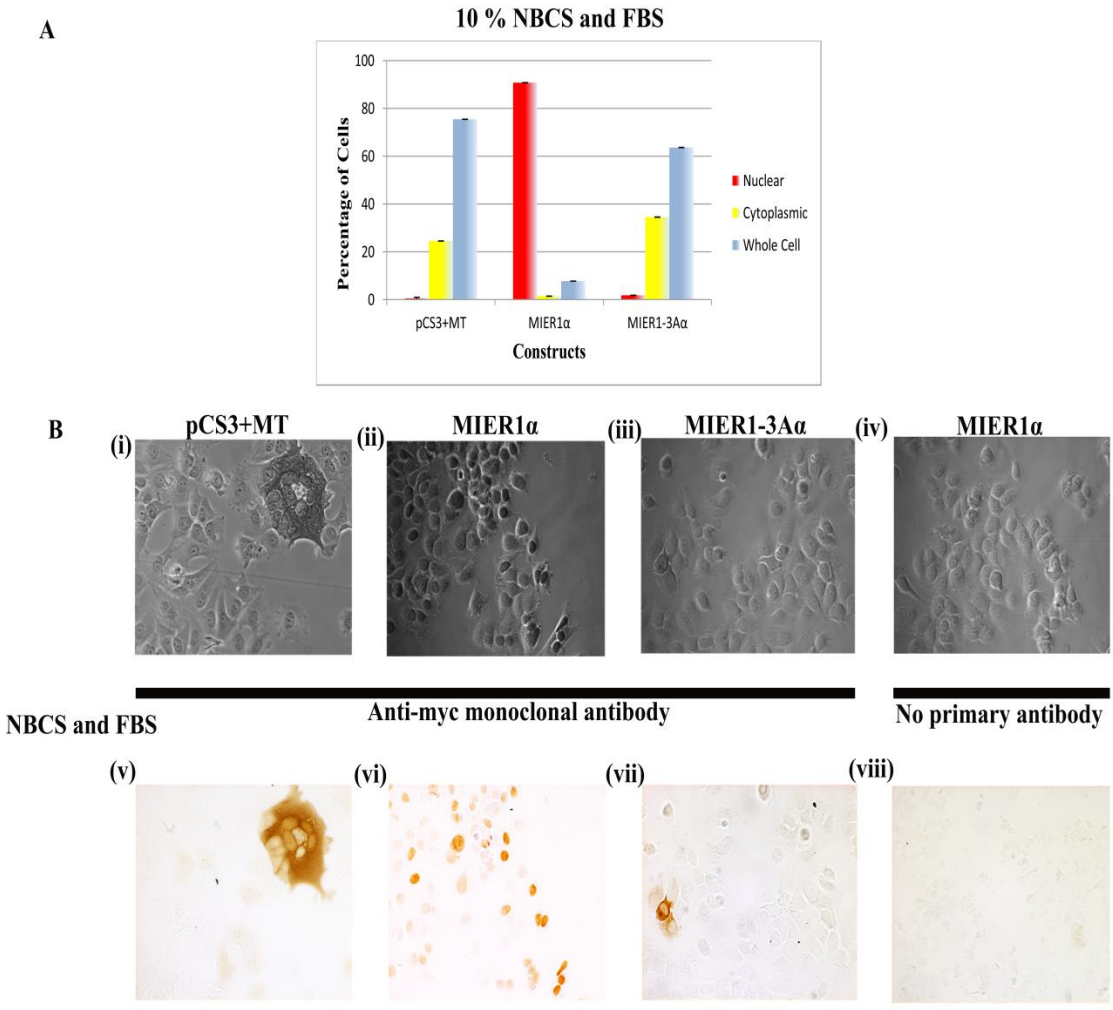
A
10 % NBCS and FBS
Percentage of Cells
100
80
60
40
20
0
pCS3+MT
MIER1α
MIER1-3Aα
Constructs
Nuclear
Cytoplasmic
Whole Cell
B
(i) pCS3+MT
(ii) MIER1α
(iii) MIER1-3Aα
(iv) MIER1α
NBCS and FBS
Anti-myc monoclonal antibody
No primary antibody
(v)
(vi)
(vii)
(viii)

Figure 3.8.2: The Effect of 10 % NBCS and FBS on the Localization of MIER1 Isoforms in MCF7 Cells 96 hours after Transfection

MCF7 cells were transfected with pCS3+MT tagged control (denoted pCS3+MT), pCS3+MT*MIER1*α (denoted MIER1α) and pCS3+MT*MIER1-3A*α (denoted MIER1-3Aα), and incubated for 24 hrs in DMEM without antibiotics. Following the 24 hrs, MCF7 transfected cells were seeded at a density of 50,000 cells/well of 8-well chamber slides and grown in MCF7 DMEM media supplemented with 10 % NBCS and FBS. The chamber slides were incubated for 96 hrs after transfection and ICC performed using an anti-myc tag antibody to analyze localization. Figure 3.8.2 A represents the localization of pCS3+MT tagged control (denoted pCS3+MT) (n=5), pCS3+MT*MIER1*α (denoted MIER1α) (n=6) and pCS3+MT*MIER1-3A*α (denoted MIER1-3Aα) (n=6) in MCF7 cells incubated in 10 % NBCS and FBS for 96 hrs after transfection ± S.D.. The y-axis represents the percentage of cells in each category and the x-axis represents the MIER1 constructs. The appeared increase in MIER1-3Aα nuclear localization in 10 % Tet-approved FBS (Figure 3.8.4) compared to incubation in 10 % NBCS and FBS after 96 hrs of incubation was significant ($p=0.0041$). The appeared increase in whole cell localization of MIER1α in 10 % Tet-approved FBS (Figure 3.8.4) compared to incubation in 10 % NBCS and FBS after 96 hrs of incubation was significant ($p=0.00076$). The appeared decrease in MIER1α and MIER-3Aα cytoplasmic localizations in 10 % Tet-approved FBS (Figure 3.8.4) compared to incubation in 10 % NBCS and FBS after 96 hrs of incubation were significant ($p=0.035$ and $p=0.00011$, respectively). Figure 3.8.2 B are representative ICC images at 200x magnification of MCF7 cells transfected with pCS3+MT tagged control (denoted pCS3+MT) (i); pCS3+MT*MIER1*α (denoted MIER1α) (ii); pCS3+MT*MIER1-3A*α (denoted MIER1-3Aα) (iii); and MIER1α control (iv) and incubated in the DMEM media supplemented with 10 % NBCS and FBS for 96 hrs after transfection. The latter images, v, vi, vii, viii, of Figure 3.8.2 B were taken in bright field.

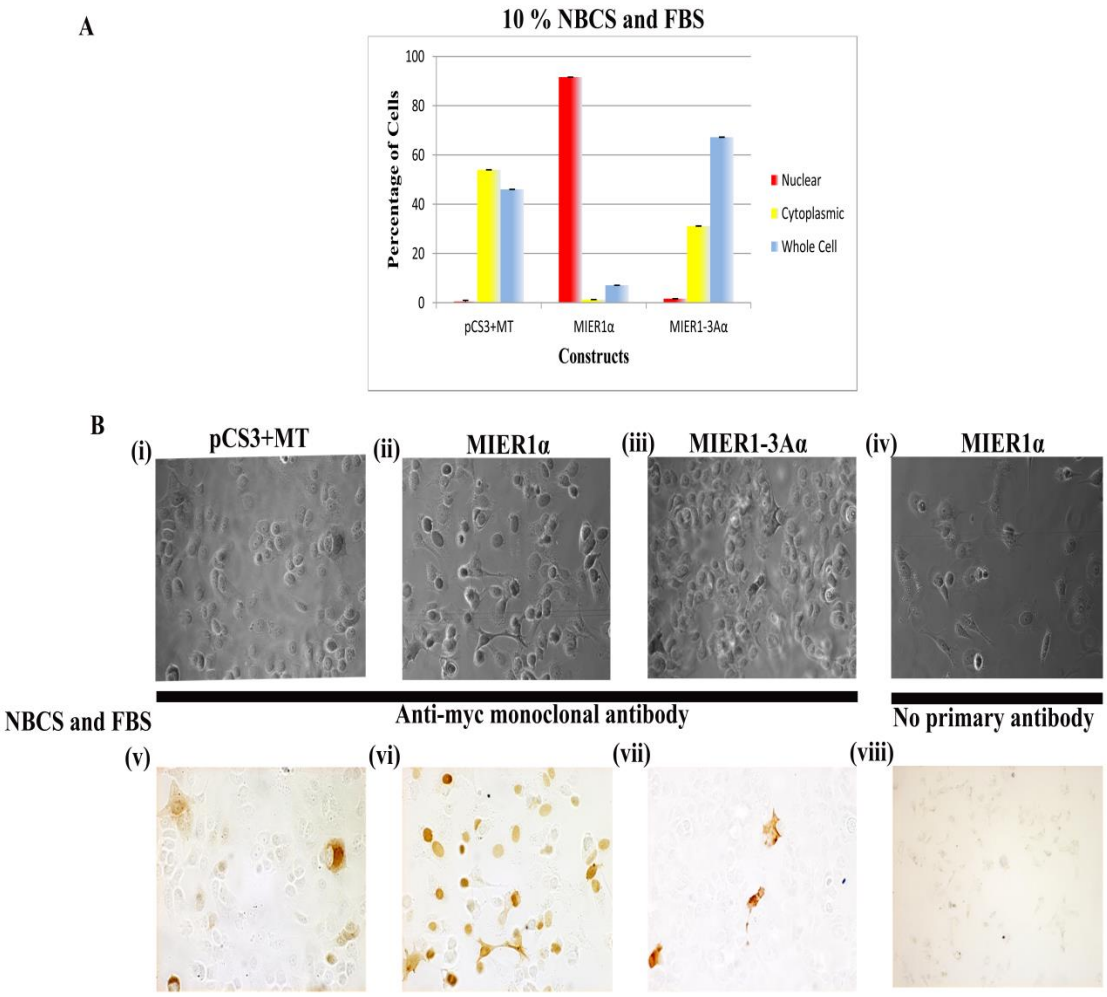
A
10 % NBCS and FBS
Percentage of Cells
100
80
60
40
20
0
pCS3+MT
MIER1α
MIER1-3Aα
Constructs
Nuclear
Cytoplasmic
Whole Cell
B
(i) pCS3+MT
(ii) MIER1α
(iii) MIER1-3Aα
(iv) MIER1α
NBCS and FBS
Anti-myc monoclonal antibody
No primary antibody
(v)
(vi)
(vii)
(viii)

Figure 3.8.3: The Effect of 10 % Tet-approved FBS on the Localization of MIER1 Isoforms in MCF7 Cells 72 hours after Transfection

MCF7 cells were transfected with pCS3+MT tagged control (denoted pCS3+MT), pCS3+MT*MIER1*α (denoted MIER1α) and pCS3+MT*MIER1-3A*α (denoted MIER1-3Aα), and incubated for 24 hrs in DMEM without antibiotics. Following the 24 hrs, MCF7 transfected cells were seeded at a density of 50,000 cells/well of 8-well chamber slides and grown in MCF7 DMEM media supplemented with 10 % Tet-approved FBS. The chamber slides were incubated for 72 hrs after transfection and ICC performed using an anti-myc tag antibody to analyze localization. Figure 3.8.3 A represents the localization of pCS3+MT tagged control (denoted pCS3+MT) (n=4) pCS3+MT*MIER1*α (denoted MIER1α) (n=4) and pCS3+MT*MIER1-3A*α (denoted MIER1-3Aα) (n=4) in MCF7 cells incubated in 10 % Tet-approved FBS for 72 hrs after transfection ± S.D.. The asterisk represents significant differences between two categories. The y-axis represents the percentage of cells in each category and the x-axis represents the MIER1 constructs. The appeared increase in MIER1α and MIER1-3Aα nuclear localizations in 10 % Tet-approved FBS compared to incubation in 10 % NBCS and FBS (Figure 3.8.1) after 72 hrs of incubation were significant ($p=0.000031$ and $p=0.023$, respectively). The appeared increase in whole cell localization of MIER1-3Aα in 10 % Tet-approved FBS compared to incubation in 10 % NBCS and FBS after 72 hrs of incubation was significant ($p=0.016$). The appeared decrease in MIER1α whole cell localization in 10 % Tet-approved FBS compared to incubation in 10 % NBCS and FBS (Figure 3.8.1) after 72 hrs of incubation was significant ($p=0.0012$). The appeared decrease in MIER1α and MIER-3Aα cytoplasmic localizations in 10 % Tet-approved FBS compared to incubation in 10 % NBCS and FBS after 72 hrs of incubation were significant ($p=0.0010$ and $p=0.00013$, respectively). Figure 3.8.3 B are representative ICC images at 200x magnification of MCF7 cells transfected with pCS3+MT tagged control (denoted pCS3+MT) (i); pCS3+MT*MIER1*α (denoted MIER1α) (ii); pCS3+MT*MIER1-3A*α (denoted MIER1-3Aα) (iii); and MIER1α control (iv) and incubated in the DMEM media supplemented with 10 % Tet-approved FBS for 72 hrs after transfection. The latter images, v, vi, vii, viii, of Figure 3.8.3 B were taken in bright field.

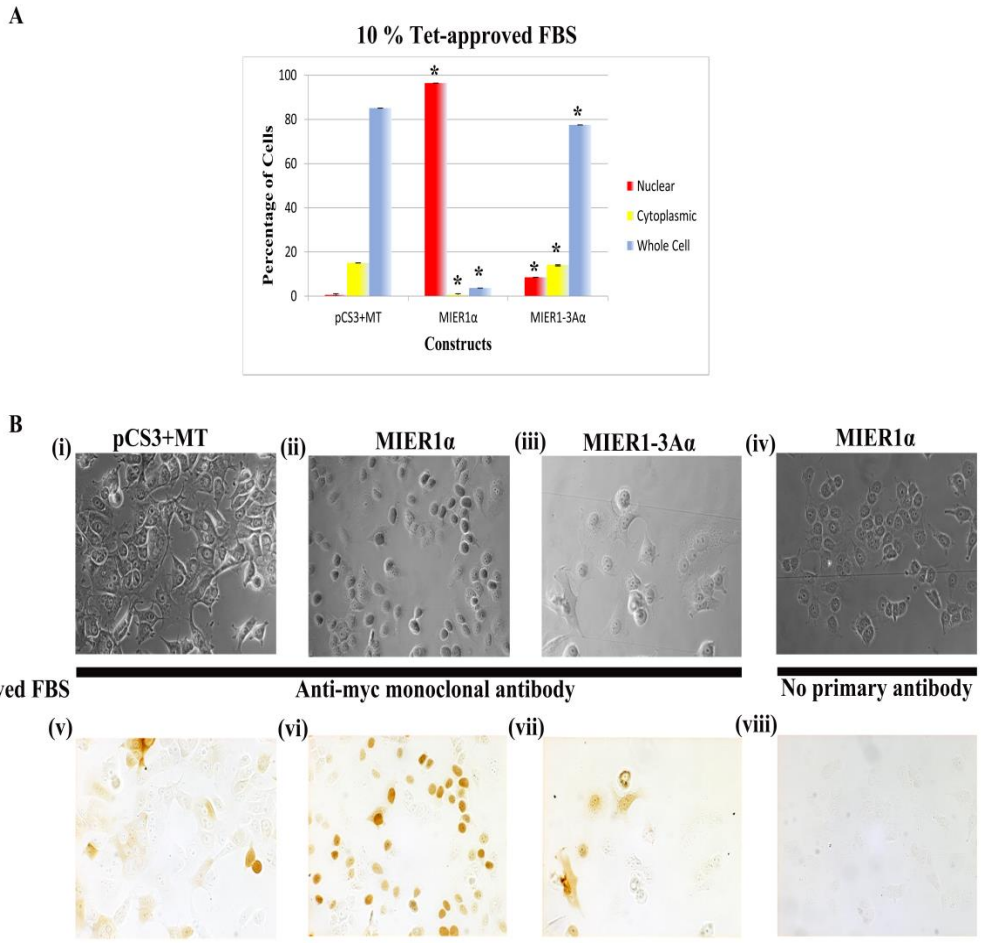
A
10 % Tet-approved FBS
Percentage of Cells
100
80
60
40
20
0
pCS3+MT
MIER1α
MIER1-3Aα
Constructs
Nuclear
Cytoplasmic
Whole Cell
B
(i) pCS3+MT
(ii) MIER1α
(iii) MIER1-3Aα
(iv) MIER1α
Tet-approved FBS
Anti-myc monoclonal antibody
No primary antibody
(v)
(vi)
(vii)
(viii)

Figure 3.8.4: The Effect of 10 % Tet-approved FBS on the Localization of MIER1 Isoforms in MCF7 Cells 96 hrs after Transfection

MCF7 cells were transfected with pCS3+MT tagged control (denoted pCS3+MT), pCS3+MT*MIER1*α (denoted MIER1α) and pCS3+MT*MIER1-3A*α (denoted MIER1-3Aα), and incubated for 24 hrs in DMEM without antibiotics. Following the 24 hrs, MCF7 transfected cells were seeded at a density of 50,000 cells/well of 8-well chamber slides and grown in MCF7 DMEM media supplemented with 10 % Tet-approved FBS. The chamber slides were incubated for 96 hrs after transfection and ICC performed using an anti-myc tag antibody to analyze localization. Figure 3.8.4 A represents the localization of pCS3+MT tagged control (denoted pCS3+MT) (n=3) pCS3+MT*MIER1*α (denoted MIER1α) (n=4) and pCS3+MT*MIER1-3A*α (denoted MIER1-3Aα) (n=4) in MCF7 cells incubated in 10 % Tet-approved FBS for 96 hrs after transfection ± S.D.. The asterisks represent significant differences between two categories. The y-axis represents the percentage of cells in each category and the x-axis represents the MIER1 constructs. The appeared increase in MIER1-3Aα nuclear localization in 10 % Tet-approved FBS compared to incubation in 10 % NBCS and FBS after 96 hrs of incubation was significant ($p=0.0041$). The appeared increase in whole cell localization of MIER1α in 10 % Tet-approved FBS compared to incubation in 10 % NBCS and FBS after 96 hrs of incubation was significant ($p=0.00076$). The appeared decrease in MIER1α and MIER-3Aα cytoplasmic localizations in 10 % Tet-approved FBS compared to incubation in 10 % NBCS and FBS after 96 hrs of incubation were significant ($p=0.035$ and $p=0.00011$, respectively). Figure 3.8.4 B are representative ICC images at 200x magnification of MCF7 cells transfected with pCS3+MT tagged control (denoted pCS3+MT) (i); pCS3+MT*MIER1*α (denoted MIER1α) (ii); pCS3+MT*MIER1-3A*α (denoted MIER1-3Aα) (iii); and MIER1α control (iv) and incubated in the DMEM media supplemented with 10 % Tet-approved FBS for 96 hrs after transfection. The latter images, v, vi, vii, viii, of Figure 3.8.4 B were taken in bright field.

A

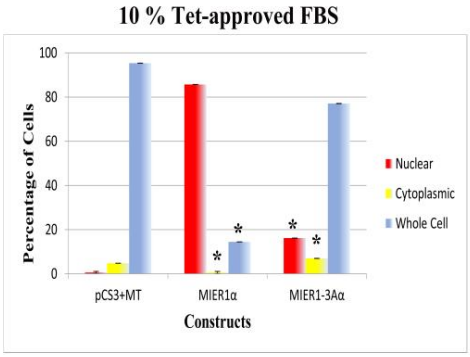
10 % Tet-approved FBS
Percentage of Cells
100
80
60
40
20
0
pCS3+MT
MIER1α
MIER1-3Aα
Constructs
Nuclear
Cytoplasmic
Whole Cell
*
*
*
*

B

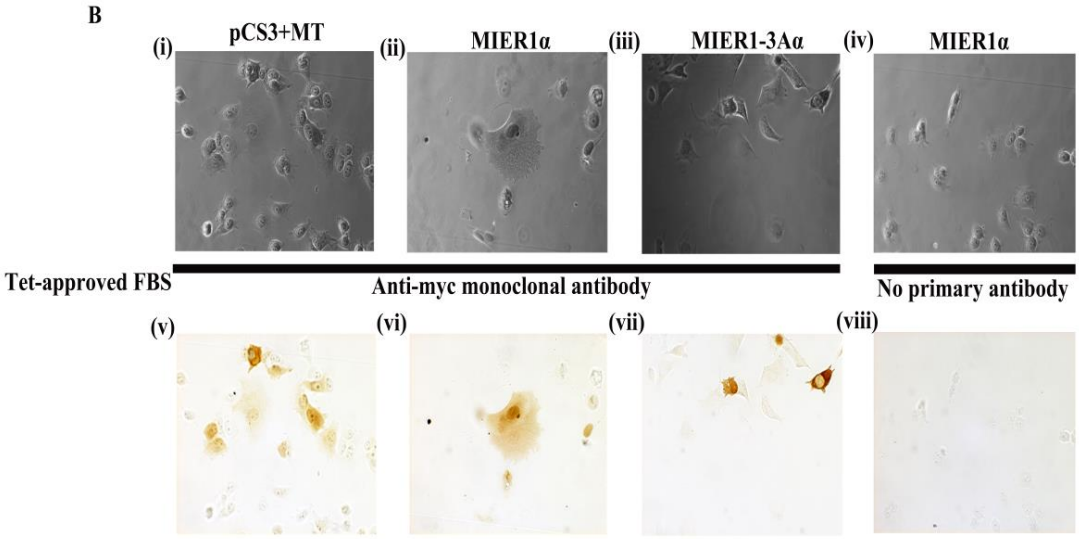
(i) pCS3+MT
(ii) MIER1α
(iii) MIER1-3Aα
(iv) MIER1α
Tet-approved FBS
Anti-myc monoclonal antibody
No primary antibody
(v)
(vi)
(vii)
(viii)

Figure 3.9: Protein Expression of MIER1 Isoforms, MIER1α and MIER1-3Aα, Incubated in Different Types of Serum for 72 and 96 hours after Transfection

MCF7 cells were transfected with pCS3+MT tagged control, pCS3+MT*MIER1*α and pCS3+MT *MIER1-3A*α, and incubated for 24 hrs in DMEM medium without antibiotics. Following the 24 hrs, MCF7 transfected cells were seeded at a density of 40,000 cells/well of 24-well plates and grown in MCF7 DMEM media supplemented with 10 % NBCS and FBS and 10 % Tet-approved FBS for 72 and 96 hrs after transfection. Cell lysates were then prepared as described in the Materials and Methods section, and loaded on the gel for Western blot. The molecular weight of the proteins is indicated on the right. Figure 3.9 A represents the protein expression of MIER1α and MIER1-3Aα 72 hrs after transfection. In lanes 2, 3 and 4, MIER1-3Aα, MIER1α and pCS3+MT tagged control cell extracts incubated in 10 % Tet-approved FBS were loaded onto the gel, respectively. In lanes 6, 7 and 8, MIER1-3Aα, MIER1α and pCS3+MT tagged control cell extracts incubated in 10 % NBCS and FBS were loaded onto the gel. Figure 3.9 B represents the protein expression of MIER1α and MIER1-3Aα 96 hrs after transfection. In lanes 2, 3 and 4, MIER1-3Aα, MIER1α and pCS3+MT tagged control cell extracts incubated in 10 % Tet-approved FBS were loaded onto the gel, respectively. In lanes 6, 7 and 8, MIER1-3Aα, MIER1α and pCS3+MT tagged control cell extracts incubated in 10 % NBCS and FBS were loaded onto the gel. β-actin was used as a loading control.

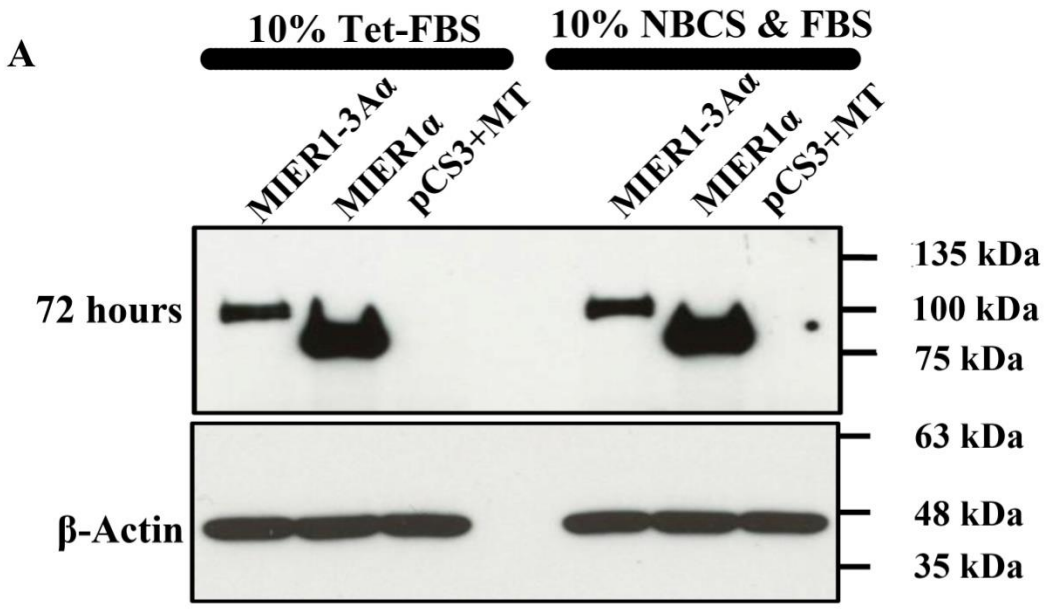
A
10% Tet-FBS
10% NBCS & FBS
MIER1-3Aα
MIER1α
pCS3+MT
MIER1-3Aα
MIER1α
pCS3+MT
72 hours
135 kDa
100 kDa
75 kDa
63 kDa
β-Actin
48 kDa
35 kDa

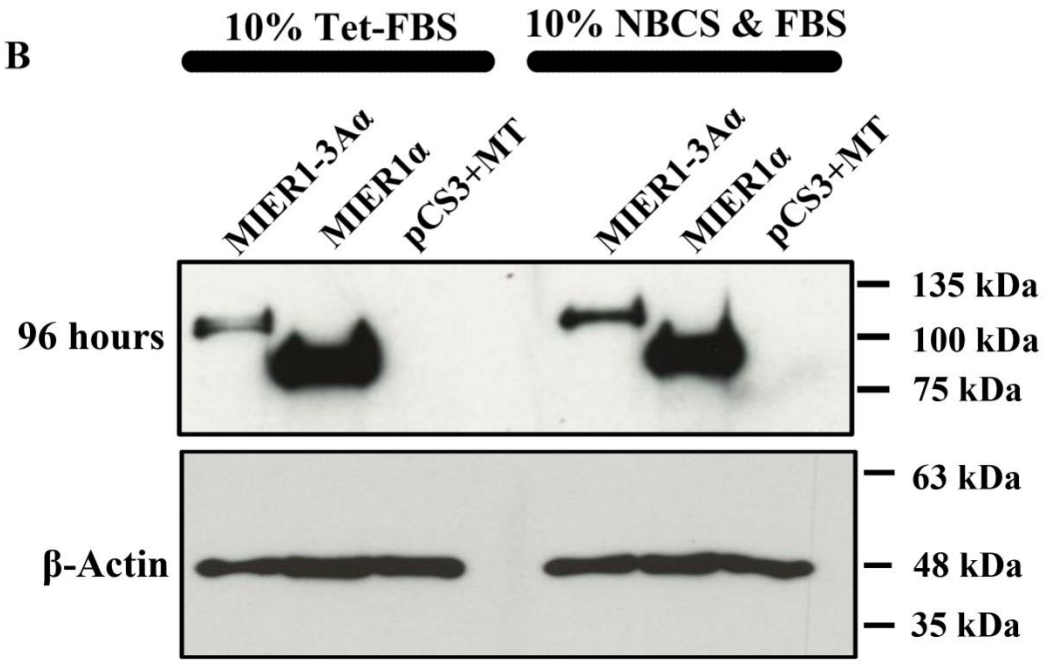
B
10% Tet-FBS
10% NBCS & FBS
MIER1-3Aα
MIER1α
pCS3+MT
MIER1-3Aα
MIER1α
pCS3+MT
96 hours
135 kDa
100 kDa
75 kDa
63 kDa
β-Actin
48 kDa
35 kDa

3.10 The Effect of Low Serum Concentrations on the Localization of MIER1 Isoforms in MCF7 Cells

To determine if low serum concentrations have an effect on the nuclear localization of MIER1 isoforms, MIER1α and MIER1-3Aα, in MCF7 cells, cells were transfected with pCS3+MT tagged control (denoted pCS3+MT), pCS3+MT*MIER1*α (denoted MIER1α) and pCS3+MT*MIER1-3A*α (denoted MIER1-3Aα) and seeded in 8-well chamber slides. The cells were incubated in DMEM media supplemented with 0.2 % NBCS and FBS and 0.2 % Tet-approved FBS for 72 hrs after transfection. The stained cells were categorized as having nuclear, cytoplasmic or whole cell staining.

Figure 3.10.1 A represents the localization of pCS3+MT, MIER1α, and MIER1-3Aα in MCF7 cells incubated in 0.2 % NBCS and FBS compared to those incubated in 0.2 % Tet-approved FBS (Figure 3.10.2 A) for 72 hrs after transfection. As shown in Figure 3.10.1 A, MIER1α localization appeared nuclear in 73.5 %, cytoplasmic in 1 % and whole cell in 25.5 % of cells in 0.2 % NBCS and FBS compared to nuclear in 93.5 %, cytoplasmic in 0 % and whole cell in 6.5 % of cells in 0.2 % Tet-approved FBS (Figure 3.10.2 A) after 72 hrs of incubation. MIER1-3Aα localization appeared nuclear in 5.6 %, cytoplasmic in 25.8 % and whole cell in 68.5 % of cells in 0.2 % NBCS and FBS compared to 16.9 % nuclear, 18.6 % cytoplasmic and 64.4 % whole cell in 0.2 % Tet-approved FBS after 72 hrs of incubation.

Figure 3.10.1 B and Figure 3.10.2 B are representative ICC images of MCF7 transfected cells and the MIER1α control incubated in DMEM media supplemented with 0.2 % NBCS and FBS and 0.2 % Tet-approved FBS for 72 hrs after transfection, respectively. The MIER1α control represents MCF7 cells transfected with

pCS3+MT*MIER1*α but, not stained with the primary antibody, anti-myc tag antibody, when ICC was performed 72 hrs after transfection. Therefore, the secondary antibody has no primary antibody to bind and as a result no staining was observed.

The results from Figures 3.6.1 A, 3.6.2 A, 3.6.3 A, 3.8.1 A, 3.8.2 A, 3.8.3 A, 3.8.4 A, 3.10.1 A and 3.10.2 A, have shown that serum concentration and composition appear to have an effect on nuclear localization. Serum, as stated in the introduction, contains many components including hormones and growth factors. These growth factors are shown in Appendix 1, and include, but not limited to, insulin-like growth factor, epidermal growth factor and fibroblast growth factor. Therefore, it was important to investigate if one of these growth factors has an effect on the localization of MIER1α in MCF7 cells.

3.11 The Effect of Insulin on Nuclear Localization of MIER1α in MCF7 Cells

Insulin is an exogenous growth factor that can promote proliferation through stimulation of the insulin receptor (IR) and IGF-1R, and activation of the extracellular-signaling-regulated kinase cascade (ERK; Hunt *et al.*, 1997; Sciacca *et al.*, 2012). In MCF7 cells, insulin stimulates IR tyrosine kinase activity and initiates a mitogenic effect via the insulin receptors and IGF-1R (Milazzo *et al.*, 1992). Studies have shown that insulin causes translocation of proteins from the nucleus to the cytoplasm

Figure 3.10.1 : The Effect of 0.2 % NBCS and FBS on the Localization of MIER1 Isoforms in MCF7 Cells

MCF7 transfected cells were seeded at a density of 50,000 cells/well of 8-well chamber slides and grown in MCF7 DMEM media supplemented with 0.2 % NBCS and FBS. The chamber slides were incubated for 72 hrs after transfection and ICC performed using an anti-myc tag antibody to analyze localization. Figure 3.10.1 A represents the localization of pCS3+MT tagged control (denoted pCS3+MT) (n=6), pCS3+MT*MIER1*α (denoted MIER1α) (n=6) and pCS3+MT*MIER1-3A*α (denoted MIER1-3Aα) (n=5) in MCF7 cells incubated in 0.2 % NBCS and FBS for 72 hrs after transfection ± S.D.. The y-axis represents the percentage of cells in each category and the x-axis represents the MIER1 constructs. The appeared increase in MIER1α and MIER1-3Aα nuclear localizations in 0.2 % Tet-approved FBS (Figure 3.10.2) compared to incubation in 0.2 % NBCS and FBS after 72 hrs of incubation were significant (p=0.0000000000012 and p=0.025, respectively). The appeared decrease in MIER1α whole cell localization in 0.2 % Tet-approved FBS (Figure 3.10.2) compared to incubation in 0.2 % NBCS and FBS after 72 hrs of incubation was significant (p=0.0000000000088). Figure 3.10.1 B represents ICC images at 200x magnification of different cells transfected with pCS3+MT tagged control (denoted pCS3+MT) (i); pCS3+MT*MIER1*α (denoted MIER1α) (ii); pCS3+MT*MIER1-3A*α (denoted MIER1-3Aα) (iii); and MIER1α control (iv) and incubated in DMEM media supplemented with 0.2 % NBCS and FBS for 72 hrs after transfection. The latter images, v, vi, vii and viii, of Figure 3.10.1 B were taken in bright field.

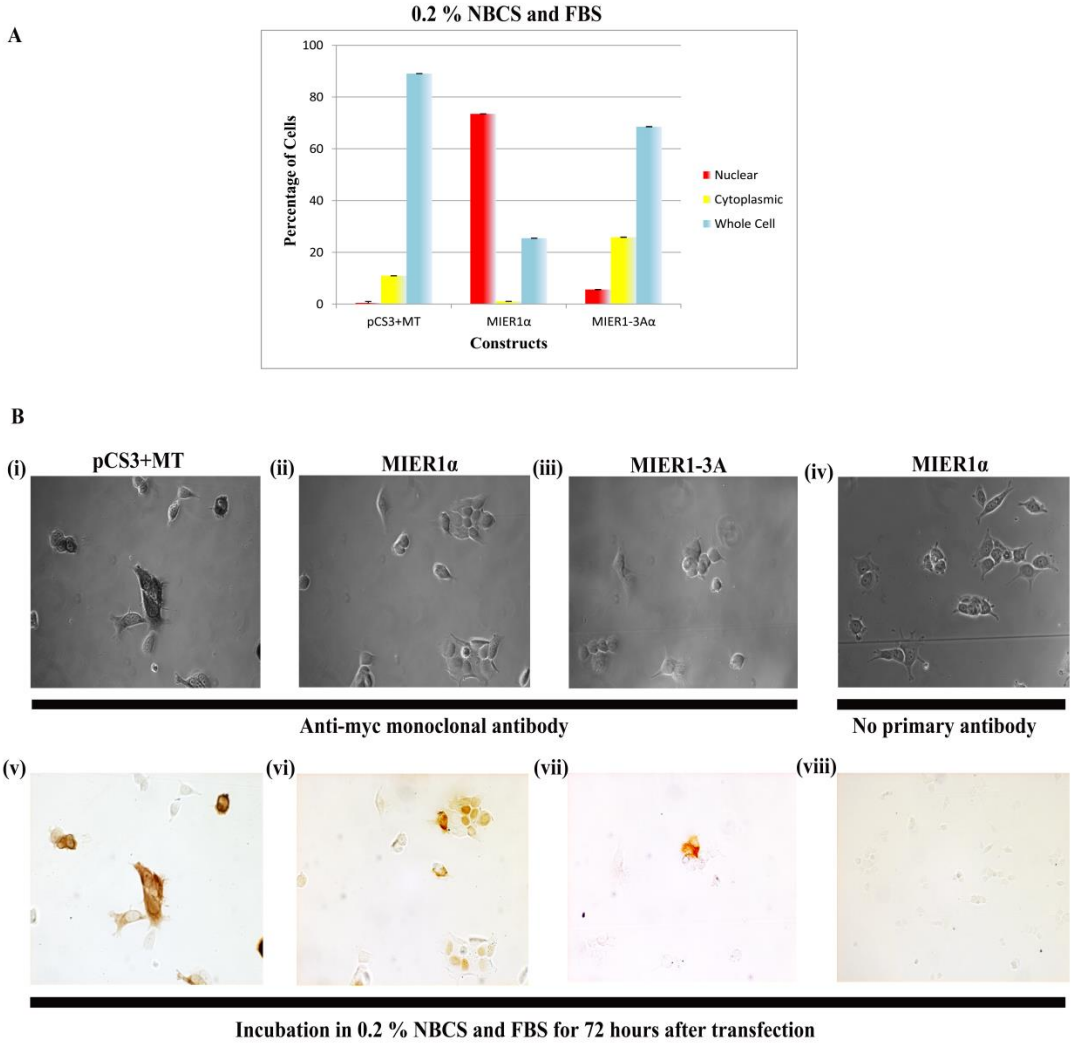
A
0.2 % NBCS and FBS
Percentage of Cells
100
80
60
40
20
0
pCS3+MT
MIER1α
MIER1-3Aα
Constructs
Nuclear
Cytoplasmic
Whole Cell
B
(i) pCS3+MT
(ii) MIER1α
(iii) MIER1-3A
(iv) MIER1α
Anti-myc monoclonal antibody
No primary antibody
(v)
(vi)
(vii)
(viii)
Incubation in 0.2 % NBCS and FBS for 72 hours after transfection

Figure 3.10.2 : The Effect of 0.2 % Tet-approved FBS on the Localization of MIER1 Isoforms in MCF7 Cells

MCF7 transfected cells were seeded at a density of 50,000 cells/well of 8-well chamber slides and grown in MCF7 DMEM media supplemented with 0.2 % Tet-approved FBS. The chamber slides were incubated for 72 hrs after transfection and ICC performed using an anti-myc tag antibody to analyze localization. Figure 3.10.2 A represents the localization of pCS3+MT tagged control (denoted pCS3+MT) (n=5), pCS3+MT*MIER1*α (denoted MIER1α) (n=5) and pCS3+MT*MIER1-3A*α (denoted MIER1-3Aα) (n=4) in MCF7 cells incubated in 0.2 % Tet-approved FBS for 72 hrs after transfection ± S.D.. The asterisks represent significant differences between two categories. The y-axis represents the percentage of cells in each category and the x-axis represents the MIER1 constructs. The appeared increase in MIER1α and MIER1-3Aα nuclear localizations in 0.2 % Tet-approved FBS compared to incubation in 0.2 % NBCS and FBS (Figure 3.10.1) after 72 hrs of incubation were significant (p=0.0000000000012 and p=0.025, respectively). The appeared decrease in MIER1α whole cell localization in 0.2 % Tet-approved FBS compared to incubation in 0.2 % NBCS and FBS (Figure 3.10.1) after 72 hrs of incubation was significant (p=0.0000000000088).Figure 3.10.2 B represents ICC images at 200x magnification of different cells transfected with pCS3+MT tagged control (denoted pCS3+MT) (i); pCS3+MT*MIER1*α (denoted MIER1α) (ii); pCS3+MT*MIER1-3A*α (denoted MIER1-3Aα) (iii); and MIER1α control (iv) and incubated in DMEM media supplemented with 0.2 % Tet-approved FBS for 72 hrs after transfection. The latter images, v, vi, vii and viii, of Figure 3.10.2 B were taken in bright field.

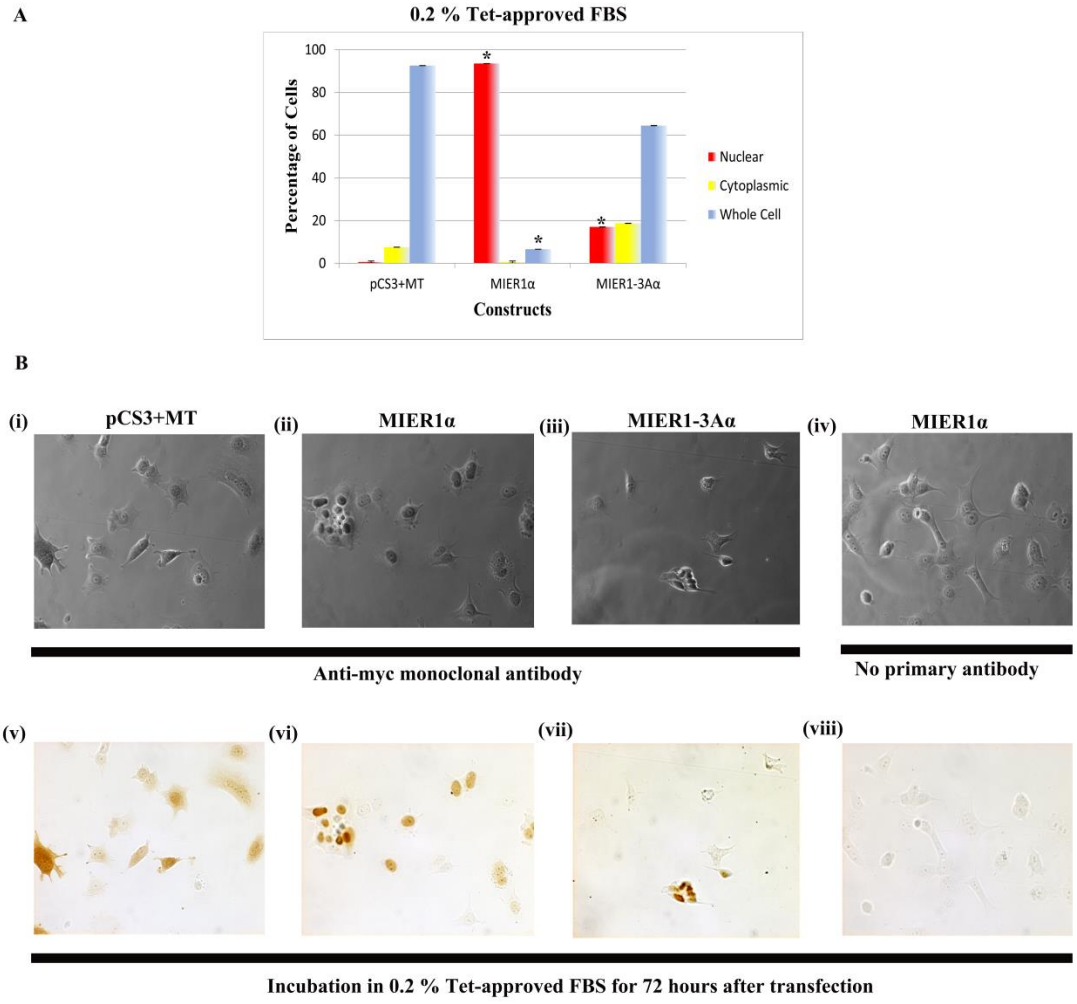
A
0.2 % Tet-approved FBS
Percentage of Cells
100
80
60
40
20
0
pCS3+MT
MIER1α
MIER1-3Aα
Constructs
Nuclear
Cytoplasmic
Whole Cell
B
(i) pCS3+MT
(ii) MIER1α
(iii) MIER1-3Aα
(iv) MIER1α
Anti-myc monoclonal antibody
No primary antibody
(v)
(vi)
(vii)
(viii)
Incubation in 0.2 % Tet-approved FBS for 72 hours after transfection

(Rden, 1999; Wuescher *et al*., 2011). To determine the effect of insulin on nuclear localization of MIER1α in MCF7 cells, Mirus™ transfection of pCS3+MT and MIER1α in MCF7 cells was performed. MCF7 cells were seeded at a density of 20,000 cells/200 uL in two 8-well chamber slides and incubated in DMEM media supplemented with 10 % NBCS and FBS overnight. Twenty-four hours later, Mirus™ Transfection of pCS3+MT and MIER1α in MCF7 cells was performed. Twenty four hours after transfection, the media was aspirated from each well and in one slide, 200 uL of DMEM media with 10 % NBCS and FBS was added, and in the other slide, 200 uL of DMEM with 10 % NBCS and FBS plus 4 ug/mL insulin was added. Twenty-eight hrs following transfection, ICC was performed using an anti-myc tag antibody to analyze localization. The stained cells were categorized as having nuclear, cytoplasmic or whole cell staining.

As shown in Figure 3.11.2 A, after four hours incubation in 10 % NBCS and FBS plus insulin, nuclear localization of MIER1α appeared to decrease and cytoplasmic and whole cell localizations appeared to increase compared to incubation in 10 % NBCS and FBS (Figure 3.11.1 A). As shown in Figure 3.11.2 A, after incubation in 10 % NBCS and FBS plus insulin, 34.1 % of cells appeared to show nuclear localization of MIER1α compared to 60.7 % in 10 % NBCS and FBS (Figure 3.11.1 A). Cytoplasmic and whole cell localizations of MIER1α appeared to increase to 11.2 % and 54.7 % respectively, following incubation in 10 % NBCS and FBS plus insulin compared to 3.9 % and 35.4 % in 10 % NBCS and FBS.

Figure 3.11.1 B and Figure 3.11.2 B are representative ICC images of MCF7 transfected cells and the MIER1α control incubated in the DMEM media supplemented with 10 % NBCS and FBS and 10 % NBCS and FBS plus insulin for 28 hrs after transfection, respectively. The MIER1α control represents MCF7 cells transfected with pCS3+MT*MIER1*α but, not stained with the primary antibody, anti-myc tag antibody, when ICC was performed 72 hrs after transfection. Therefore, the secondary antibody has no primary antibody to bind and as a result no staining was observed.

These results showed that the addition of insulin to the DMEM media appeared to have an effect on nuclear localization of MIER1α in MCF7 cells. In future studies, it would be interesting to evaluate the effect of other growth factors, such as estrogen on the localization of MIER1α in MCF7 cells.

Figure 3.11.1: The Effect of No Insulin on Nuclear Localization of MIER1α in MCF7 Cells

Mirus™ Transfection of pCS3+MT tagged control (denoted pCS3+MT) and pCS3+MT*MIER1*α (denoted MIER1α) in MCF7 cells was performed. Twenty four hours after transfection, the media was aspirated from each well and 200 uL of DMEM media with 10 % NBCS and FBS was added. The slides were incubated for an additional 4 hrs, and ICC performed using an anti-myc tag antibody to analyze localization. Figure 3.11.1 A represents the localization of MIER1α in MCF7 cells incubated in DMEM medium with 10 % NBCS and FBS (n=3) 28 hrs after transfection ± S.D.. The y-axis represents the percentage of cells and the x-axis represents the MIER1 constructs. The appeared decrease in MIER1α nuclear localization, and the appeared increase in cytoplasmic and whole cell localizations of MIER1α after incubation in 10 % NBCS and FBS plus insulin (Figure 3.11.2) compared to incubation in 10 % NBCS and FBS were significant ($p=0.0000000000028$, $p=0.000010$ and $p=0.00000000053$, respectively). Figure 3.11.1 B represents ICC images at 200x magnification of different cells transfected with MIER1α control (i); pCS3+MT (ii); and MIER1α (iii) and incubated in DMEM medium supplemented with 10 % NBCS and FBS for 28 hrs after transfection. The latter images, iv, v and vi, of Figure 3.11.1 B were taken in bright field.

A

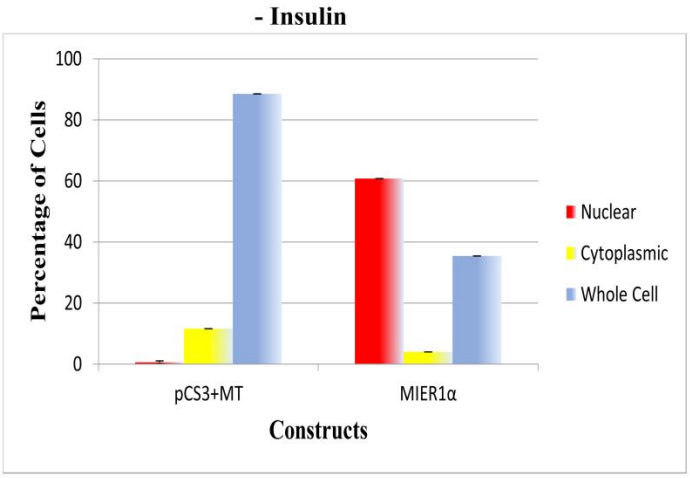
- Insulin
100
80
60
40
20
0
Percentage of Cells
Nuclear
Cytoplasmic
Whole Cell
pCS3+MT
MIER1α
Constructs

B

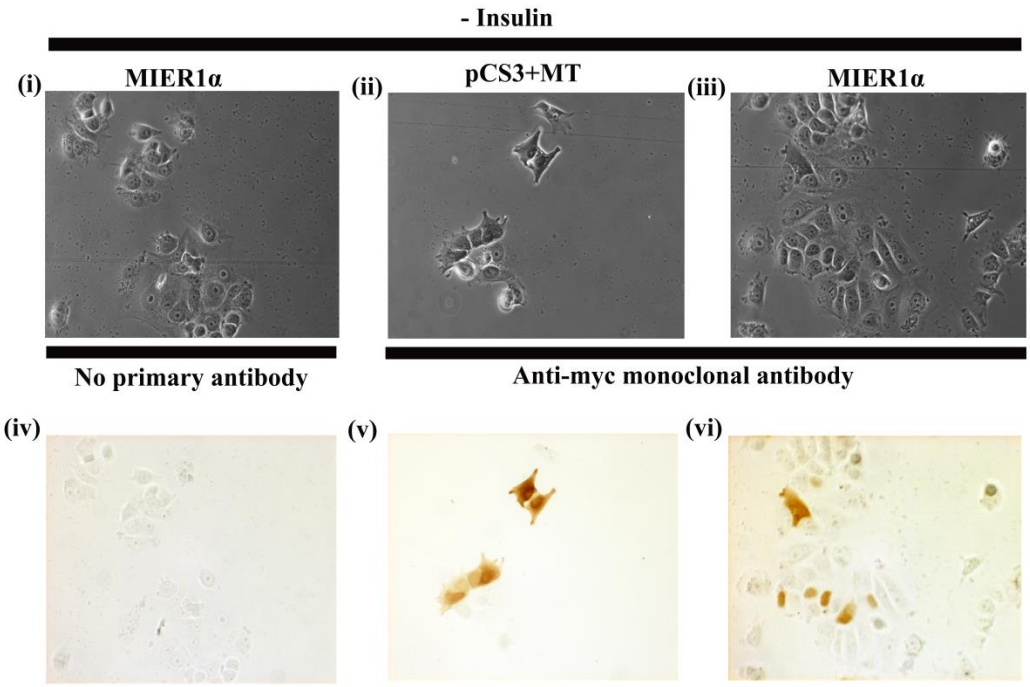
- Insulin
(i)
MIER1α
(ii)
pCS3+MT
(iii)
MIER1α
No primary antibody
Anti-myc monoclonal antibody
(iv)
(v)
(vi)

Figure 3.11.2: The Effect of Insulin on Nuclear Localization of MIER1α in MCF7 Cells

Mirus™ Transfection of pCS3+MT tagged control (denoted pCS3+MT) and pCS3+MT*MIER1*α (denoted MIER1α) in MCF7 cells was performed. Twenty four hours after transfection, the media was aspirated from each well and 200 uL of DMEM with 10 % NBCS and FBS plus 4 ug/mL insulin was added. The slides were incubated for an additional 4 hrs, and ICC performed using an anti-myc tag antibody to analyze localization. Figure 3.11.2 A represents the localization of MIER1α in MCF7 cells incubated in DMEM medium with 10 % NBCS and FBS plus 4ug/mL insulin (n=3) for 28 hrs after transfection ± S.D.. The asterisks represent significant differences between two categories. The y-axis represents the percentage of cells and the x-axis represents the MIER1 constructs. The appeared decrease in MIER1α nuclear localization, and the appeared increase in cytoplasmic and whole cell localizations of MIER1α after incubation in 10 % NBCS and FBS plus insulin compared to incubation in 10 % NBCS and FBS (Figure 3.11.1) were significant (p=0.0000000000028, p=0.000010 and p=0.00000000053, respectively).Figure 3.11.2 B represents ICC images at 200x magnification of different cells transfected with MIER1α control (i); pCS3+MT (ii); MIER1α (iii) and incubated in DMEM medium supplemented with 10 % NBCS and FBS plus 4ug/mL insulin for 28 hrs after transfection, respectively. The latter images, iv, v, and vi, of Figure 3.11.2 B were taken in bright field.

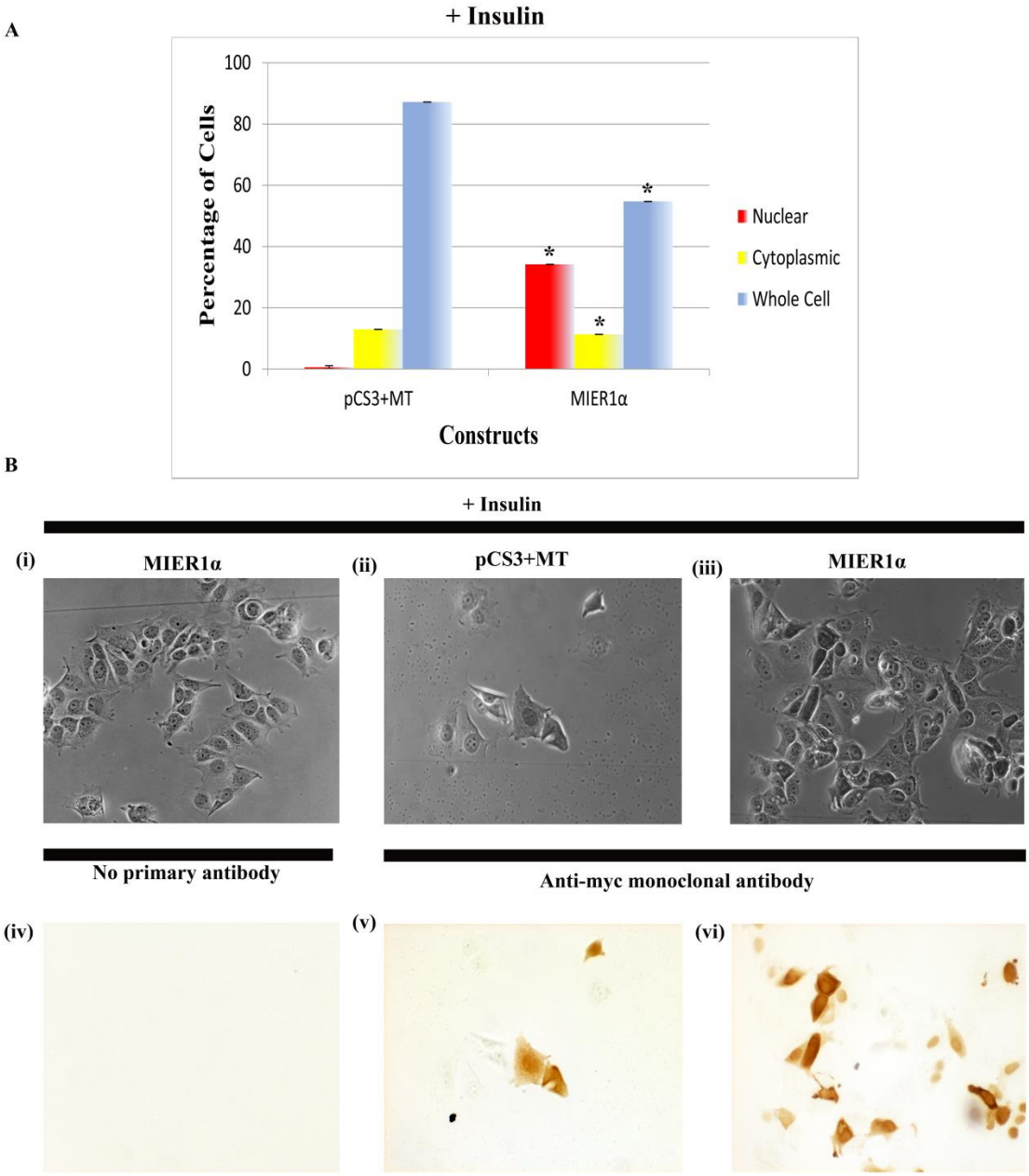
A
+ Insulin
Percentage of Cells
100
80
60
40
20
0
pCS3+MT
MIER1α
Constructs
Nuclear
Cytoplasmic
Whole Cell
*
*
*
B
+ Insulin
(i)
MIER1α
(ii)
pCS3+MT
(iii)
MIER1α
No primary antibody
Anti-myc monoclonal antibody
(iv)
(v)
(vi)

Chapter 4- Discussion

The main objectives of this study were to determine the effect of MIER1α on proliferation of breast carcinoma cell lines, to investigate the effect of factors in serum on localization of MIER1 isoforms, MIER1α and MIER1-3Aα, in MCF7 cells, and MIER1α in T47D cells, and study the effect of insulin on nuclear localization of MIER1α in MCF7 cells. MIER1α is a transcriptional repressor and contains an LXXLL motif for interaction with nuclear hormone receptors. The functional role of the interaction between MIER1α and ERα was investigated (McCarthy *et al.,* 2008). This was measured by the ability of control and MIER1α expressing T47D cells to proliferate in soft agar in the presence of E2. The results showed MIER1α expression by dox induction decreased anchorage-independent growth of T47D cells. The staining pattern of MIER1α in normal and breast carcinoma tissues was determined as nuclear, cytoplasmic or whole cell staining. The results showed a large differential between normal and invasive ductal carcinoma tissues with nuclear MIER1α. Normal tissue and hyperplasia showed 74.7 % and 76.5 % nuclear staining respectively, compared to 50.7 % in ductal carcinoma in situ (DCIS), 25.3 % in invasive lobular carcinoma (ILC) and only 4.4 % in invasive ductal carcinoma (IDC). This loss of nuclear MIER1α suggested a potential role in breast cancer progression. In this present study, the effect of MIER1α on proliferation of MCF7 and T47D cells was investigated.

MIER1α has no effect on MCF7 cell number when compared to non-transfected, pCS3+MT tagged control and mock transfected cells (Figure 3.1 A). There was no effect of MIER1α on MCF7 cell number, as initially hypothesized, and this could be the result

of the transfection efficiency. The moderate transfection efficiency of primary human cells using the electroporation method is 28.9 % to 45.3 % (Liu *et al.*, 2011). The transfection efficiency of MIER1α in these experiments was 56 %, and therefore more than the moderate level. However, in order for MIER1α to have an effect on MCF7 cell number, transfection efficiency may have to be higher. The lack of an effect could also be the result of MIER1α not being 100 % nuclear at this time. As shown in Figure 3.8.2 A, the apparent localization of MIER1α 96 hrs after transfection in 10 % NBCS and FBS was 91.6 % nuclear, 7.1 % whole cell and 1.3 % cytoplasmic. A previous study revealed that MIER1α functions as an ER corepressor and during progression to IDC, MIER1α is shuttled out of the nucleus to the cytoplasm where it is unable to apply its gene/chromatin repressor functions (McCarthy *et al.*, 2008). It is believed this may interfere with the interaction between MIER1α and ERα and could activate signal transduction pathways.

The study, by McCarthy *et al.* (2008), was conducted over an 18 day period with media, dox and E2 replaced every 4 days. In this present study, control and MIER1α expressing T47D cells were incubated for 5 days after the start of doxycycline induction, and there was no change of media or dox during this time. MIER1α had no effect on T47D cells 5 days after the start of dox induction, when compared to TDα5 cells (- dox) and TDc21 cells (+ and - dox; Figure 3.2 A). The percentage of cells expressing MIER1α 5 days after the start of dox induction is only 33 % and therefore, due to the low percentage of cells expressing, it is difficult to determine the real effect of MIER1α on T47D cells. In order to determine the effect of MIER1α on T47D cells, the number of cells expressing may have to be higher. Five days after the start of dox induction (Figure

3.6.3 A), MIER1α appeared nuclear in 17.6 % of cells, appeared cytoplasmic in 33.2 % of cells, and appeared whole cell in 49.2 % of cells. The lack of an effect of MIER1α on T47D cells 5 days after the start of dox induction could be due to the low number of cells expressing, and MIER1α was only 17.6 % nuclear at this time. As stated previously, when MIER1α is shuttled out of the nucleus it is unable to exert its gene/chromatin repressor functions. In Figure 3.2 A five days after the start of dox induction, there is an apparent difference between control and MIER1α expressing T47D cells and this difference could just be the result of clonal variation between cell clones.

The expression of MIER1α in T47D cells decreased dramatically over the 9 day incubation period as shown in Figure 3.3. The Tet-On system, utilized for gene expression in T47D cells, is favoured when gene induction is essential. In this system, gene expression is controlled by the adding of doxycycline to cell culture medium (Zhou *et al.*, 2006). Doxycycline has a half-life of 24 hrs in cell culture and therefore, to maintain stable expression dox should be replaced in medium every 48 hrs (Tet-Off and Tet-On Gene Expression Systems User Manuel, 2012). Therefore, the expression of MIER1α in the stably transfected T47D cell line was determined when dox and media were replaced every 48 hours over the 9 day period. As shown in Figure 3.4, the replacing of dox and media did not increase the expression of MIER1α in the stably transfected T47D cell line 5 days after the start of dox induction. A small increase was observed 9 days after the start of dox induction at 1.7 %, compared to 1 % when the dox and media were not replaced every 48 hours (Figure 3.3). Thus, the decrease in expression of MIER1α could be the result of *in vitro* DNA methylation. DNA methylation plays an

essential regulatory role in gene expression, and methylation of CG dinucleotides (CpGs) has been shown to repress gene transcription (Qu & Ehrlich, 1999). Methylation-induced gene silencing can occur through the inability of transcription factors to bind promoters, or the inhibition of transcription by transcriptional repressors (Doyes & Birdt, 1991; Kass *et al.*, 1997). This was shown in a study which examined the effect of methylation on the expression of plasmid DNA in stably transfected HeLa cells (Qu & Ehrlich, 1999). HeLa cells were stably transfected with methylated or mock methylated plasmids containing neomycin (*neo*) or hygromycin (*hyg*) reporter genes, and the number of colonies from these transfections were compared. The results revealed that CpG-methylation greatly decreased the number of antibiotic-resistant colonies when reporter gene expression was driven by the HSV TK Pr promoter. This decrease in gene expression as a result of CpG-methylation can be prevented with the use of an insulator. An insulator is a regulatory DNA sequence that protects a gene from condensed chromatin and position effects (Burgess-Beusse *et al.,* 2002). Insulators have been developed which can protect genes against the surrounding chromatin with their enhancer blocking ability and barrier activity. The enhancer blocking ability enables the blocking of the promoter from an enhancer, and the barrier activity prevents the activity of chromatin. This was shown in a study which investigated the effect of the cHS4 chromatin insulator on gammaretroviral vector expression in mouse bone marrow (Li & Emery, 2008). The results revealed that marrow transduced with cHS4 chromatin insulated vectors had increased histone acetylation levels and a lower frequency of methylated CpG dinucleotides than uninsulated vectors. Therefore, the cHS4 chromatin insulator was successful in preventing the silencing of the gammaretroviral vector.

When determining the percentage of T47D cells expressing MIER1α over the 9 day period, another observation was made. There appeared to be a change in the localization of MIER1α during this time (Figure 3.5 B). During this 9 day incubation period, the media was not changed on the cells. This could result in the shuttling of MIER1α out of the nucleus, and could be the result of growth factor production by autocrine signalling. Autocrine production of growth factors has been shown to promote growth and survival of carcinoma cells. These growth factors can then act on MIER1α and shuttle it out of the nucleus. This is similar to a study which evaluated the production of transforming growth factor alpha (TGF-α), vascular endothelial growth factor (VEGF), and basic fibroblast growth factor (bFGF) in human cancer cell lines that express epidermal growth factor receptor (EGFR) and TGF-α (Ciardiello *et al.*, 2001). The results showed levels of EGFR and its major ligand, TGF-α, in all cancer cell lines. Epidermal growth factor receptor has been implicated in many processes for tumour formation, not only proliferation but also, invasion, angiogenesis and metastasis. These results suggested an active TGF-α EGFR autocrine growth pathway in these cell lines, and this pathway plays a major role in the progression of human epithelial cancers. The levels of endogenous angiogenic growth factors, basic fibroblast growth factor (bFGF) and vascular endothelial growth factor (VEGF), were measured and present in all cancer cell lines, except for two. To determine the effects of blocking EGFR activation, these cell lines were then treated with a selective epidermal growth factor receptor tyrosine kinase inhibitor, ZD1839, and the levels of TGF-α, bFGF and VEGF were measured. Treatment with ZD1839 decreased the level of TGF-α, bFGF and VEGF in a dose-dependent and time-dependent manner (Ciardiello *et al.*, 2001). Therefore, T47D cells could be

producing growth factors to help promote cell growth and progression, and these growth factors could then be acting on MIER1α and transporting it out of the nucleus. This could explain the appeared increased distribution of MIER1α in the whole cell and cytoplasmic regions after 7 and 9 days of incubation, respectively.

Three days after the start of dox induction, the appeared increase in nuclear localization and the appeared decrease in cytoplasmic localization of MIER1α in T47D cells in 0.2 % Tet-approved FBS compared to 10 % Tet-approved FBS as shown in Figure 3.6.1 A, could first be due to the fact that this FBS, unlike untreated FBS, is charcoal-stripped. Therefore, this FBS contains lower levels of steroid, thyroid and peptide hormones, in particular estradiol and insulin (Cao *et al*., 2009). In charcoal-stripped FBS, estradiol is almost completely removed at 19.8 concentration in non-treated FBS and less than 10 concentration in charcoal-treated FBS. Two other hormones are greatly reduced in charcoal-treated FBS and these are L-Thyroxine (T_4) and 3, 5, 3′-triiodo-L-thyronin (T_3) at 96 % and 77 %, respectively. Vitamins and enzymes are also depleted from charcoal-stripped FBS, and insulin is not detectable. Secondly, 0.2 % Tet-approved FBS contains an even lower level of hormones, steroids and growth factors than 10 % Tet-approved FBS and therefore, less components could be acting on MIER1α and shuttling it out of the nucleus. These results are similar to a study which investigated the PI3K/Akt pathway in serum-free medium in rat C6 glioblastoma cell line (Sephton & Mousseau, 2008). As part of the study, the investigators determined the localization of the regulatory subunit of phosphatidylinositol 3'-kinase (PI3K), p85, in serum-free medium for 4 hrs. In control cells, p85 is localized throughout the cell. However, incubation in

serum-free medium changed the localization to primarily perinuclear. This was also observed for PIP3, phosphatidylinositol 3, 4, 5-trisphosphate, the lipid products of PI3K. In control cells, PIP3 is found distributed throughout the cell and becomes nuclear/perinuclear under serum-free conditions. In another study, the localization of a neuroglobin (NGB), a new neuroprotectant globin, in response to 17-β estradiol treatment was investigated (De Marinis *et al.*, 2013). The human SK-N-BE neuroblastoma cell line was grown in RPMI medium supplemented with 10 % charcoal-stripped fetal bovine serum. The neuroprotectant globin (NGB) is found in the nucleus and cytosol in SK-N-BE cells however, treatment with 1 nM E_2 for only 1 hr is able to reduce the nuclear localization of NGB. This effect is more obvious 24 hrs after treatment and is paired with an increase in localization of NGB in the cytosol and mitochondrial fractions. Thirdly, the localization of SIRT1, an NAD-dependent histone/protein deacetylase, under normal 10 % FBS culture conditions was investigated (Byles *et al.*, 2010). Under normal culture conditions, SIRT1 is localized in the cytoplasm and nucleus in DU_{145} cells. However, after serum depletion for 48 hrs, SIRT1 is greatly reduced in the cytoplasm. When serum was replaced, the decrease in SIRT1 cytoplasmic localization was restored. Lastly, a study which investigated the localization of ribosomal DNA transcription factors UBF1 and UBF2 in Chinese hamster ovary cells (CHO) cultured in serum deprived medium (Mahony *et al.*, 1992). The UBF protein is a nucleolar protein however, after 24 hrs of serum deprivation the protein localization was diffused between the nucleus and cytoplasm. The 0.2 % Tet-approved FBS contains a lower level of components than 10 % Tet-approved FBS and thus, there is an appeared increase in nuclear localization and an

appeared decrease in cytoplasmic localization of MIER1α in 0.2 % Tet-approved FBS 3 days after the start of dox induction.

Five days after the start of dox induction, the appeared decrease in nuclear localization and the appeared increase in whole cell localization of MIER1α in T47D cells in 0.2 % Tet-approved FBS compared to incubation in 10 % Tet-approved FBS (Figure 3.6.3 A), could be the result of growth factor production by autocrine signalling. The production of growth factors in low serum after 5 days incubation would increase the factors in the medium that could be acting on MIER1α and transporting it out of the nucleus. Autocrine production by cells in low serum has been investigated, and has been shown to allow continued growth of cells in the absence of growth factors (van Zoelen *et al.*, 1984). This was demonstrated in a study which investigated the increased proliferation and survival of breast cancer cell lines by autocrine signalling of vascular endothelial growth factor (VEGF; Weigand *et al.*, 2005). The results showed that breast cancer cell lines, MDA-MB-468, T47D, MCF-7 and HBL-100, secrete VEGF-A, and these levels are higher than its biological activity. In certain cell lines studied, T47D, MCF7 and HBL-100, VEGF-A stimulated phosphorylation of vascular endothelial growth factor receptor 2,VEGFR-2. The effect of VEGF-A stimulation on intracellular signalling was also investigated and led to phosphorylation of Akt in T47D cells, and ERK1/2 phosphorylation in MDA-MB-468, MCF7 and HBL-100 cells. Therefore, this study suggested VEGF-A stimulation plays a vital role in cell survival, growth, apoptosis and differentiation. This was demonstrated in another study which determined if mouse neuroblastoma Neuro-2A cells are capable of autocrine production of polypeptide growth

factor (van Zoelen *et al.*, 1984). The results showed that Neuro-2A cells produce a mitogenic transforming growth factor (TGF) in serum-free medium, and this allows the cells to proliferate in soft agar without the presence of added growth factors. In another study, the ability of Kirsten murine sarcoma virus (KiMSV)-transformed rat-1 cells to grow in serum-free medium supplemented with insulin and transferrin but no mitogenic growth factors was investigated (Kaplan *et al.*, 1982). The results revealed that the proliferative ability of the KiMSV cells in this medium is dependent on production of transforming growth factor(s) by these cells. Therefore, T47D cells could be producing growth factors after 5 days of incubation to promote growth and differentiation, and these growth factors could be acting on MIER1α and transporting it out of the nucleus. This could explain the appeared decrease in nuclear localization and the appeared increase in whole cell and cytoplasmic localizations of MIER1α after 5 days of incubation in 0.2 % Tet-approved FBS.

Five days after the start of dox induction, the appeared increase in nuclear localization of MIER1α in T47D cells in 10 % Tet-approved FBS compared to 0.2 % Tet-approved FBS (Figure 3.6.3 A), could be due to the depletion of components from the medium. Cells are cultured in cell culture media supplemented with animal serum which contains a combination of factors that mimic the properties of the *in vivo* environment of origin. Serum contains many components, as shown in Appendix 1, essential for cellular functions including growth, differentiation and proliferation (Ferruzza *et al.*, 2013; Gstraunthaler, 2003). When culturing cells *in vitro,* the culture media has to be changed every few days in order to replenish the nutrients. For these experiments the media was

not changed 5 days after the start of doxycycline induction. The media was not changed on the cells over the 5 day incubation period because the experiment was designed to determine the effect of factors in serum on localization over time. Changing the media every few days would replenish the nutrients present in the cell culture media, including factors of serum. Therefore, the factors in serum would resemble the cell culture media at day 0 and this would alter the design of the experiment. Thus, not changing the media would allow the nutrients, including factors in serum, to be depleted and enable the effect on MIER1α localization to be determined. Factors present in the media could have been depleted over time and no longer act on MIER1α and shuttle it out of the nucleus. This is shown in a study which investigated the localization of Dok1 in mouse embryonic fibroblasts (MEFs; Niu *et al.*, 2006). In D10 cell culture medium containing 10 % serum, Dok1 is localized in the cytoplasm of MEFs. However, after 27 hrs of serum starvation, Dok1 is less in the cytoplasmic region and nuclear localization is increased in a proportion of cells. This result suggested that components of serum are responsible for the localization of Dok1. To further investigate, platelet-derived growth factor (PDGF) was added to serum-starved cells and the subcellular localization of Dok1 was examined. In serum-starved cells, Dok1 is predominantly localized in the nucleus. However, treatment with 40 ng/mL PDGF for 15 mins resulted in cytoplasmic localization. These effects confirmed that serum and growth factors are involved in the shuttling of Dok1 out of the nucleus. This is shown in another study which investigated the localization of transcription factor ERK4 in human non immortalized intestinal epithelial crypt cells (HIEC; Paquin *et al.*, 2013). The effect of growth factor, lysophosphatidic acid (LPA), on nuclear translocation of ERK4 was examined. In quiescent HIEC, E2F4 is localized in the

cytoplasm however, after treatment with 10 uM LPA, E2F4 was translocated to the nucleus. This result indicated that LPA is an important growth factor in serum for E2F4 localization in HIEC (Paquin *et al.*, 2013). Components of serum could therefore be responsible for the localization of MIER1α in T47D cells. Following 5 days incubation, the components of serum are depleted and therefore, no factors present to keep MIER1α out of the nucleus. Therefore, MIER1α nuclear localization appeared to increase, and whole cell and cytoplasmic localizations appeared to decrease.

Seventy two hours after transfection, MIER1α nuclear localization appeared to increase and whole cell localization appeared to decrease in 10 % Tet-approved FBS (Figure 3.8.3) compared to 10 % NBCS and FBS. Seventy-two and ninety six hours after transfection, MIER1-3Aα nuclear localizations appeared to increase and cytoplasmic localizations of MIER1α and MIER1-3Aα appeared to decrease in 10 % Tet-approved FBS (Figures 3.8.3 A and 3.8.4 A) compared to incubation in 10 % NBCS and FBS (Figures 3.8.1 A and 3.8.2 A). This appeared increase in nuclear localizations and the appeared decrease in cytoplasmic localizations of MIER1α and MIER1-3Aα, and the appeared small decrease in whole cell localization of MIER1α, could again be due to the fact that this FBS, unlike fetal bovine serum, is charcoal-stripped. This medium contains less hormones and growth factors, in particular estradiol, than untreated NBCS and FBS and therefore, less components of serum could be acting on MIER1α and MIER1-3Aα and exporting them out of the nucleus. This is similar to a study which investigated the localization of estrogen receptors, ESR1 and ESR2, after treatment with E_2 (Lucas *et al.*, 2008). In the absence of E_2, these estrogen receptors exhibit nuclear localization in

cultured rat Sertoli cells. However, after 10 mins treatment with E_2 nuclear localization of ESR1 and ESR2 was weakly detected and detection was observed in other regions of the cell. This is similar to another study which investigated the localization of estradiol receptor α (ERα) in MCF7 cells in response to estradiol treatment (Lombardi *et al.*, 2008). Thirty minutes treatment with 10 nM E_2 induced nuclear export of ERα in MCF7 cells. This study determined that estradiol induced nuclear export of ERα in a CRM1-dependent manner. Following 72 hrs incubation, the appeared increase in nuclear localization and the appeared decrease in whole cell localization of MIER1α, and following 72 and 96 hrs incubation, the appeared increase in nuclear localization of MIER1-3Aα and the appeared decrease in cytoplasmic localizations of MIER1α and MIER1-3Aα could be the result of less components present in 10 % Tet-approved FBS serum that could be acting on MIER1α and MIER1-3Aα and shuttling them out of the nucleus.

The appeared small increase in whole staining of MIER1-3Aα and MIER1α in MCF7 cells in 10 % Tet-approved FBS 72 and 96 hrs after transfection, respectively (Figures 3.8.3 A and 3.8.4 A) could be due to autocrine production of growth factors by MCF7 cells. This would increase the factors in the medium that could be acting on MIER1α and MIER1-3Aα and transporting them out of the nucleus. This is shown in a study which investigated the ability of FaO rat hepatoma cells to grow in the absence of serum (Sancho & Fabregat, 2010). After 24 hrs incubation in serum-free medium, reactive oxygen species (ROS) was increased and required for autocrine proliferation of FaO rat hepatoma cells. There was an increase in NOX1 mRNA levels correlating with ROS production and therefore, NOX1 and ROS production are required for autocrine

growth in FaO cells. Investigators studied the effect of NOX1 knockdown on autocrine growth. The results revealed that knockdown or inhibition of NOX1 decreased FaO autocrine growth by inhibiting expression of epidermal growth factor receptor (EGFR) and transforming growth factor-α (TGF-α). In a different study, a clone of the MCF7 cell line, MCF-7ras, was established to investigate if growth factors had a potential role in expression of the tumorigenic phenotype (Dickson *et al.*, 1987). The results of this study revealed that the tumorigenic line, MCF7ras, exhibited increased levels of type α transforming growth factor-like growth factor and insulin like growth factor, and promoted tumorigenesis in MCF7 cells. This study revealed that growth factor secretion could replace estrogen dependence by breast cancer cells for a tumorigenic phenotype. Therefore, after 72 and 96 hrs incubation, MCF7 cells could be producing growth factors by autocrine signalling and these growth factors could be acting on MIER1-3Aα and MIER1α and transporting them out of the nucleus. This could explain the appeared increase in whole cell localizations of MIER1-3Aα and MIER1α in 10 % Tet-approved FBS after 72 and 96 hrs incubation respectively.

As shown in Figure 3.10.2 A, nuclear localizations of MIER1α and MIER1-3Aα appeared to increase after 72 hrs incubation in 0.2 % Tet-approved FBS. This appeared increase in nuclear localization of MIER1 isoforms in 0.2 % Tet-approved FBS could again be due to the fact that this FBS, unlike fetal bovine serum, is charcoal-stripped. Once more, this FBS contains lower levels of growth factors and hormones, in particular insulin and estradiol (Cao *et al.*, 2009). Therefore, incubation in Tet-approved FBS provides less growth factors and hormones that could be acting on these isoforms and

shuttling them out of the nucleus. This is similar to a study which investigated the localization of ER1β splice variants fused to GFP in Chinese hamster ovary cells (CHO) cultured in media 2 x charcoal stripped (Price *et al.*, 2001). The results showed that cells expressing GFP alone were localized in the cytoplasm and nucleus, and that the presence of estradiol (E_2) did not have an effect on localization. However, in the absence of steroids, ERα, ERβ1 and ERβ2 fused to GFP showed nuclear localization. In another study the localization of ERα and ERβ in the presence of E_2 in MCF7 cells was investigated (Chen *et al.*, 2004). The results showed that cells not treated with E_2 showed little ERα and ERβ in the mitochondria however, the amount of mitochondrial ER1α and ER1β increased with time of E_2 treatment. Lastly, a study investigated the effect of 0.5 % charcoaled-stripped FBS media supplemented with estrogen on the localization of steroid hormone regulation EMP2 in RL95-2 cells (Wadehra *et al.*, 2008). In vehicle control cells, EMP2 expression was found localizing in the Golgi apparatus at 31.7 of total EMP2, and the plasma membrane. Following estradiol treatment, less EMP2 expression was observed on the plasma membrane and there was increased expression in intracellular compartments of the Golgi apparatus at 42.5 of total GMP2. The cell culture media supplemented with 0.2 % Tet-approved FBS contains less components, such as hormones and growth factors, than 0.2 % NBCS and FBS that could act on the MIER1 isoforms, MIER1α and MIER1-3Aα, and shuttle them out of the nucleus.

Seventy-two hours after transfection, whole cell localization of MIER1α also decreased in 0.2 % Tet-approved FBS at 6.5 % compared to 25.5 % in 0.2 % NBCS and FBS. This appeared increase in nuclear localizations of MIER1α and MIER1-3Aα, and

appeared decrease in whole cell staining of MIER1α is similar to a study which investigated the localization of glyceraldehyde 3-phosphate dehydrogenase (GAPDH) in human diploid fibroblasts (HDFs; Kwon *et al.*, 2010). HDFs were maintained in culture medium containing 10 % FBS for 2 days and then incubated in serum free medium. Almost all GAPDH was present in the cytosol of HDFs after 2 days incubation in 10 % FBS however, serum withdrawal induced nuclear localization of GAPDH and nuclear localization increased until 5 days. After serum depletion for 4 to 5 days, 90 % of HDFs showed nuclear GADPH. In another study, a change in localization of androgen receptor (AR) under different serum conditions was observed (Gerdes *et al.*, 1998). In the PS-1 rat prostate smooth muscle cell line, AR exhibited cytoplasmic localization in serum containing medium. The PS-1 cells were seeded in serum containing medium and allowed to attach for 24 hrs, and then the medium was changed to serum-free medium for 24 hrs. After 24 hrs in serum-free medium, there was induced nuclear localization of AR. Therefore, 0.2 % Tet-approved FBS provides less growth factors and hormones that can act on MIER1 isoforms in MCF7 cells and shuttle them out of the nucleus.

As shown in Figure 3.11.2 A, twenty-eight hours after transfection in 10 % NBCS and FBS plus insulin, MIER1α nuclear localization appeared to decrease, and cytoplasmic and whole cell localizations appeared to increase, compared to incubation in 10 % NBCS and FBS (Figure 3.11.1 A). The appeared nuclear localization of MIER1α after incubation in 10 % NBCS and FBS plus insulin was 34.1 % compared to 60.7 % in 10 % NBCS and FBS. Cytoplasmic and whole cell localizations of MIER1α appeared to increase to 11.2 % and 54.7 %, respectively following incubation in 10 % NBCS and FBS plus insulin compared to 3.9 % and 35.4 % in 10 % NBCS and FBS. This is similar to the

results of a study in which the localization of a member of the forkhead of transcription factors, FKHR1, in serum deprived medium after 24 hrs was investigated (Rden, 1999). In serum free medium, FKHR1 was found in the nucleus in 90 % of cells. It was believed extracellular growth signals were responsible for nuclear export of the transcription factor. Therefore, serum-deprived cells were treated with insulin-like growth factor and FKHR1 was exported from the nucleus in 70 % of cells. In another study the investigators determined the effect of insulin on menin, the nuclear protein product of the *MEN1* gene, expression in primary hepatocytes (Wuescher *et al.*, 2011). After 24 hrs exposure to 100 nM insulin, induced translocation of menin from the nucleus to the cytoplasm. Insulin is an extracellular growth factor which when added to the media could therefore be acting on MIER1α and transporting it out of the nucleus

The subcellular localization of proteins is increasingly important for the regulation of protein function. As stated in section 1.3, the nuclear localization of retinoblastoma protein (pRb) in cyclin-dependent kinase 4 wild-type ($Cdk4^{WT}$) mouse embryo fibroblasts (MEFs) is essential for its role as a negative regulator of cell proliferation (Jiao *et al.*, 2006). However, when the localization of pRb changes from nuclear to cytoplasmic in cyclin-dependent kinase 4 mutant ($Cdk4^{R/R}$) MEFs due to a cyclin-dependent kinase 4 mutant ($Cdk4^{R24C}$), these cells showed increased cell growth and tumorigenesis. This is similar to another study which investigated the localization of peroxisome proliferator-activated receptor PPARγ in breast cancer cell lines (Cheng *et al.*, 2013). In MCF7 cells (ER positive), PPARγ is localized in the nucleus however, in MDA-MB-231 (ER negative) PPARγ is localized in the cytoplasm. The nuclear export of PPARγ inhibits its ability to transactivate nuclear target genes thereby, reducing the ability of PPARγ to

decrease cell proliferation and induce apoptosis in breast cancer cells. The regulation of subcellular localization is important for another tumour suppressor, p53. p53 is known as the "guardian of the genome", and the cellular localization of p53 is important for its function (O'Brate & Giannakakou, 2003). If cellular stress occurs, the nuclear localization of p53 is important to evoke its function and inhibit the growth of malignant cells. In many tumour types, p53 activity is loss and this is associated with cytoplasmic localization. These tumour types have a decreased response to the stresses of radiotherapy and chemotherapy, and poor long-term patient survival. The cytoplasmic sequestering of p53 inactivates the gene, leading to a decreased DNA damage response in many tumours including colorectal carcinoma, retinoblastoma and inflammatory breast adenocarcinoma. This is similar to another study which investigated the subcellular localization of insulin-like growth factor binding protein 5 (IGFBP5) in MDA-MB-435 breast cancer cells (Akkiprik *et al.,* 2009). Wild-type IGFBP5 was localized mainly in the nucleolus of MDA-MB-435 cells, and mutant IGFBP5 was detected at a low level in the cytoplasm. Overexpression of wild-type IGFBP5 inhibited BrdU incorporation however, overexpression of mutant IGFBP5 increased BrdU incorporation. The results revealed that wild-type IGFBP5 decreased cell growth when compared to the control, and mutant IGFBP5 promoted cell growth when compared to the control. This study confirmed that the function of IGFBP5 in cells is dependent on its subcellular localization. When the nuclear localization signal of IGFBP5 is deleted, the function of IGFBP5 changes from a growth inhibitor to a growth stimulator. As stated previously, the localization of MIER1α changes with breast cancer progression from predominantly nuclear in normal breast tissue, to predominantly cytoplasmic in invasive breast carcinoma (McCarthy *et al.*,

2008). This revealed that loss of nuclear MIER1α might contribute to breast cancer progression. It is important to study the subcellular localization of MIER1α because, the change in MIER1α nuclear localization to cytoplasmic localization in invasive breast carcinoma could affect the ability of MIER1α to apply its gene/chromatin repressor functions (McCarthy *et al*., 2008). Therefore, like the insulin-like growth factor binding protein 5 mentioned above, the function of MIER1α could be dependent on its subcellular localization. As a result, the change from nuclear to cytoplasmic localization could alter MIER1α from a tumour suppressor to a tumour promoter.

This study provided preliminary results on the effect of MIER1α on cell number in MCF7 and T47D cells. To increase the transfection efficiency of MIER1α in MCF7 cells, a Tet-On stable MCF7 cell line could be established. Future studies should also focus on increasing the number of T47D cells expressing MIER1α after doxycycline induction, and establishing the time period at which expression is the highest. If a stable MCF7 cell line is established, continued experiments on the effect of MIER1α on MCF7 cells should be conducted. For additional studies, it would also be interesting to look at the effect of E_2 stimulated proliferation on MCF7 cells. In the future, more experiments on the effect of factors in serum on localization of MIER1 isoforms should be conducted. It would be interesting to investigate the effect of 10 % FBS compared to 10 % Tet-approved FBS on the localization of MIER1 isoforms in MCF7 cells. In this present study, the effect of 10 % NBCS and FBS compared to 10 % Tet-approved FBS was investigated however, it would be interesting to determine if the results would change when NBCS is eliminated from the medium. It would be interesting to eliminate NBCS from the medium because, this serum contains a higher number of proteins and

immunoglobins and a lower number of growth factors than FBS. Therefore if NBCS is eliminated, the effect of untreated-FBS compared to charcoal-treated FBS on localization of MIER1 isoforms in MCF7 cells could be closely analyzed. Secondly, it would be interesting to evaluate the effect of estrogen addition to RPMI medium supplemented with 10 % Tet-approved FBS on the localization of MIER1α in T47D cells. Lastly, antibodies against growth factors in serum could be used to determine if the localization of MIER1 isoforms in MCF7 cells, and MIER1α in T47D cells, changes when certain growth factors are eliminated from culture.

In conclusion, this study provided interesting results on the effect of factors in serum on the localization of MIER1 isoforms, MIER1α and MIER1-3Aα, in MCF7 cells, and MIER1α in T47D cells. These results determined that factors in serum appeared to have an effect on nuclear localization of MIER1α in MCF7 and T47D cells, and MIER1-3Aα in MCF7 cells. These results also showed that insulin appeared to have an effect on nuclear localization of MIER1α in MCF7 cells. This could be important for future research because, as stated previously, MIER1α functions as an ER corepressor and during progression to IDC, MIER1α is forced out of the nucleus. This shuttling of MIER1α out of the nucleus to the cytoplasm, inhibits its ability to apply its gene/chromatin repressor functions (McCarthy *et al.*, 2008). It is believed this may interfere with the interaction between MIER1α and ERα and could activate signal transduction pathways (McCarthy *et al.*, 2008). Therefore, if a method to sequester MIER1α in the nucleus is achieved, the tumour suppressive potential of MIER1α can be controlled.

References

Akkiprik, M., Hu, L., Sahin, A., Hao, X., & Zhang, W. (2009). The subcellular localization of IGFBP5 affects its cell growth and migration functions in breast cancer. *BMC cancer*, *9*, 103. doi:10.1186/1471-2407-9-103

Badri, K. R., Zhou, Y., Dhru, U., Aramgam, S., & Schuger, L. (2008). Effects of the SANT domain of tension-induced/inhibited proteins (TIPs), novel partners of the histone acetyltransferase p300, on p300 activity and TIP-6-induced adipogenesis. *Molecular and cellular biology*, *28,* 6358–72. doi:10.1128/MCB.00333-08

Bhikoo, R., Srinivasa, S., Yu, T. C., Moss, D., & Hill, A. G. (2011). Systematic review of breast cancer biology in developing countries (part 1): Africa, the middle East, eastern europe, Mexico, the Caribbean and South america. *Cancers*, *3,* 2358–81. doi:10.3390/cancers3022358

Blackmore, T. M., Mercer, C. F., Paterno, G. D., & Gillespie, L. L. (2008). The transcriptional cofactor MIER1-beta negatively regulates histone acetyltransferase activity of the CREB-binding protein. *BMC research notes*, *1,* 68. doi:10.1186/1756-0500-1-68

Boyer, L. A., Langer, M. R., Crowley, K. A., Tan, S., Denu, J. M., & Peterson, C. L. (2002). Essential role for the SANT domain chromatin remodeling enzymes. *Molecular Cell, 10,* 935–942.

Brunner, D., Frank, J., Appl, H., Schöffl, H., Pfaller, W., & Gstraunthaler, G. (2010). Serum-free cell culture: the serum-free media interactive online database. *Altex*, *27,* 53–62.

Burgess-Beusse, B., Farrell, C., Gaszner, M., Litt, M., Mutskov, V., Recillas-Targa, F., & Felsenfeld, G. (2002). The insulation of genes from external enhancers and silencing chromatin. *Proceedings of the National Academy of Sciences of the United States of America*, *99*, 16433–7. doi:10.1073/pnas.162342499

Byles, V., Chmilewski, L. K., Wang, J., Zhu, L., Forman, L. W., & Faller, D. V. (2010). Aberrant cytoplasm localization and protein stability of SIRT1 is regulated by PI3K / IGF-1R signaling in human cancer cells. *International Journal of Biological Sciences, 6,* 599–612.

Canadian Cancer Society's Advisory Committee (2013): Canadian Cancer Statistics 2013. Toronto: Canadian Cancer Society ISSN 0835-2976

Cao, Z., West, C., Norton-Wenzel, C. S., Rej, R., Davis, F. B., & Davis, P. J. (2009). Effects of resin or charcoal treatment on fetal bovine serum and bovine calf serum. *Endocrine research*, *34,* 101–8. doi:10.3109/07435800903204082

Chan, S. K., Hill, M. E., & Gullick, W. J. (2006). The role of the epidermal growth factor receptor in breast cancer. *Journal of mammary gland biology and neoplasia*, *11,* 3–11. doi:10.1007/s10911-006-9008-2

Chen, J. Q., Delannoy, M., Cooke, C., & Yager, J. D. (2004). Mitochondrial localization of ERalpha and ERbeta in human MCF7 cells. *American journal of physiology-Endocrinology and metabolism*, *286,* E1011–22. doi:10.1152/ajpendo.00508.2003

Cheng, H., Meng, J., Wang, G., Meng, Y., Li, Y., Wei, D., & Dai, S. (2013). Skp2 regulates subcellular localization of PPARγ by MEK signaling pathways in human breast cancer. *International journal of molecular sciences*, *14,* 16554–69. doi:10.3390/ijms140816554

Ciardiello, F., Caputo, R., Bianco, R., Damiano, V., Fontanini, G., Cuccato, S., & Bianco, A. R. (2001). Inhibition of growth factor production and angiogenesis in human cancer cells by ZD1839 (Iressa), a selective epidermal growth factor receptor tyrosine kinase inhibitor. *Clinical Cancer Research, 7,* 1459–1465.

Clements, J. A., Mercer, F. C., Paterno, G. D., & Gillespie, L. L. (2012). Differential splicing alters subcellular localization of the alpha but not beta isoform of the MIER1 transcriptional regulator in breast cancer cells. *PloS one*, *7,* e32499. doi:10.1371/journal.pone.0032499

Curigliano, G. (2011). Immunity and autoimmunity: revising the concepts of response to breast cancer. *Breast (Edinburgh, Scotland)*, *20,* S71–4. doi:10.1016/S0960-9776(11)70298-3

Dang, C. V. (1999). c-Myc target genes involved in cell growth , apoptosis , and metabolism. *Molecular and Cellular Biology, 19,* 1-11.

De la Chapelle, A., & Hampel, H. (2010). Clinical relevance of microsatellite instability in colorectal cancer. *Journal of clinical oncology : official journal of the American Society of Clinical Oncology*, *28,* 3380–7. doi:10.1200/JCO.2009.27.0652

De Marinis, E., Fiocchetti, M., Acconcia, F., Ascenzi, P., & Marino, M. (2013). Neuroglobin upregulation induced by 17β-estradiol sequesters cytocrome c in the mitochondria preventing H2O2-induced apoptosis of neuroblastoma cells. *Cell death & disease*, *4,* e508. doi:10.1038/cddis.2013.30

Dickson, R. B., Kasid, A., Huff, K. K., Bates, S. E., Knabbe, C., Bronzert, D., & Lippman, M. E. (1987). Activation of growth factor secretion in tumorigenic states of breast cancer induced by 17 beta-estradiol or v-Ha-ras oncogene. *Proceedings of the National Academy of Sciences of the United States of America*, *84,* 837–41.

Ding, Z., Gillespie, L. L., Mercer, F. C., & Paterno, G. D. (2004). The SANT domain of human MI-ER1 interacts with Sp1 to interfere with GC box recognition and repress transcription from its own promoter. *The Journal of biological chemistry*, *279,* 28009–16. doi:10.1074/jbc.M403793200

Ding, Z., Gillespie, L. L., & Paterno, G. D. (2003). Human MI-ER1 alpha and beta function as transcriptional repressors by recruitment of histone deacetylase 1 to their conserved ELM2 domain. *Molecular and Cellular Biology, 23,* 250–258. doi:10.1128/MCB.23.1.250

Doyes, J., & Birdt, A. (1991). DNA methylation via a methyl-CpG inhibits transcription binding protein indirectly. *Cell, 64,* 1123–1134.

Duffy, M. J. (2006). Estrogen receptors: role in breast cancer. *Critical reviews in clinical laboratory sciences*, *43,* 325–47. doi:10.1080/10408360600739218

Ellis, M., Chew, Y. P., Fallis, L., Freddersdorf, S., Boshoff, C., Weiss, R. A., & Mittnacht, S. (1999). Degradation of p27 Kip cdk inhibitor triggered by Kaposi's sarcoma virus cyclin – cdk6 complex. *The EMBO Journal, 18,* 644–653.

Engstrøm, M. J., Opdahl, S., Hagen, A. I., Romundstad, P. R., Akslen, L. A., Haugen, O. A., & Bofin, A. M. (2013). Molecular subtypes, histopathological grade and survival in a historic cohort of breast cancer patients. *Breast cancer research and treatment*, *140*, 463–73. doi:10.1007/s10549-013-2647-2

Fernández-Cuesta, L., Oakman, C., Falagan-Lotsch, P., Smoth, K.-S., Quinaux, E., Buyse, M., & Olivier, M. (2012). Prognostic and predictive value of TP53 mutations in node-positive breast cancer patients treated with anthracycline- or anthracycline/taxane-based adjuvant therapy: results from the BIG 02-98 phase III trial. *Breast cancer research : BCR*, *14,* R70. doi:10.1186/bcr3179

Ferruzza, S., Rossi, C., Sambuy, Y., & Scarino, M. L. (2013). Serum-reduced and serum-free media for differentiation of Caco-2 cells. *Altex*, *30,* 159–68.

Florea, A. M., & Busselberg, D. (2013). Breast cancer and possible mechanisms of therapy resistance. *Journal of Global and Local Health Science, 2013:2,* 1-9.

Fukazawa, H., Mizuno, S., & Uehera, Y. (1995). A microplate assay for quantification of anchorage-independent growth of transformed cells. *Analytical Biochemistry, 228,* 83-90.

Fukazawa, H., Noguchi, K., Murakami, Y., & Uehara, Y. (2002). Mitogen-activated Protein / Extracellular Signal-regulated Kinase Kinase (MEK) Inhibitors Restore Anoikis Sensitivity in Human Breast Cancer Cell Lines with a Constitutively Activated Extracellular- regulated Kinase (ERK) Pathway. *Molecular Cancer Therapeutics, 1,* 303-309.

Gerdes, M. J., Dang, T. D., Larsen, M., & Rowley, D. R. (1998). Transforming growth factor-beta1 induces nuclear to cytoplasmic distribution of androgen receptor and inhibits androgen response in prostate smooth muscle cells. *Endocrinology*, *139,* 3569–77.

Gerl, R., & Vaux, D. L. (2005). Apoptosis in the development and treatment of cancer. *Carcinogenesis*, *26,* 263–70. doi:10.1093/carcin/bgh283

Gillespie, L.L. and Paterno, G.D. (2012). MIER1 (mesoderm induction early response 1 homolog (Xenopus laevis). *Atlas Genet Cytogenet Oncol Haematol, 16,* 127-130. *http://atlasgeneticsoncology.org//Genes/MIER1ID50389ch1p31.html*

Good, J. S., & Harrington, K. J. (2013). The hallmarks of cancer and the radiation oncologist: updating the 5Rs of radiobiology. *Clinical Oncology*, *25,* 569–77. doi:10.1016/j.clon.2013.06.009

Gstraunthaler, G. (2003). Alternatives to the use of fetal bovine serum: serum-free cell culture. *Altex*, *20*, 275–81.

Gutschner, T. and Diederichs, S. (2012). A long non-coding RNA point of view. *RNA Biology, 9,* 703–719.

Hamelers, I. H. L., van Schaik, R. F. M. A., Sipkema, J., Sussenbach, J. S., & Steenbergh, P. H. (2002). Insulin-like growth factor I triggers nuclear accumulation of cyclin D1 in MCF-7S breast cancer cells. *The Journal of biological chemistry*, *277,* 47645–52. doi:10.1074/jbc.M208727200

Hanahan, D., & Weinberg, R. A. (2011). Hallmarks of cancer: the next generation. *Cell*, *144,* 646–74. doi:10.1016/j.cell.2011.02.013

Haria, D., & Naora, H. (2013). Homeobox gene deregulation: impact on the hallmarks of cancer. *Cancer Hallm., 1,* 67-76. doi:10.1166/ch.2013.1007.

Harrington, K., Jankowska, P., & Hingorani, M. (2007). Molecular biology for the radiation oncologist: the 5Rs of radiobiology meet the hallmarks of cancer. *Clinical Oncology*, *19,* 561–71. doi:10.1016/j.clon.2007.04.009

Hoelz, A., Debler, E. W., & Blobel, G. (2011). The structure of the nuclear pore complex. *Annual review of biochemistry*, *80,* 613–43. doi:10.1146/annurev-biochem-060109-151030

Horovitz-Fried, M., Brutman-Barazani, T., Kesten, D., & Sampson, S. R. (2008). Insulin increases nuclear protein kinase Cdelta in L6 skeletal muscle cells. *Endocrinology*, *149,* 1718–27. doi:10.1210/en.2007-1572

Hunt, S. M. N., Pak, S. C. O., Bridges, M. W., Gray, P. P., & Sleigh, M. J. (1997). Chinese hamster ovary cells produce sufficient recombinant insulin-like growth factor I to support growth in serum-free medium. *Cytotechnology, 24,* 55–64.

Jiao, W., Datta, J., Lin, H. M., Dundr, M., & Rane, S. G. (2006). Nucleocytoplasmic shuttling of the retinoblastoma tumor suppressor protein via Cdk phosphorylation-dependent nuclear export. *The Journal of biological chemistry*, *281,* 38098–108. doi:10.1074/jbc.M605271200

Kaplan, P. L., Anderson, M., & Ozanne, B. (1982). Transforming growth factor(s) production enables cells to grow in the absence of serum: an autocrine system. *Proceedings of the National Academy of Sciences of the United States of America*, *79*, 485–9.

Kaplan, R. C., Strickler, H. D., Rohan, T. E., Muzumdar, R., & Brown, D. L. (2005). Insulin-like growth factors and coronary heart disease. *Cardiology in review*, *13,* 35–9. doi:10.1097/01.crd.0000134914.10407.40

Kass, S. U., Pruss, D., & Wolffe, A. P. (1997). How does DNA methylation repress transcription. *Trends in Genetics, 13,* 444–449.

Kelland, L. (2007). Targeting the limitless replicative potential of cancer: the telomerase/telomere pathway. *Clinical cancer research : an official journal of the American Association for Cancer Research*, *13,* 4960–3. doi:10.1158/1078-0432.CCR-07-0422

Kenemans, P., Verstraeten, R. A., & Verheijen, R. H. M. (2004). Oncogenic pathways in hereditary and sporadic breast cancer. *Maturitas*, *49,* 34–43. doi:10.1016/j.maturitas.2004.06.005

Klinge, C. M. (2001). Estrogen receptor interaction with estrogen response elements. *Nucleic acids research*, *29,* 2905–19.

Kwon, H. J., Rhim, J. H., Jang, I. S., Kim, G. E., Park, S. C., & Yeo, E. J. (2010). Activation of AMP-activated protein kinase stimulates the nuclear localization of glyceraldehyde 3-phosphate dehydrogenase in human diploid fibroblasts. *Experimental & molecular medicine*, *42,* 254–69. doi:10.3858/emm.2010.42.4.025

Lamothe, B., Baudry, A., Christoffersen, C. T., Meyts, P. De, Jami, J., Bucchini, D., & Joshi, R. L. (1998). Insulin receptor-decient cells as a new tool for dissecting complex interplay in insulin and insulin-like growth factors. *FEBS Letters, 426*, 381–385.

Laron, Z. (2001). Insulin-like growth factor 1 (IGF-1): a growth hormone. *J. Clin Pathol: Molecular Pathology, 54,* 311–316.

Lenormand, P., Sardet, C., Pages, G., L'Allemain, G. Brunet, A., & Pouyssogur, J. (1993). Growth factors induce nuclear translocation of MAP kinases (p42 mapk and p44 mapk) but not of their activator MAP kinase kinase (p45 mapkk) in fibroblasts. *The Journal of Cell Biology, 122,* 1079-1088.

Lerebours, F., & Lidereau, R. (2002). Molecular alterations in sporadic breast cancer. *Critical reviews in oncology/hematology*, *44,* 121–41.

Lewis, A. E., Fikaris, A. J., Prendergast, G. V, & Meinkoth, J. L. (2004). Thyrotropin and serum regulate thyroid cell proliferation through differential effects on p27 expression and localization. *Molecular endocrinology (Baltimore, Md.)*, *18,* 2321–32. doi:10.1210/me.2004-0104

Li, C. L., & Emery, D. W. (2008). The cHS4 chromatin insulator reduces gammaretroviral vector silencing by epigenetic modifications of integrated provirus. *Gene therapy*, *15,* 49–53. doi:10.1038/sj.gt.3303009

Li, S., Paterno, G. D., & Gillespie, L. L. (2013). Nuclear localization of the transcriptional regulator MIER1α requires interaction with HDAC1/2 in breast cancer cells. *PloS one*, *8,* e84046. doi:10.1371/journal.pone.0084046

Liu, L., Johnson, C., Fujimura, S., Teque, F., & Levy, J. A. (2011). Transfection optimization for primary human CD8+ cells. *Journal of immunological methods*, *372,* 22–9. doi:10.1016/j.jim.2011.06.026

Lombardi, M., Castoria, G., Migliaccio, A., Barone, M. V., Di Stasio, R., Ciociola, A., & Auricchio, F. (2008). Hormone-dependent nuclear export of estradiol receptor and DNA synthesis in breast cancer cells. *The Journal of cell biology*, *182,* 327–40. doi:10.1083/jcb.200712125

Lucas, T. F. G., Siu, E. R., Esteves, C. A., Monteiro, H. P., Oliveira, C. A., Porto, C. S., & Lazari, M. F. M. (2008). 17beta-estradiol induces the translocation of the estrogen receptors ESR1 and ESR2 to the cell membrane, MAPK3/1 phosphorylation and proliferation of cultured immature rat Sertoli cells. *Biology of reproduction*, *78,* 101–14. doi:10.1095/biolreprod.107.063909

Mahony, D. J. O., Xie, W., Smith, S. D., Singer, H. A., & Rothblum, L. I. (1992). Differential phosphorylation and localization of the transcription factor UBF *in vivo* in response to serum deprivation. *The Journal of Biological Chemistry, 267,* 35–38.

Marfori, M., Mynott, A., Ellis, J. J., Mehdi, A. M., Saunders, N. F. W., Curmi, P. M., & Kobe, B. (2011). Molecular basis for specificity of nuclear import and prediction of nuclear localization. *Biochimica et biophysica acta*, *1813,* 1562–77. doi:10.1016/j.bbamcr.2010.10.013

McCarthy, P. L., Mercer, F. C., Savicky, M. W. J., Carter, B. A., Paterno, G. D., & Gillespie, L. L. (2008). Changes in subcellular localisation of MI-ER1 alpha, a novel oestrogen receptor-alpha interacting protein, is associated with breast cancer progression. *British journal of cancer*, *99,* 639–46. doi:10.1038/sj.bjc.6604518

Milazzo, G., Giorgino, F., Damante, G., Giorgine, F., Sung, C., Stampfer, M. R., & Belfiore, A. (1992). Insulin receptor expression and function in human breast cancer cell lines insulin receptor expression and function in human breast cancer cell lines. *Cancer Research, 52,* 3924–3930.

Millard, C. J., Watson, P. J., Celardo, I., Gordiyenko, Y., Cowley, S. M., Robinson, C. V., & Schwabe, J. W. R. (2013). Class I HDACs share a common mechanism of regulation by inositol phosphates. *Molecular Cell*, *51,* 57–67. doi:10.1016/j.molcel.2013.05.020

Miralles, F., Posern, G., Zaromytidou, A., & Treisman, R. (2003). Actin dynamics control SRF activity by regulation of its coactivator MAL. *Cell, 113,* 329–342.

Mukherjee, S., & Conrad, S. E. (2005). c-Myc suppresses p21WAF1/CIP1 expression during estrogen signaling and antiestrogen resistance in human breast cancer cells. *The Journal of biological chemistry*, *280,* 17617–25. doi:10.1074/jbc.M502278200

Narla, G., Difeo, A., Reeves, H. L., Schaid, D. J., Hirshfeld, J., Hod, E., & Martignetti, J. A. (2005). A germline DNA polymorphism enhances alternative splicing of the KLF6 tumor suppressor gene and is associated with increased prostate cancer risk. *Cancer research*, *65*, 1213–22. doi:10.1158/0008-5472.CAN-04-4249

Narod, S. A., and Salmena, L. (2011). BRCA1 and BRCA2 mutations and breast cancer. *Discov Med, 12,* 445-453. Retrieved from:

http://www.discoverymedicine.com/Steven-A-Narod/2011/11/25/brca1-and-brca2-mutations-and-breast-cancer/

Negrini, S., Gorgoulis, V. G., & Halazonetis, T. D. (2010). Genomic instability--an evolving hallmark of cancer. *Nature reviews. Molecular cell biology*, *11,* 220–8. doi:10.1038/nrm2858

Niu, Y., Roy, F., Saltel, F., Andrieu-Soler, C., Dong, W., Chantegrel, A. L., & Sylla, B. S. (2006). A nuclear export signal and phosphorylation regulate Dok1 subcellular localization and functions. *Molecular and cellular biology*, *26,* 4288–301. doi:10.1128/MCB.01817-05

O'Brate, A., & Giannakakou, P. (2003). The importance of p53 location: nuclear or cytoplasmic zip code? *Drug Resistance Updates*, *6,* 313–322. doi:10.1016/j.drup.2003.10.004

Panigrahi, A. R., Pinder, S. E., Chan, S. Y., Paish, E. C., Robertson, J. F. R., & Ellis, I. O. (2004). The role of PTEN and its signalling pathways, including AKT, in breast cancer; an assessment of relationships with other prognostic factors and with outcome. *The Journal of pathology*, *204,* 93–100. doi:10.1002/path.1611

Paquin, M. C., Cagnol, S., Carrier, J. C., Leblanc, C., & Rivard, N. (2013). ERK-associated changes in E2F4 phosphorylation, localization and transcriptional activity during mitogenic stimulation in human intestinal epithelial crypt cells. *BMC cell biology*, *14,* 33. doi:10.1186/1471-2121-14-33

Paterno, G. D. (1997). cDNA cloning of a novel, developmentally regulated immediate early gene activated by fibroblast growth factor and encoding a nuclear protein. *Journal of Biological Chemistry*, *272,* 25591–25595. doi:10.1074/jbc.272.41.25591

Paterno, G. D., Ding, Z., Lew, Y. Y., Nash, G. W., Mercer, F. C., & Gillespie, L. L. (2002). Genomic organization of the human mi-er1 gene and characterization of alternatively spliced isoforms: regulated use of a facultative intron determines subcellular localization. *Gene*, *295,* 79–88.

Pomorski, T., Hrafnsdóttir, S., Devaux, P. F., & van Meer, G. (2001). Lipid distribution and transport across cellular membranes. *Seminars in cell & developmental biology*, *12*, 139–48. doi:10.1006/scdb.2000.0231

Post, J. N., Gillespie, L. L., & Paterno, G. D. (2001). Nuclear localization signals in the Xenopus FGF embryonic early response 1 protein. *FEBS letters*, *502,* 41–5.

Prevarskaya, N., Skryma, R., & Shuba, Y. (2010). Ion channels and the hallmarks of cancer. *Trends in molecular medicine*, *16,* 107–21. doi:10.1016/j.molmed.2010.01.005

Price, R. H., Butler, C. A., Webb, P., Uht, R., Kushner, P., & Handa, R. J. (2001). A splice variant of estrogen receptor beta missing exon 3 displays altered subnuclear localization and capacity for transcriptional activation. *Endocrinology*, *142,* 2039–49.

Qu, G. Z., & Ehrlich, M. (1999). Demethylation and expression of methylated plasmid DNA stably transfected into HeLa cells. *Nucleic acids research*, *27,* 2332–8.

Rden, K. A. C. A. (1999). Protein kinase B ¯Akt-mediated phosphorylation promotes nuclear exclusion of the winged helix transcription factor FKHR1. *Proc. Natl. Acad. Sci., 96,* 7421–7426.

Reilly, J. T., & Nash, J. R. (1988). Vitronectin (serum spreading factor): its localisation in normal and fibrotic tissue. *Journal of clinical pathology*, *41*, 1269–72.

Rodríguez, E., Aburjania, N., Priedigkeit, N. M., DiFeo, A., & Martignetti, J. A. (2010). Nucleo-cytoplasmic localization domains regulate Krüppel-like factor 6 (KLF6) protein stability and tumor suppressor function. *PloS one*, *5,* e12639. doi:10.1371/journal.pone.0012639

Saha Roy, S., & Vadlamudi, R. K. (2012). Role of estrogen receptor signaling in breast cancer metastasis. *International journal of breast cancer*, *2012,* 654698. doi:10.1155/2012/654698

Sancho, P., & Fabregat, I. (2010). NADPH oxidase NOX1 controls autocrine growth of liver tumor cells through up-regulation of the epidermal growth factor receptor pathway. *The Journal of biological chemistry*, *285*, 24815–24. doi:10.1074/jbc.M110.114280

Schafer, K. A. (1998). The cell cycle: a review. *Veterinary Pathology*, *35*, 461–478. doi:10.1177/030098589803500601

Sciacca, L., Le Moli, R., & Vigneri, R. (2012). Insulin analogs and cancer. *Frontiers in endocrinology*, *3,* 21. doi:10.3389/fendo.2012.00021

Sephton, C. F., & Mousseau, D. D. (2008). Dephosphorylation of Akt in C6 cells grown in serum-free conditions corresponds with redistribution of p85 / PI3K to the nucleus. *Journal of Neuorscience Research, 682,* 675–682. doi:10.1002/jnr

Sera for Cell Culture: Highest quality, consistencty, total trust. (n.d.). *PAA The Cell Culture Company*. Retrieved from *http://www.brunschwigch.com/pdf/downloads/PA_Serum_Brochure.pdf*

Sledge, G., & Miller, K. (2003). Exploiting the hallmarks of cancer. *European Journal of Cancer*, *39*, 1668–1675. doi:10.1016/S0959-8049(03)00273-9

Smith, C. (2013). Stable vs. transient transfection of eukaryotic cells. *Biocompare: The Buyer's Guide for Life Scientists*. Retrieved from: *http://www.biocompare.com/Editorial-Articles/126324-Transfection/*

Sonnenschein, C., & Soto, A. M. (2013). The aging of the 2000 and 2011 hallmarks of cancer reviews: A critique. *Journal of Biosciences*, *38*, 651–663. doi:10.1007/s12038-013-9335-6

Sterner, D. E., Wang, X., Bloom, M. H., Simon, G. M., & Berger, S. L. (2002). The SANT domain of Ada2 is required for normal acetylation of histones by the yeast SAGA complex. *The Journal of biological chemistry*, *277*, 8178–86. doi:10.1074/jbc.M108601200

Suter, R., & Marcum, J. A. (2007). The molecular genetics of breast cancer and targeted therapy. *Biologics : targets & therapy*, *1,* 241–58.

Tapia, C., Savic, S., Wagner, U., Schönegg, R., Novotny, H., Grilli, B., & Bubendorf, L. (2007). HER2 gene status in primary breast cancers and matched distant metastases. *Breast cancer research : BCR*, *9,* R31. doi:10.1186/bcr1676

Teplitsky, Y., Paterno, G. D., & Gillespie, L. L. (2003). Proline365 is a critical residue for the activity of XMI-ER1 in Xenopus embryonic development. *Biochemical and Biophysical Research Communications*, *308,* 679–683. doi:10.1016/S0006-291X(03)01461-X

Tet-Off and Tet-On Gene Expression Systems User Manuel. (2012). *Clontech*. Retrieved from: *www.clontech.com/xxclt_ibcGetAttachment.jsp?cItemId=17553*

Thompson, M. E. (2010). BRCA1 16 years later: nuclear import and export processes. *The FEBS journal*, *277,* 3072–8. doi:10.1111/j.1742-4658.2010.07733.x

Tinoco, G., Warsch, S., Glück, S., Avancha, K., & Montero, A. J. (2013). Treating breast cancer in the 21st century: emerging biological therapies. *Journal of Cancer*, *4,* 117–32. doi:10.7150/jca.4925

Turpin, P., Ossareh-Nazari, B., & Dargemont, C. (1999). Nuclear transport and transcriptional regulation. *FEBS letters*, *452*, 82–6.

Van Zoelen, E. J., Twardzik, D. R., van Oostwaard, T. M., van der Saag, P. T., de Laat, S. W., & Todaro, G. J. (1984). Neuroblastoma cells produce transforming growth factors during exponential growth in a defined hormone-free medium. *Proceedings of the National Academy of Sciences of the United States of America*, *81,* 4085–9.

Vermeulen, K., Van Bockstaele, D. R., & Berneman, Z. N. (2003). The cell cycle: a review of regulation, deregulation and therapeutic targets in cancer. *Cell proliferation*, *36*, 131–49.

Voron, T., Marcheteau, E., Pernot, S., Colussi, O., Tartour, E., Taieb, J., & Terme, M. (2014). Control of the immune response by pro-angiogenic factors. *Frontiers in oncology*, *4,* 70. doi:10.3389/fonc.2014.00070

Wadehra, M., Mainigi, M., Morales, S. A., Rao, R. G., Gordon, L. K., Williams, C. J., & Braun, J. (2008). Steroid hormone regulation of EMP2 expression and localization in the endometrium. *Reproductive biology and endocrinology : RB&E*, *6,* 15. doi:10.1186/1477-7827-6-15

Walerych, D., Napoli, M., Collavin, L., & Del Sal, G. (2012). The rebel angel: mutant p53 as the driving oncogene in breast cancer. *Carcinogenesis*, *33,* 2007–17. doi:10.1093/carcin/bgs232

Weigand, M., Hantel, P., Kreienberg, R., & Waltenberger, J. (2005). Autocrine vascular endothelial growth factor signalling in breast cancer. Evidence from cell lines and primary breast cancer cultures in vitro. *Angiogenesis*, *8,* 197–204. doi:10.1007/s10456-005-9010-0

Willmarth, N. E., Albertson, D. G., & Ethier, S. P. (2004). Chromosomal instability and lack of cyclin E regulation in hCdc4 mutant human breast cancer cells. *Breast cancer research : BCR*, *6,* R531–9. doi:10.1186/bcr900

Wuescher, L., Angevine, K., Hinds, T., Ramakrishnan, S., Najjar, S. M., & Mensah-Osman, E. J. (2011). Insulin regulates menin expression, cytoplasmic localization, and interaction with FOXO1. *American journal of physiology. Endocrinology and metabolism*, *301,* E474–83. doi:10.1152/ajpendo.00022.2011

Xu, J., Chen, Y., & Olopade, O. I. (2010). MYC and breast cancer. *Genes & cancer*, *1,* 629–40. doi:10.1177/1947601910378691

Yang, P., Du, C. W., Kwan, M., Liang, S. X., & Zhang, G. J. (2013). The impact of p53 in predicting clinical outcome of breast cancer patients with visceral metastasis. *Scientific reports*, *3,* 2246. doi:10.1038/srep02246

Yu, H., Chen, J. K., Feng, S., Dalgarno, D. C., Brauer, A. W., & Schreiber, S. L. (1994). Structural basis for the binding of proline-rich peptides to SH3 domains. *Cell*, *76,* 933–45.

Zhang, D., Meyron-Holtz, E., & Rouault, T. A. (2007). Renal iron metabolism: transferrin iron delivery and the role of iron regulatory proteins. *Journal of the American Society of Nephrology : JASN*, *18,* 401–6. doi:10.1681/ASN.2006080908

Zhang, H.Y., Liang, F., Jia, Z. L., Song, S. T., & Jiang, Z. F. (2013). PTEN mutation, methylation and expression in breast cancer patients. *Oncology letters*, *6,* 161–168. doi:10.3892/ol.2013.1331

Zhou, X., Vink, M., Klaver, B., Berkhout, B., & Das, A. T. (2006). Optimization of the Tet-On system for regulated gene expression through viral evolution. *Gene therapy*, *13,* 1382–90. doi:10.1038/sj.gt.3302780

Appendix 1: Components of Serum

This table represents the typical components found in serum (Brunner *et al.*, 2010)

Serum Proteins	Albumin Globulins (e.g. Immunglobulins, IgG) Complement Factors α1-Antitrypsin (Protease Inhibitor) α2-Macroglobulin (Protease Inhibitor)
Transport Proteins	Transferrin Transcortin Thyroxine-binding Globulin α1-Lipoprotein β1-Lipoprotein Apolipoprotein
Attachment and Spreading Factors	Fibronectin Laminin Serum Spreading Factor Collagen α1
Enzymes	Lactate Dehydrogenase Alkaline Phosphatase γ-Glutamyl Transferase Alanine Aminotransferase (ALT/GPT) Aspartate Aminotransferase (AST/GOT) Carboxypeptidase Creatine Kinase
Hormones	Insulin Glucagon Corticosteroids Vasopressin Thyroid Hormones Parathyroid Hormone Growth Hormone Pituitary Glandotropic Factors Prostaglandins
Growth Factors and Cytokines	Epidermal Growth Factor (EGF) Fibroblast Growth Factor (FGF) Nerve Growth Factor (NGF) Endothelial Cell Growth Factor (ECGF) Platelet-derived Growth Factor (PDGF) Insulin-like Growth Factors (IGFs) Interleukins Interferons Transforming Growth Factors (TGFs)

Fatty Acids and Lipids	Free and Protein-bound Fatty Acids Triglycerides Phospholipids Cholesterol Ethanolamine Phosphatidylethanolamine
Vitamins and Trace Elements	Retinol/Retinoic Acid (Vitamin A) Vitamin B-Group: Thiamine Riboflavin Pyridoxine/Pyridoxalphosphate Cobalamin Folic Acid Niacinamide/Nicotinic Acid Panthotenic Acid Biotin Ascorbic Acid (Vitamin C) α-Tocopherol (Vitamin E) Selenium, Iron, Zinc, and Cu, Co, Cr, I, F, Mn, Mo, V, Ni, Sn,
Carbohydrates	Glucose Galactose Fructose Mannose Ribose Glycolytic Metabolites
Nonprotein Nitrogens	Urea Purines/Pyrimidines Polyamines Creatinine Amino Acids